AD-765 519

THE EFFECTS OF SURFACE LAYER ON PLASTIC DEFORMATION AND CRACK PROPAGATION

Irvin R. Kramer

Martin Marietta Corporation

Prepared for:

Army Materials and Mechanics Research Center
Advanced Research Projects Agency

July 1973

AMMRC CR 71-2/6

THE EFFECTS OF SURFACE LAYER ON PLASTIC DEFORMATION AND CRACK PROPAGATION

July 1973

Irvin R. Kramer
Martin Marietta Corporation, Denver Division
P. O. Box 179, Denver, Colorado 80201

Final Report

Contract DAAG 46-70-C-0102

Approved for public release; distribution unlimited

Prepared for

ARMY MATERIALS AND MECHANICS RESEARCH CENTER
Watertown, Massachusetts 02172

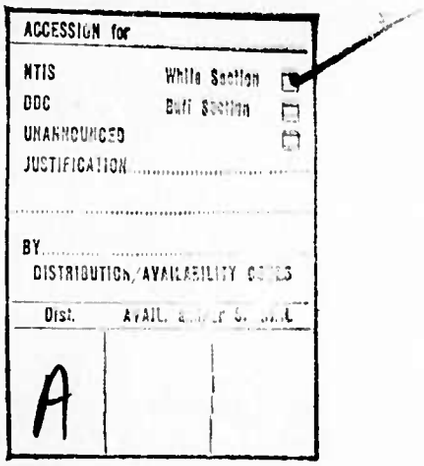

The findings in this report are not to be construed as an official Department of the Army position, unless so designated by other authorized documents.

Mention of any trade names or manufacturers in this report shall not be construed as advertising nor as an official indorsement or approval of such products or companies by the United States Government.

DISPOSITION INSTRUCTIONS

Destroy this report when it is no longer needed.
Do not return it to the originator.

Unclassified
Security Classification

DOCUMENT CONTROL DATA - R&D

(Security classification of title, body of abstract and indexing annotation must be entered when the overall report is classified)

1 ORIGINATING ACTIVITY (Corporate author)

Martin Marietta Corporation

2a REPORT SECURITY CLASSIFICATION

Unclassified

2b GROUP

3 REPORT TITLE

The Effects of Surface Layer on Plastic Deformation and Crack Propagation

4 DESCRIPTIVE NOTES (Type of report and inclusive dates)

Final Report

5 AUTHOR(S) (Last name, first name, initial)

Irvin R. Kramer

6 REPORT DATE	7a TOTAL NO. OF PAGES	7b NO. OF REFS
July 1973	~~94~~ 103	76

8a CONTRACT OR GRANT NO.	9a ORIGINATOR'S REPORT NUMBER(S)
DAAG 46-70-C-0102	AMMRC CR 71-2/6
b. PROJECT NO ARPA Order 188-0-7400	
c.	9b. OTHER REPORT NO(S) (Any other numbers that may be assigned this report)
d	Details of illustrations in this document ~~may be better studied~~ on microfiche.

10 AVAILABILITY/LIMITATION NOTICES

Approved for public release; distribution unlimited.

11 SUPPLEMENTARY NOTES	12 SPONSORING MILITARY ACTIVITY
	Army Materials and Mechanics Research Ctr Watertown, Massachusetts 02172

13 ABSTRACT

Chapter I - The crack propagation of 2014-T6 aluminum, titanium (6Al-4V), and 4130 steel (YS = 180,000 psi) was measured under plane stress and plane strain, and a comparison was made to determine the effect of eliminating or decreasing the surface layer (SLE treatment) on the cracking resistance of the specimens. The data show that, in all cases, the SLE treatment improves the crack resistance. The improvement is on the order of 2 to 5 times, depending on the stress intensity factor. A comparison between the SLE-treated and shot-peened specimens shows that the SLE treatment also improves the cracking resistance by about a factor of 2 over that obtained from shot-peening. The endurance limit of titanium (6Al-4V) tubing was increased from 70,000 to 90,000 psi by the SLE treatment. Tests made to assess the effectiveness of the SLE treatment on commercial 4130 steel tanks were inconclusive due to the large scatter in the crack propagation rates.

Chapter II - It was shown that when specimens of 2014-T6 aluminum, titanium (6Al-4V), and 4130 steel (YS = 180,000 psi) were fatigued, the surface-layer stress increased. The number of cycles required to initiate a propagating crack was determined. The data show that a crack is initiated when the surface-layer stress attains a critical value. This value is independent of the cyclic stress amplitude. Based on these results, a new theory of fatigue has been proposed.

DD FORM 1 JAN 64 1473

1a

Unclassified
Security Classification

14 KEY WORDS	LINK A		LINK B		LINK C	
	ROLE	WT	ROLE	WT	ROLE	WT
Crack Propagation						
Stress Intensity						
Crack Growth						
Surface Layer						
Fatigue						

INSTRUCTIONS

1. ORIGINATING ACTIVITY: Enter the name and address of the contractor, subcontractor, grantee, Department of Defense activity or other organization *(corporate author)* issuing the report.

2a. REPORT SECURITY CLASSIFICATION: Enter the overall security classification of the report. Indicate whether "Restricted Data" is included. Marking is to be in accordance with appropriate security regulations.

2b. GROUP: Automatic downgrading is specified in DoD Directive 5200.10 and Armed Forces Industrial Manual. Enter the group number. Also, when applicable, show that optional markings have been used for Group 3 and Group 4 as authorized.

3. REPORT TITLE: Enter the complete report title in all capital letters. Titles in all cases should be unclassified. If a meaningful title cannot be selected without classification, show title classification in all capitals in parenthesis immediately following the title.

4. DESCRIPTIVE NOTES: If appropriate, enter the type of report, e.g., interim, progress, summary, annual, or final. Give the inclusive dates when a specific reporting period is covered.

5. AUTHOR(S): Enter the name(s) of author(s) as shown on or in the report. Enter last name, first name, middle initial. If military, show rank and branch of service. The name of the principal author is an absolute minimum requirement.

6. REPORT DATE: Enter the date of the report as day, month, year, or month, year. If more than one date appears on the report, use date of publication.

7a. TOTAL NUMBER OF PAGES: The total page count should follow normal pagination procedures, i.e., enter the number of pages containing information.

7b. NUMBER OF REFERENCES: Enter the total number of references cited in the report.

8a. CONTRACT OR GRANT NUMBER: If appropriate, enter the applicable number of the contract or grant under which the report was written.

8b, 8c, & 8d. PROJECT NUMBER: Enter the appropriate military department identification, such as project number, subproject number, system numbers, task number, etc.

9a. ORIGINATOR'S REPORT NUMBER(S): Enter the official report number by which the document will be identified and controlled by the originating activity. This number must be unique to this report.

9b. OTHER REPORT NUMBER(S): If the report has been assigned any other report numbers *(either by the originator or by the sponsor)*, also enter this number(s).

10. AVAILABILITY/LIMITATION NOTICES: Enter any limitations on further dissemination of the report, other than those imposed by security classification, using standard statements such as:

(1) "Qualified requesters may obtain copies of this report from DDC."

(2) "Foreign announcement and dissemination of this report by DDC is not authorized."

(3) "U. S. Government agencies may obtain copies of this report directly from DDC. Other qualified DDC users shall request through _____."

(4) "U. S. military agencies may obtain copies of this report directly from DDC. Other qualified users shall request through _____."

(5) "All distribution of this report is controlled. Qualified DDC users shall request through _____."

If the report has been furnished to the Office of Technical Services, Department of Commerce, for sale to the public, indicate this fact and enter the price, if known.

11. SUPPLEMENTARY NOTES: Use for additional explanatory notes.

12. SPONSORING MILITARY ACTIVITY: Enter the name of the departmental project office or laboratory sponsoring *(paying for)* the research and development. Include address.

13. ABSTRACT: Enter an abstract giving a brief and factual summary of the document indicative of the report, even though it may also appear elsewhere in the body of the technical report. If additional space is required, a continuation sheet shall be attached.

It is highly desirable that the abstract of classified reports be unclassified. Each paragraph of the abstract shall end with an indication of the military security classification of the information in the paragraph, represented as *(TS), (S), (C), or (U)*

There is no limitation on the length of the abstract. However, the suggested length is from 150 to 225 words.

14. KEY WORDS: Key words are technically meaningful terms or short phrases that characterize a report and may be used as index entries for cataloging the report. Key words must be selected so that no security classification is required. Identifiers, such as equipment model designation, trade name, military project code name, geographic location, may be used as key words but will be followed by an indication of technical context. The assignment of links, rules, and weights is optional.

AMMRC CR 71-2/6

THE EFFECTS OF SURFACE LAYER ON PLASTIC DEFORMATION AND CRACK PROPAGATION

Irvin R. Kramer
Martin Marietta Corporation
P. O. Box 179, Denver, Colorado 80201

July 1973

Final Report

Contract DAAG 46-70-C-0102

Sponsored by Advanced Research Project Agency
ARPA Order No. 188-0-7400

Prepared for

ARMY MATERIALS AND MECHANICS RESEARCH CENTER
Watertown, Massachusetts 02172

FOREWORD

This report was prepared by the Denver Division of Martin Marietta Corporation under U.S. Army Contract DAAG 46-70-C-0102. This contract is sponsored by the Advanced Research Project Agency under ARPA Order 188-0-7400 and is administered by the Army Materials and Mechanics Research Center, Watertown, Massachusetts, with Dr. Eric B. Kula, AMXMR-EM, serving as Technical Supervisor.

This report has been divided into two chapters, each independent from the other:

Chapter I - Enhancement of Crack Propagation Resistance by Elimination of the Surface Layer

Chapter II - A Mechanism of Fatigue Failure

ABSTRACT

Chapter I

The crack propagation of 2014-T6 aluminum, titanium (6Aℓ-4V), and 4130 steel (YS = 180,000 psi) was measured under plane stress and plane strain, and a comparison was made to determine the effect of eliminating or decreasing the surface layer (SLE treatment) on the cracking resistance of the specimens. The data show that, in all cases, the SLE treatment improves the crack resistance at low stress intensities. The improvement is on the order of 2 to 5 times, depending on the stress intensity factor. A comparison between the SLE-treated and shot-peened specimens shows that the SLE treatment also improves the cracking resistance by about a factor of 2 over that obtained from shot-peening. The endurance limit of titanium (6Aℓ-4V) tubing was increased from 70,000 to 90,000 psi by the SLE treatment. Tests made to assess the effectiveness of the SLE treatment on commercial 4130 steel tanks were inconclusive due to the large scatter in the crack propagation rates.

Chapter II

It was shown that when specimens of 2014-T6 aluminum, titanium (6Aℓ-4V), and 4130 steel (YS = 180,000 psi) were fatigued, the surface-layer stress increased. The number of cycles required to initiate a propagating crack was determined. The data show that a crack is initiated when the surface-layer stress attains a critical value. This value is independent of the cyclic stress amplitude. Based on these results, a new theory of fatigue has been proposed.

CONTENTS

Table

A Mechanism of Fatigue Failure

I. INTRODUCTION

In this phase of the research effort performed under Contract DAAG 46-70-C-0102, the objectives were directed toward determining the degree of improvement imparted by the SLE process to crack propagation resistance and fatigue life. The SLE treatment consists of a process in which the metal is prestressed (usually up to the proportional limit) and the surface layer formed as a result of this prestressing operation is eliminated either by chem-milling or by relaxation. (The surface layer is the high-dislocation region that forms at free surfaces as a result of plastic deformation.)

The existance of the surface layer was shown previuously from observations on single and polycrystalline metals (Ref 1). In the earlier work, the presence of the surface layer was demonstrated by observations that the plastic deformation characteristics of single and polycrystalline metals were altered markedly when the surface metal was removed during deformation. These changes were accompanied by a decrease in the apparent activation energy for deformation and an increase in the activation volume. These latter changes showed that the dislocation density in the surface layer was greater than that in the interior. The depth of the surface layer and the back stress it imposed on moving dislocations was measured (Ref 2) by determining the decrease in the initial flow stress after removing the surface layer from plastically deformed specimens. The difference between the unloading stress and the stress at which plastic flow started after eliminating the surface was defined as the surface-layer stress. The presence of the surface layer was also shown by Kitajama, *et al.* (Ref 3), using an etch pit technique on single crystals of copper, and by G. Vellaikal (Ref 4) on polycrystalline copper.

A recent publication (Ref 5) described the metallurgical changes that occur when a metal is stressed to the proportional limit, as in the SLE process. The essential data are reproduced in Fig. 1 and 2 for convenience. By observing the appearance of slip bands, the percentage of deformed surface grains was measured as a function of stress for 2014-T6 aluminum (Fig. 1). No slip bands were detected until the applied stress was about 3.5 kg/mm^2 (5000 psi). Past this value, the number of surface grains that deformed plastically increased rapidly, and at 10 kg/mm^2(14,000 psi) approximately 80% of the surface grains were deformed. Afterwards the number of deformed grains increased slowly with stress; and at the proportional limit (42 kg/mm^2, or 59,000 psi), about 85% of the surface grains were deformed.

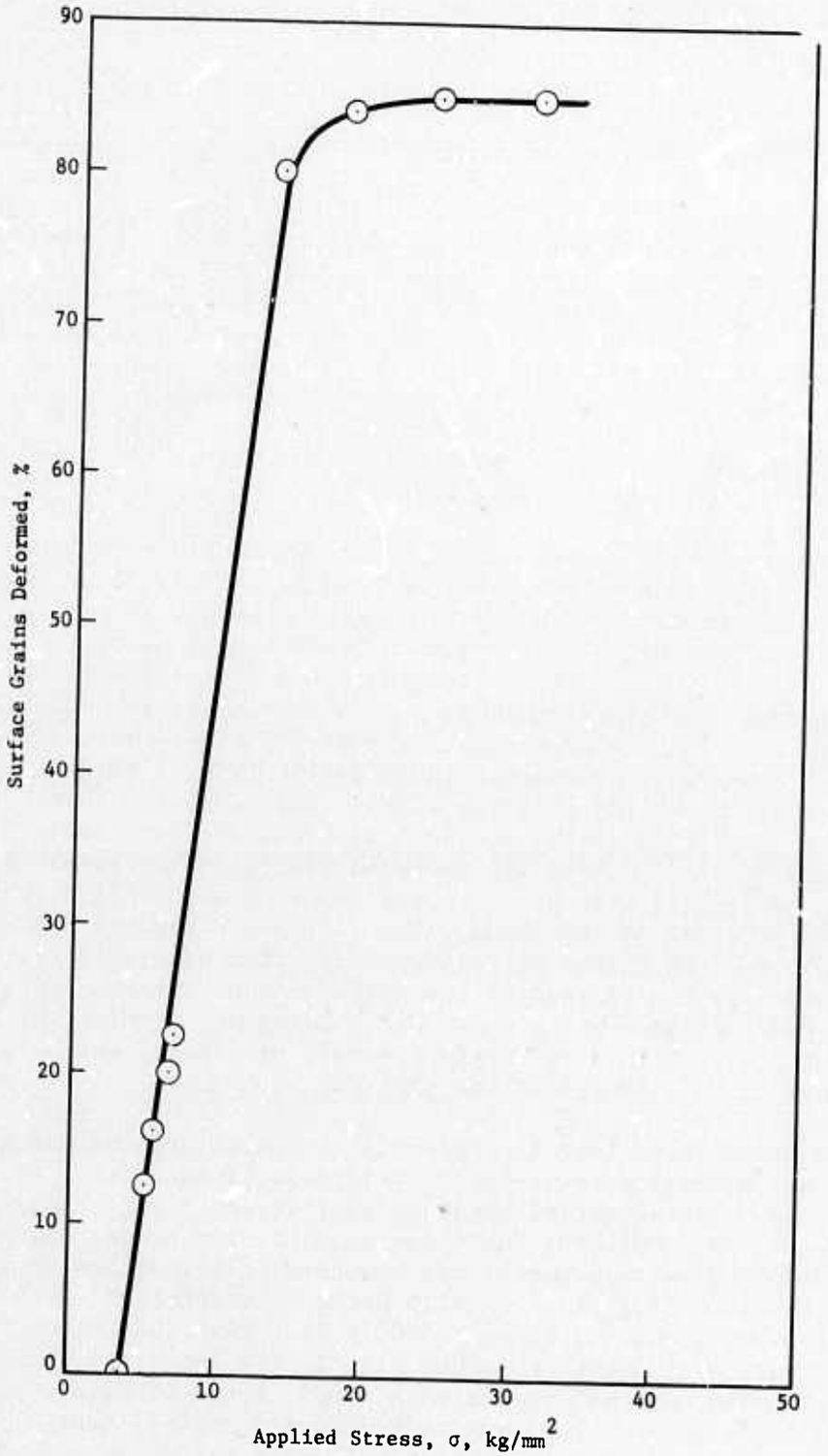

Fig. 1 Percentage of Surface Grains Deformed as a Function of Applied Stress in 2014-T6 Aluminum

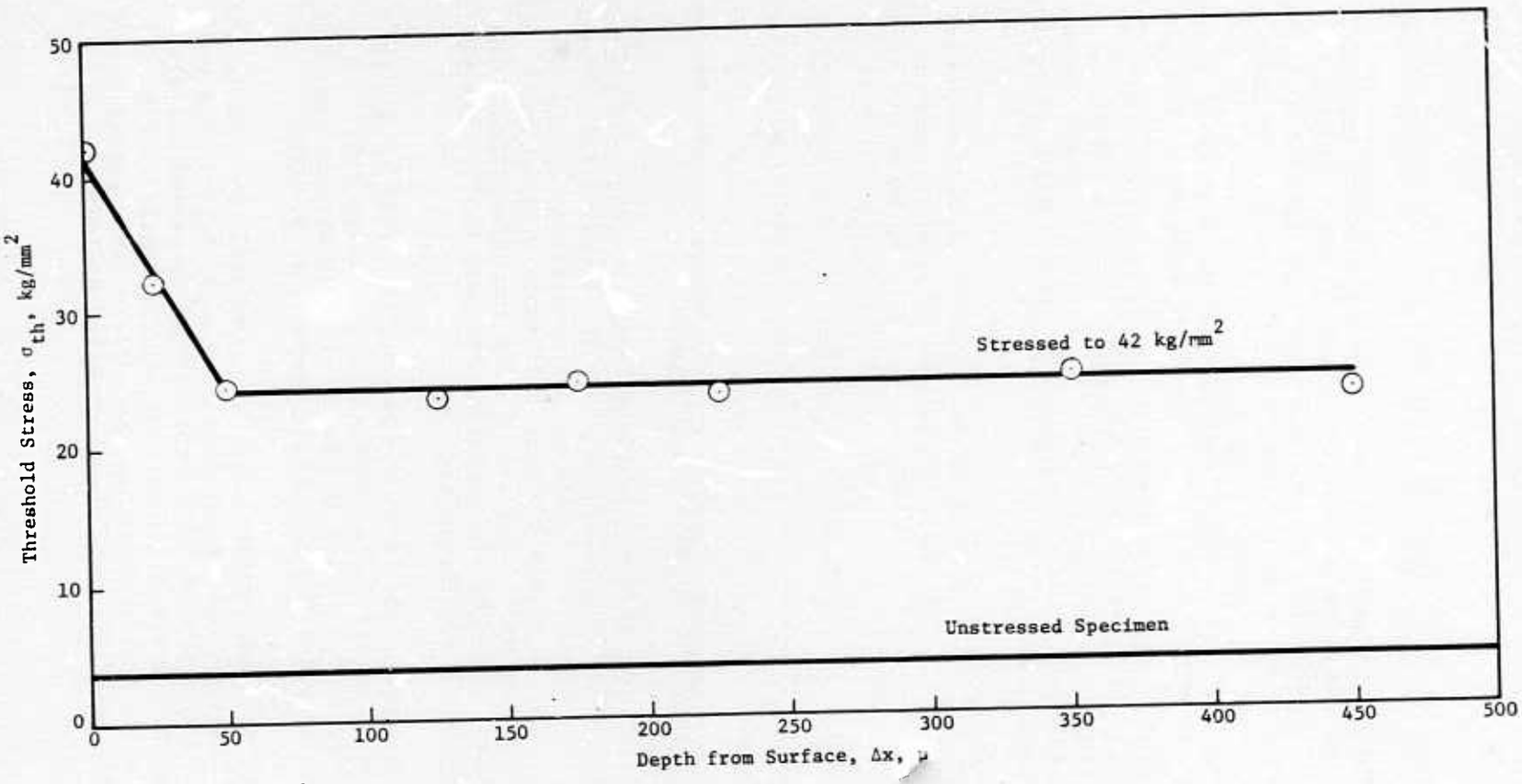

Fig. 2 Threshold Stress for Plastic Flow as a Function of Depth from Surface in 2014-T6 Aluminum

Figure 2 shows the plastic deformation characteristics as a function of depth from the surface after the specimens were stressed to the proportional limit. When the surface region was removed by electromechanical polishing, and when the sample was restressed, the onset of plastic flow--as measured by the appearance of slip bands--decreased with the distance from the surface. Beyond a distance of about 50 μ (0.002 in.), the threshold stress, σ_{th}, remained constant at 23.8 kg/mm^2 (33,500 psi). Thus. when this material is prestressed to the proportional limit (59,000 psi), a surface layer about 0.002 in. deep is formed. In the SLE treatment, this outer layer is removed; and on restressing the specimen, the surface layer should not begin to reform until the stresses attain 33,500 psi.

The effect of the surface layer on ductility or crack propagation appears to be most readily explained in terms of "pileup" arrays of dislocations against barriers (Ref 6 thru 8). In this concept, the stress field exerted by a "pileup" of dislocations of like sign is $\sigma = N \sigma_a$, where N is the number of dislocations in the pileup and σ_a is the applied stress. When $\sigma \geq \sigma_F$, where σ_F is the fracture strength, fracture occurs. Accordingly, the conditions to promote brittle fracture require the presence of a strong barrier and a critical number of dislocations in the piled-up array for a given applied stress.

The evidence that the surface layer may become a sufficiently strong barrier was first presented in 1968 (Ref 9). To determine the influence of the surface layer on brittle fracture, polycrystalline specimens of molybdenum were pulled in an electrolytic cell containing sulphuric acid and metal was removed at a constant rate during the deformation. The increase in temperature during the deplating was only 0.5°C. The results of this test are presented in Fig. 3.

Note that when the surface layer was removed at a rate of 6×10^{-4} in./minute, the ductile-brittle temperature was decreased 15°C. In comparison, a hundredfold decrease in the strain rate without removing the surface layer decreased the transition temperature by 25°C.

It is unlikely that the surface layer was completely removed in these tests, since the surface-layer stress increases with strain. Furthermore, as reported previously (Ref 10), this stress increases rapidly as the temperature is decreased. Thus, the data presented in Fig. 3 imply that brittle fracture occurs when the surface layer become strong enough to support a critical-sized pileup array of dislocations.

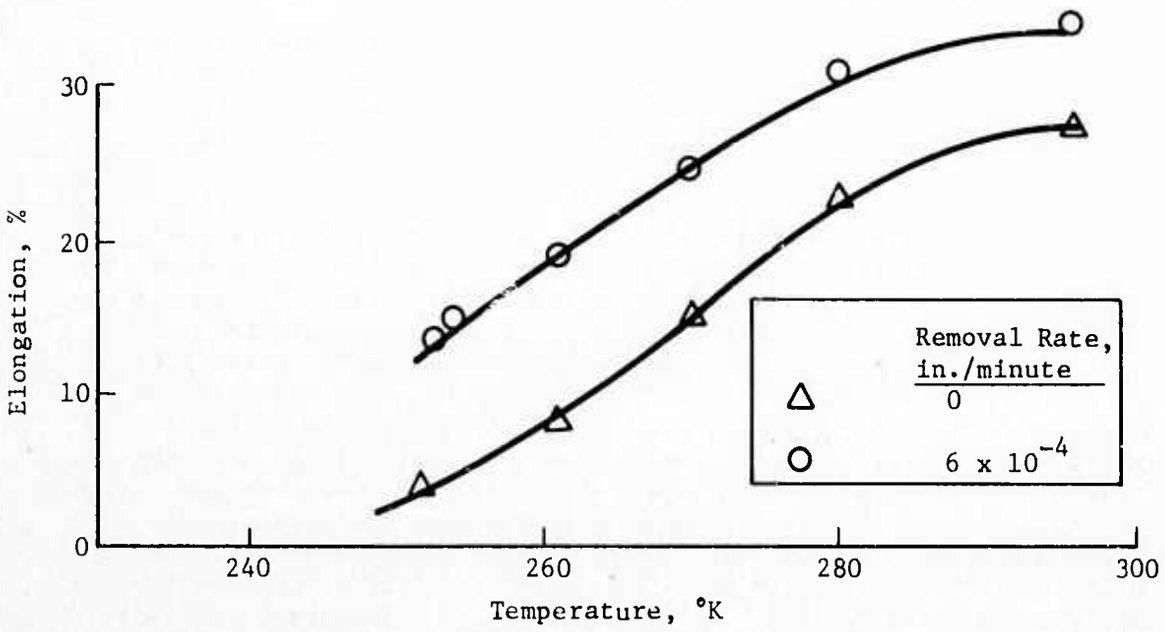

Fig. 3 Effect of Removing Surface Layer on the Ductile-Brittle Transition Temperature of Molybdenum (from Ref 9)

Similarly, it was reported that during cycling either between fixed plastic strain limits or at constant stress amplitudes, the surface-layer stress increased. Further research (Ref 11) showed that when the surface layer reached a critical value, fatigue failure occurred. From the relationship between the rate of change of the surface-layer stress, σ_s, the stress amplitude during cycling, σ, and the number of cycles needed to cause fatigue failure, N_F, a Basquin (Ref 12)-type equation was derived; that is, $N_F = \sigma_s^* / k\,\sigma^{-P}$, where P and k are constants and σ_s^* is the critical value of the surface-layer stress. It was also shown (Ref 11) that if the surface layer was prevented from attaining a critical value, the fatigue life was extended indefinitely--limited only by the finite size of the specimen. These observations imply that fatigue failures, in much the same manner as the ductile-brittle transition temperature, are influenced strongly by the surface-layer stress: Fatigue cracking starts when the surface layer attains sufficient strength to sustain a critical-sized pileup of dislocations that exceed the fracture strength.

In this theory the pileup need not be a classical linear-type array; rather, the critical stress field probably arises from the addition of the force fields of a large number of dislocations of like sign, arranged somewhat randomly in the slip planes within the surface layer.

From the above discussion, it should be clear that a process that inhibits or prevents the formation of the surface layer would enhance fatigue resistance and crack propagation resistance. The improvements obtained by decreasing the surface-layer stress were demonstrated in previous reports in terms of the crack propagation behavior under both plane stress and plane strain conditions. In this report, in addition to measuring the crack propagation rates, an evaluation was made to determine the effect of the SLE treatment on weldments of titanium and 4130 steel and on the fatigue life of titanium tubing. The fatigue life of a commercial-type steel pressure bottle was also determined. Since shot-peening is rather extensively employed to improve the fatigue resistance of metals, tests were also conducted to compare its effectiveness against that of the SLE treatment. In addition, we wanted to determine the extent to which shot-peening affected the initiation and crack propagation stages. Since the amount of work-hardening is often reported to be temperature-sensitive, the influence of prestressing the specimens in liquid nitrogen (LN_2) during the SLE treatment was also investigated.

In the previous work, it was shown that under cyclic stress testing below the proportional limit, the surface-layer stress increased linearly as a function of the number of cycles. This curve, when extrapolated to the life of the specimen, indicated that fracture occurred at a critical surface-layer stress. it is apparent that the number of cycles required for fracture will depend on the size of the specimen; that is, on the critical crack length. As a result, in this investigation it was decided to determine the surface-layer stress necessary for crack initiation. These results are reported in Chapter II.

II. EXPERIMENTAL TECHNIQUES

A. MATERIALS

The sheet and plate materials used in this investigation are listed below.

Material	Thickness, in.	Vendor
2014-T6 Aluminum	0.125	Alcoa
2014-T6 Aluminum	1.0	Kaiser
Titanium (6Aℓ-4V)	0.067	Timet
Titanium (6Aℓ-4V)	0.625	Timet
4130 Steel	0.125	U.S. Steel
4130 Steel	0.625	U.S. Steel

The 4130 pressure vessels were purchased from the Pressed Steel Tank Company as industrial oxygen tanks. The vessels were approximately 18 in. long by 6 in. in diameter (Fig. 4), and their wall thickness was determined to be 0.18 in. According to the vendor, they were austenitized at 1600°F, oil-quenched, and tempered at 1200°F. The strength of both tanks was reported to be between 100 and 120 ksi. The tanks had a design pressure of 3360 psi and a burst pressure of 5000 psi. Their chemical composition is listed below:

Carbon	0.32	Nickel	0.11
Manganese	0.52	Chromium	0.90
Phosphorus	0.013	Molybdenum	0.17
Sulphur	0.026	Copper	0.19
Silicon	0.32		

The titanium tubing was purchased from the Wolverine Tube Division of O. O. E. Products Corporation. These tubes had a 1/2-in. O.D. and a thickness of 0.049 in. According to the vendor, the tubing was annealed at 1400°F for 4 hr after being drawn. The 4130 steel was obtained in two forms: hot-rolled plates 5/8- and 1/16-in. thick, and

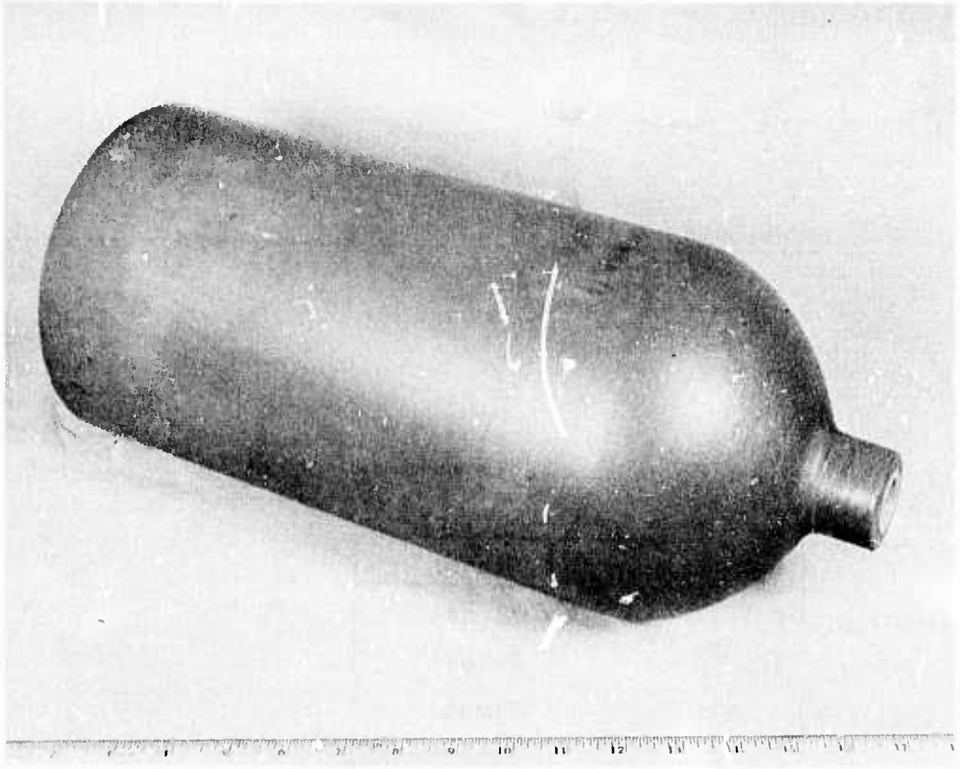

Fig. 4 4130 Steel Pressure Vessel

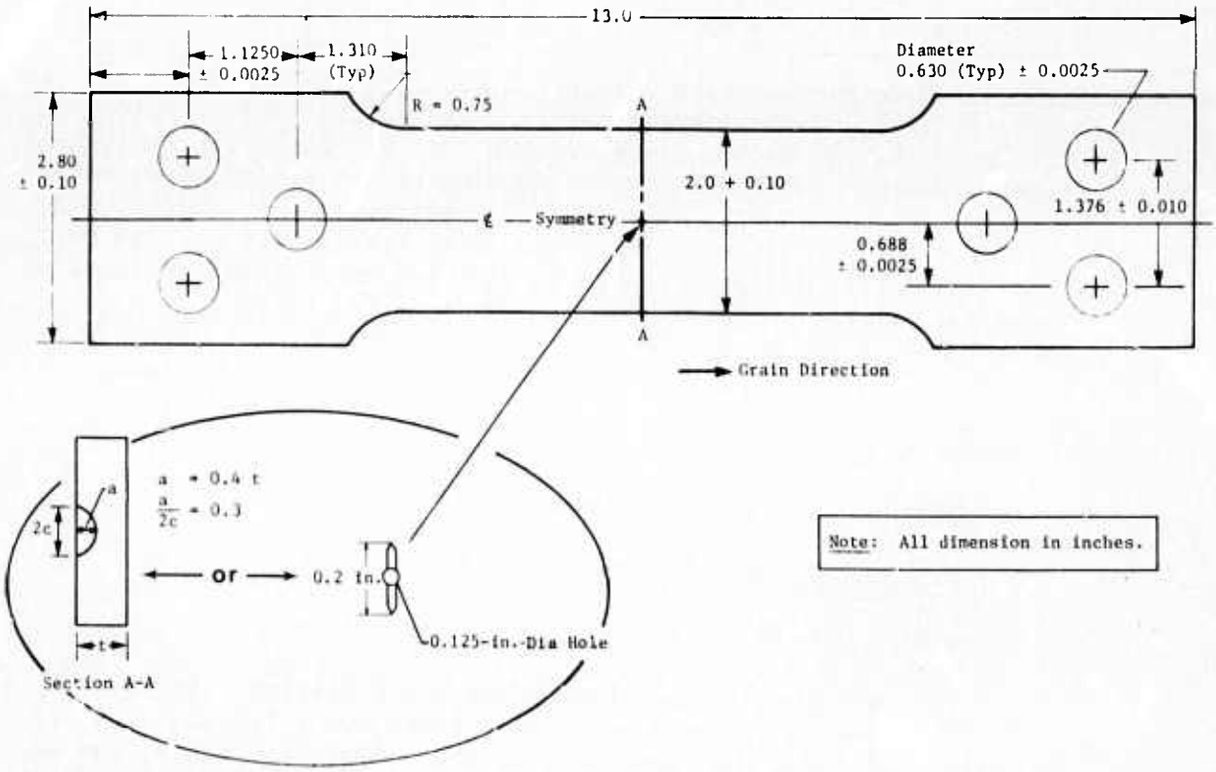

Fig. 5 Center-Cracked and Surface-Flawed Plane Stress Specimen

5/8-in. rods. These materials were heat-treated by austenitizing them at 1600°F and then oil-quenching them. They were then tempered at 800°F (YS = 180,000 psi) and 1200°F (YS = 100,000 psi).

B. SPECIMEN CONFIGURATION

Three types of test specimens were used in these investigations. For the plane stress condition, a symmetrical center-cracked plate with the configuration shown in Fig. 5 was used. This specimen was 13 in. long and 2 in. wide at the gage section. The center-notched flaw was 0.2 in. wide. The surface-flawed specimen was the same as the center-cracked specimen except that a "part-through" elliptical flaw was used (Fig. 5). The depth, a, was 0.4 of the thickness, t, and the axial ratio $\frac{a}{2c}$, was 0.3 in. These flaws were put in by the electrical discharge machining (EDM) method. Plane strain testing was done using a compact tension specimen (Fig. 6) whose dimensions conformed to the recommendations of the ASTM's committee E-24 on fracture toughness. The current recommendation is that the thickness be not less than $2.5 \left(K_{Ic}/\sigma_y\right)^2$. This stipulation dictated that for plane strain testing, the aluminum 2014-T6 was to be 1 in. thick, whereas the titanium (6Aℓ-4V) and 4130 steel specimens were to be 0.625 in. thick.

The following equations were used to calculate the stress intensity factor, K_I:

1) Compact tension specimen (from Ref 13):

$$K_I = \frac{L\sqrt{a}}{Bw} \cdot y, \qquad (1)$$

where $y = 23.12 - 67.67\left(\frac{a}{w}\right) + 97.31\left(\frac{a}{w}\right)^2$;

2) Part-through surface-cracked specimen:

$$K_I = 1.1\,\sigma\sqrt{\frac{\pi a}{Q}}; \qquad (2)$$

3) Center-notched specimen:

$$K_I = \frac{L}{Bw}\sqrt{w \tan\frac{\pi a}{w}}, \qquad (3)$$

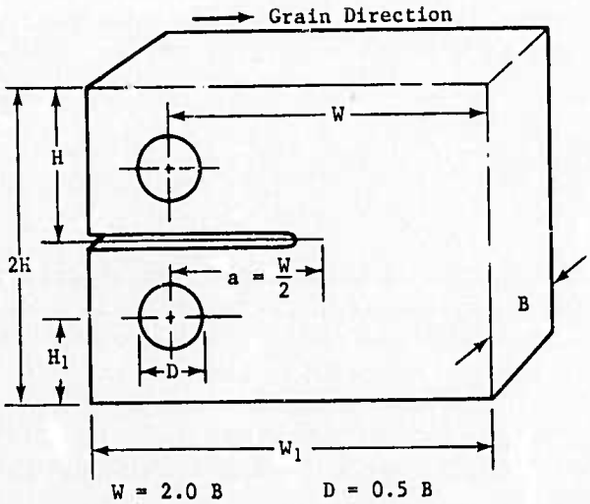

Fig. 6 Modified Compact Tension Specimen

where:

a = crack length,

B = thickness,

w = width,

L = load,

Q = flaw shape parameter.

For testing the 4130 steel pressure vessels, five part-through starter cracks were machined around the circumference by the electro-discharge method. These cracks were elliptical, with $\frac{a}{2c} = 0.33$ and a = 0.07 in.

1. Preparation of Specimens and Heat Treatment

The specimen blanks for the plane stress and plane strain tests were machined from the "as-received" sheets with the longitudinal direction parallel to the rolling direction. After being machined the specimens were subjected to a stress-relieving treatment to eliminate the residual stresses imparted by the machining operation. A 250°F 1-hr treatment was used for the aluminum specimens; the titanium (6Aℓ-4V) was annealed at 1300°F for 1 hr in vacuum ($\sim 10^{-6}$ torr). The 4130 steel was austenitized at 1650°F for 1 hour, then oil-quenched and tempered at either 800°F (for YS = 180,000 psi) or 1200°F (for YS = 100,000 psi). The decarburized layer was removed from the steel before the specimen was machined. For those specimens to be given the SLE treatment, the prestressing was done on specimen blanks before the final machining, but after the stress-relieving treatment. The notches were machined in after the prestress and after the surface layer had been removed. All specimens were chem-milled to obtain the same surface finish.

To prepare the welded specimens, strips 7 by 6 by 0.125 in. were first cut from a large sheet. The ends were machined flat and two 7-in. pieces were arc-welded to form a 14-in. length. The 4130 steel was welded manually using a Class 2, Type A weld rod with a nominal composition of: carbon, 0.28/0.33; manganese, 0.40/0.60; silicon, 0.20/0.65; chrominum, 0.80/1.30; molybdenum, 0.15/0.55; vanadium, 0.30; phosphorous, $\leq$0.025; and sulphur, $\leq$0.025. The titanium specimens were TIG-welded and the beads were then machined flush with the surface of the specimen blank. Approximately 0.01 in. was then ground from each face to obtain the desired degree of flatness and to remove decarburized or oxidized layers, and the specimens were then heat-treated. The steel was austenitized at 1600°F, oil-quenched, and tempered at 1200°F for 2 hr. The titanium blanks were annealed in vacuum for 4 hr at 1400°F, and the center-notched specimens were then machined from these blanks. The SLE specimens were prepared by stressing these specimens before the notches were machined and by chem-milling them to remove about 0.006 in. from each face. The notches were placed in the heat-affected zone and in the center of the welds.

The titanium tubing was annealed at 1400°F for 4 hr in vacuum and chem-milled to remove mill imperfections inside and outside the tubes. In an attempt to prevent the fatigue failures from occurring outside the gage section, the diameter along the central portion of the tubes was gradually reduced by abrasive-grinding the material on a lathe; the wall thickness was reduced from 0.049 to 0.035 in. at the smallest diameter. For the SLE treatment, tube lengths of about 5 ft were stressed in a tensile machine. These were then cut to the appropriate length (12 in.) and chem-milled.

The 4130 steel pressure bottles were used in the "as received" heat-treated condition. Before treating them a pressure-deformation curve was obtained by pressurizing a tank in a hydrostat. Two strain gages were attached in the hoop direction and another two in the longitudinal direction, and the tanks were stressed using water as a fluid. These tests indicated that the proportional limit occurred at 4800 psig, and the yield, at 5700 psig. The burst pressure was 7400 psig. In preparation for the SLE treatment, five tanks were pressurized to 4800 psig and then chem-milled to remove 0.008 in. from the diameter. No metal was removed from the interior of the tanks. Immediately afterwards, the tanks were baked at 350°F for 4 hr to minimize the loss of ductility associated with hydrogen embrittlement. One tank was pressurized and the surface layer was left on to determine whether it could be eliminated by relaxation. Five EDM notches were machined into the tanks after the chem-mill and hydrogen bakeout treatment.

To compare the effectiveness of the SLE and shot-peening treatments, compact tension specimens of 2014-T6 aluminum were treated by the Metal Improvement Company. The aluminum was peened with S-230 shot; the resulting Alman test indicated a value of 0.010/0.014. The shot-peening was done on both untreated and SLE-treated specimens.

2. Test Methods

The crack-propagation rates on the specimens were measured by means of an electrohydraulic testing machine. The crack growth in the plane stress specimens was measured optically. Cycling was conducted between fixed stress limits at 20 Hz; however, the system was operated at 1 Hz periodically to measure the crack length. Measurements were taken about every 5000 cycles. The crack growth in the compact tension specimen was measured by the crack opening displacement (COD) method. For this purpose, a COD gage was placed on V-shaped holders fixed to the faces of the specimen. The output of the COD gages was recorded on a strip chart recorder at 1-hr intervals during the propagation phase. The tests were conducted at 20 Hz until the fatigue crack was formed; afterwards, the cycling was at a rate of 1 Hz. To calibrate the crack length in terms of COD, cracks of known lengths were milled into the specimens and the COD/load ratio was measured in terms of the crack length.

The fatigue life of the titanium tubing was measured in reverse bending using a four-point fixture. The distance between the loading points was 4 in. and that between the support points was 8 in. The overall length of the specimen was 12 in. The tests were conducted on an electrohydraulic testing machine at 6 Hz. Because of the strong

propensity of titanium to cause fretting corrosion when in contact with other metals, linen-phenolic rods were used as roller bearings to impart the forces to the specimen.

To detect the presence of a crack, the tube was filled with distilled water and pressurized using a toy balloon. A 2x4-in. wire mesh grid, placed 0.01 in. above an aluminum foil, was placed directly under the fatigue specimen. Fine poweder of NaCl was sprinkled on the aluminum foil. When the tube developed a crack and a drop of water came in contact with this detection assembly, an electrical circuit was energized and the fatigue machine was shut off. Preliminary experiments showed that a small drop of water from a hypodermic needle was sufficient for detection.

The 4130 pressure bottles were tested in a hydrostat using water as a fluid. The cycling was conducted at about 4 Hz between the pressure limits. The pressure limits were controlled by fixed valves that changed the fluid flow direction as a function of the preset pressures. The cycle-pressure profile was recorded on strip chart recorders. A through crack was detected by means of a conductivity cell that sensed the change in electrical resistance when water leaked through the EDM flaw.

III. RESULTS AND DISCUSSION

A. 4130 STEEL

The crack propagation behavior of 4130 steel (YS = 100,000 psi) under plane stress is presented in Fig. 7 and 8. The data in Figure 7 show the increase in the crack length as a function of the number of cycles needed to propagate the crack, N_p. Compared to the untreated material, when the prestress for the SLE treatment was 60,000 psi the crack growth was very slow. However, when the prestress was increased to 80,000 psi to induce a small amount of plastic strain, the crack propagation resistance decreased.

Figure 7 also includes the results obtained when the specimens were prestressed to 100,000 psi in liquid nitrogen. These low-temperature stress experiments were conducted to ascertain whether the cryoformed condition would further enhance the improvement. It is apparent that prestressing at the low temperature did not give as much improvement as prestressing to 60,000 psi at room temperature.

Figure 8 shows the crack propagation rage, da/dN, as a function of the change in the stress intensity factor, ΔK. Note that at the lower ΔK values, the crack velocity of the SLE-treated specimens is about 4 times lower than that of the untreated specimens. This improvement tends to decrease as the stress in front of the crack approaches that of the prestress. At about 13,000 psi $\sqrt{in.}$, the curves merge.

The data for the crack propagation rate under plane strain conditions for the 4130 steel heat-treated to a yield strength of 180,000 psi are presented in Fig. 9. This figure also includes points obtained from duplicate specimens. Note that the reproducibility is excellent.

Again, these curves show that the SLE treatment improves crack propagation resistance. At a ΔK of about 16,000 psi $\sqrt{in.}$, the SLE-treated specimens have a crack velocity 4 times smaller than that of the untreated specimens. As ΔK increase, the degree of improvement decreases; and at values in excess of 18,000 psi $\sqrt{in.}$, the improvement is 40%. This degree of improvement remains constant at least to a ΔK of 22,000 psi $\sqrt{in.}$

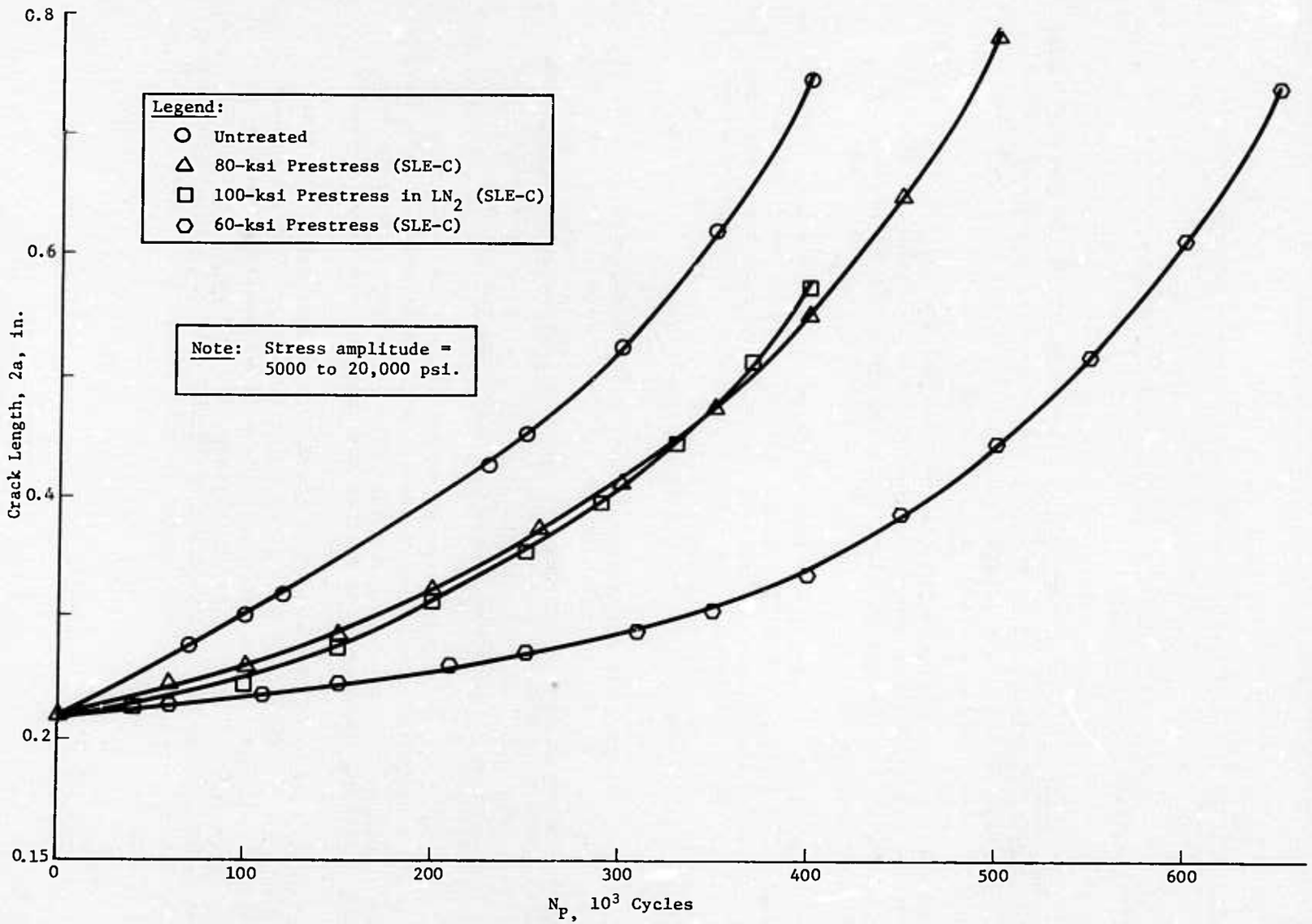

Fig. 7 Crack Growth in 4130 Steel Center-Notched Specimens 0.06 in. Thick, YS = 100 ksi

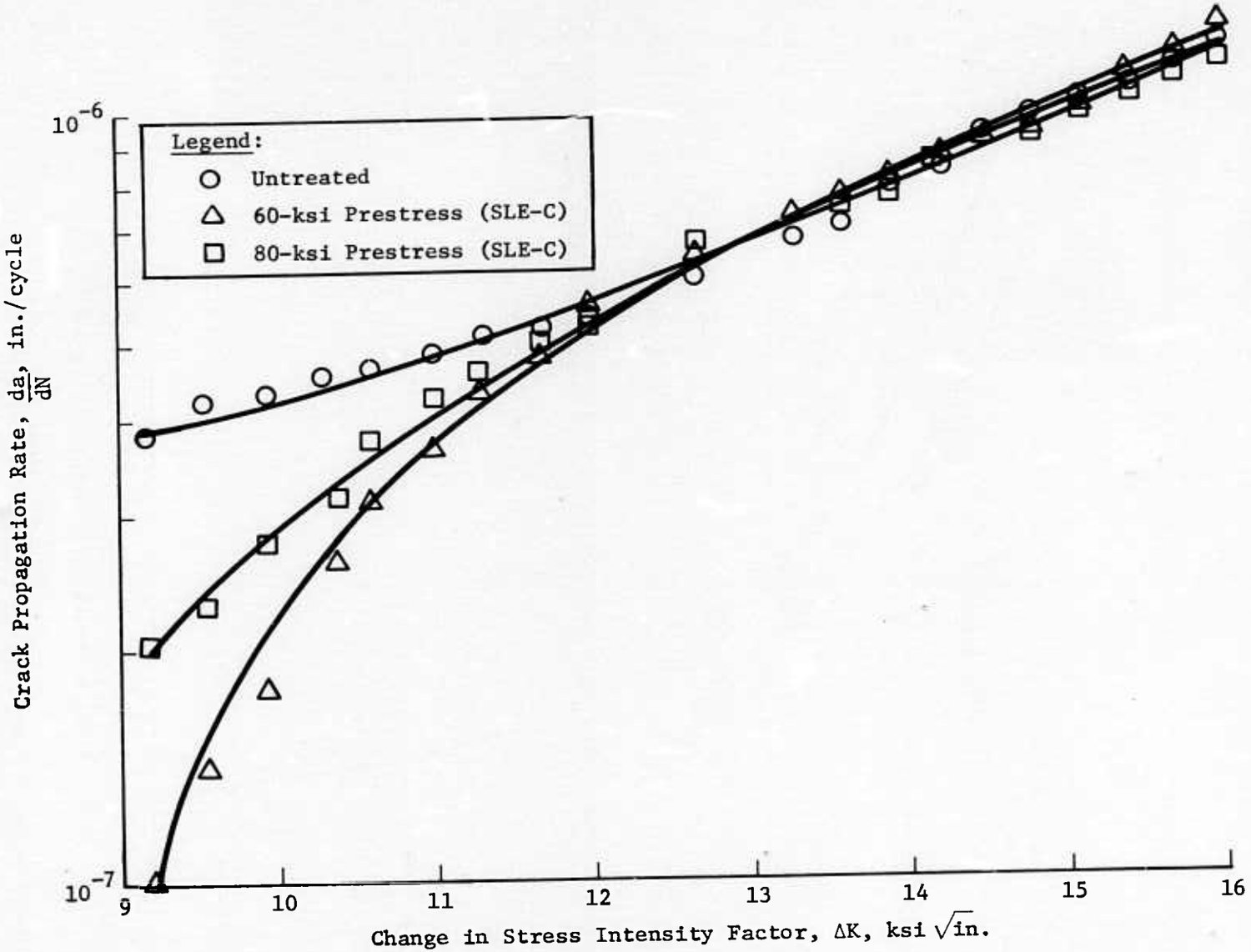

Fig. 8 Crack Propagation Rate in 4130 Steel under Plane Stress Conditions, YS = 100 ksi

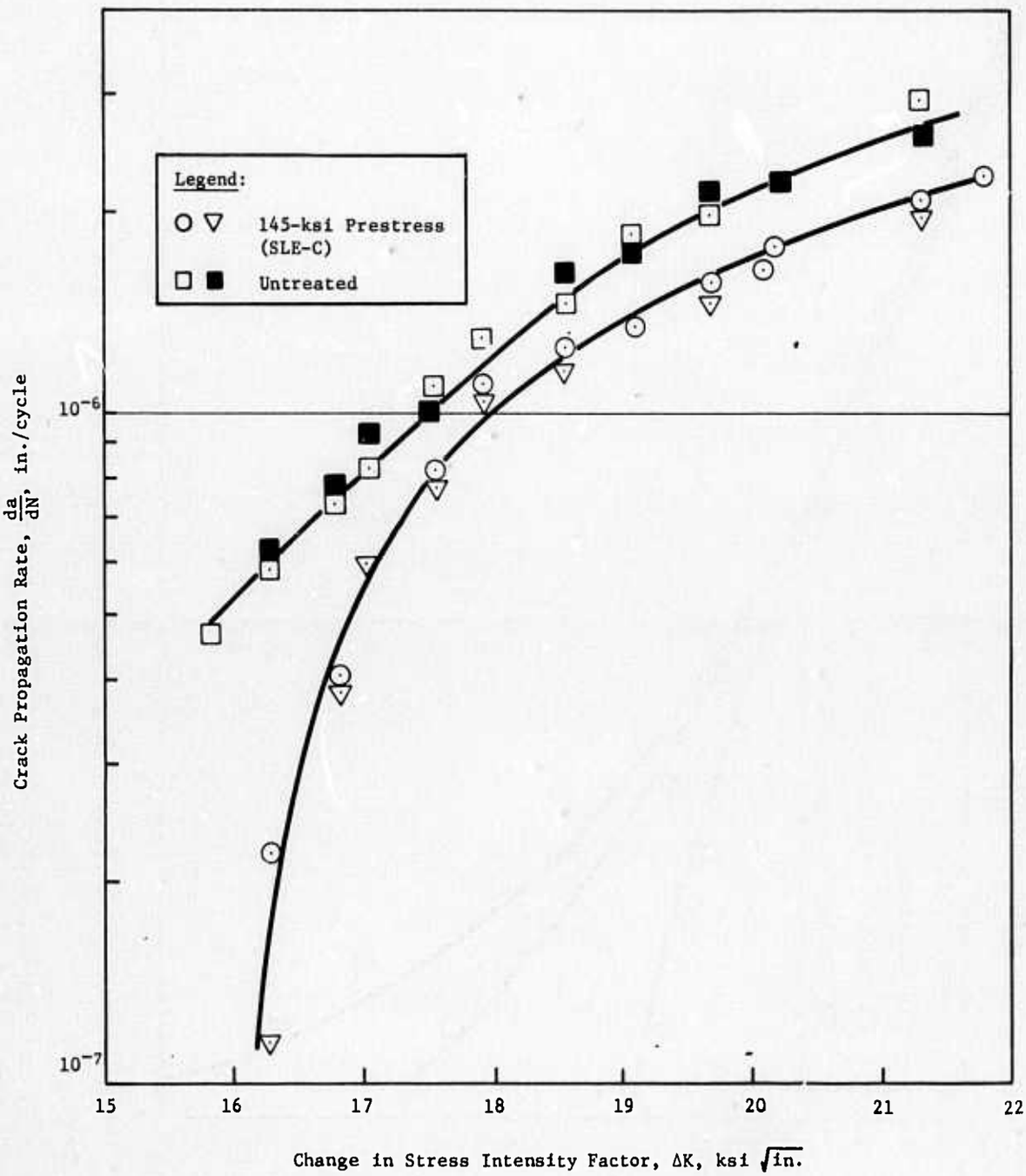

Fig. 9 Crack Propagation Behavior of 4130 Steel Compact-Tension Specimens 0.625 in. Thick under Plane Strain Conditions, YS = 180 ksi

B. 2014-T6 ALUMINUM

The crack propagation behavior of 2014-T6 aluminum under plane stress conditions is presented in Fig. 10 and 11. Figure 10 shows the crack growth as a function of the number of cycles required to propagate the crack growth as a function of the number of cycles required to propagate the crack, N_p, when the stress was varied between 2250 and 9000 psi (R = 0.25). Also included are data that show the influence of the prestress used in the SLE treatment. It is apparent that prestressing the specimen at 55,000 psi before removing the surface layer resulted in more improvement than prestressing to 45,000 psi. When the prestressing was done at the temperature of liquid nitrogen, the amount of improvement was rather small.

The degree of improvement in terms of the crack propagation rate is given in Fig. 11. For the SLE-treated specimens stressed to 55,000 psi, the crack propagation rate is decreased by about a factor of 4 at ΔK values near 4000 psi $\sqrt{in.}$ This improvement decreases as ΔK increases, and at ΔK near 6000 psi $\sqrt{in.}$, the crack velocity of the SLE-treated specimens is about 40% of that of the untreated specimen.

The change in crack length when plane strain specimens were cycled between 300 and 1200 lb is shown in Fig. 12. Again, it is apparent that the SLE treatment improves the crack propagation resistance. As seen from Fig. 13, the crack propagation rage at ΔK values of 6000 psi $\sqrt{in.}$ has been decreased by about a factor of 2.

C. TITANIUM (6Al-4V)

The crack propagation rate of titanium (6Al-4V) plane stress specimens is shown in Fig. 14. Again, the SLE treatment improved the crack resistance. At the lower values of ΔK--for example at 8000 psi $\sqrt{in.}$--the resistance improved by a factor of about 6. The arrow shown in Fig. 14 indicates that propagating crack did not form at the stress amplitude used in this test (4500 to 18,000 psi). The ΔK value was calculated on the basis of the loads and machined notch depth, whereas the actual ΔK value should be based on a sharp crack. However, the data serve merely as a rough basis of comparison.

For the untreated specimens tested under this stress amplitude, the crack formed in about 175,000 cycles and the specimen was completely broken in approximately 300,000 cycles. In comparison, the SLE-treated specimen was cycled 6,300,000 times and the test was terminated since no propagating crack was formed.

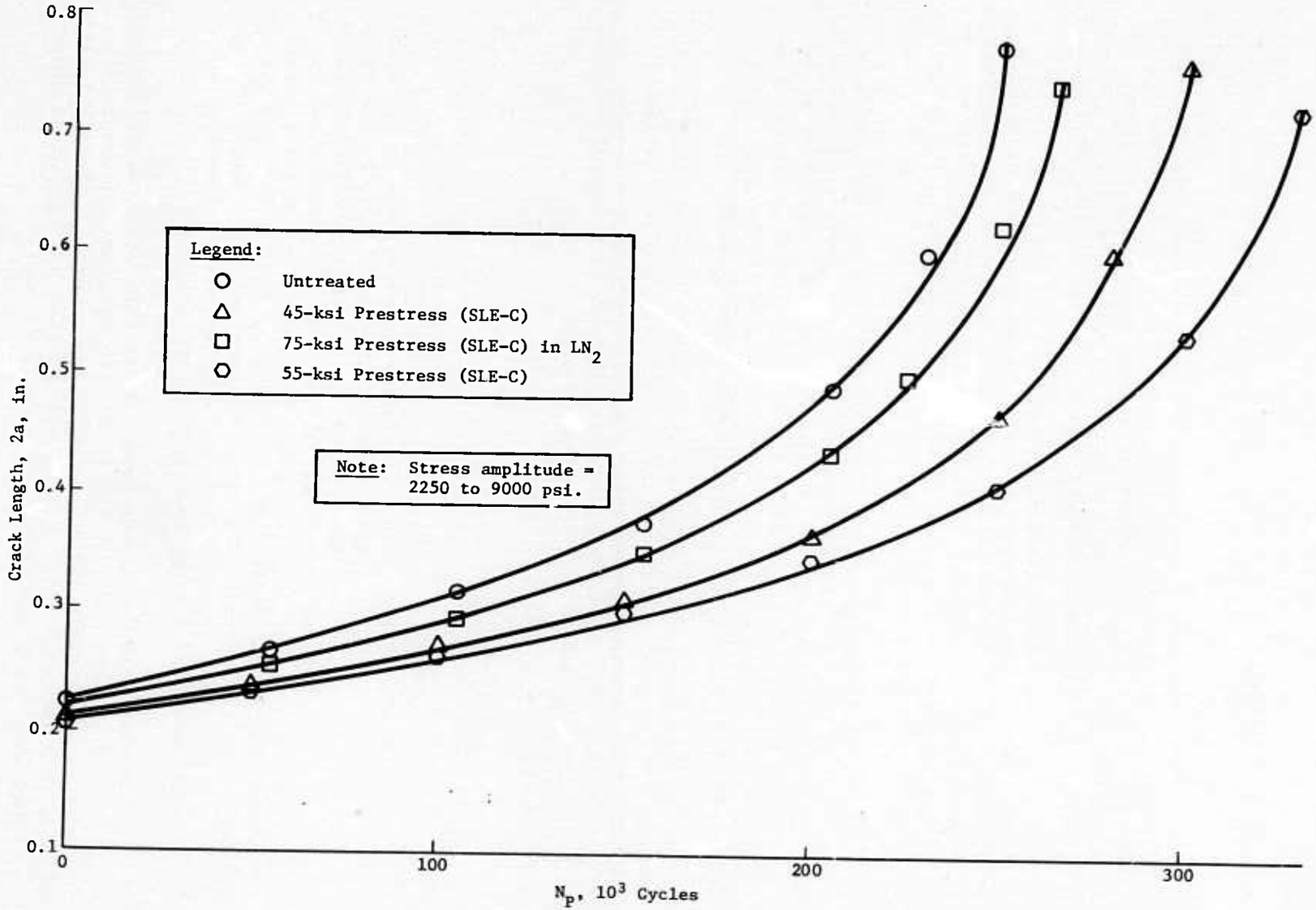

Fig. 10 Crack Growth in 2014-T6 Aluminum Center-Notched Specimens 0.125 in. Thick

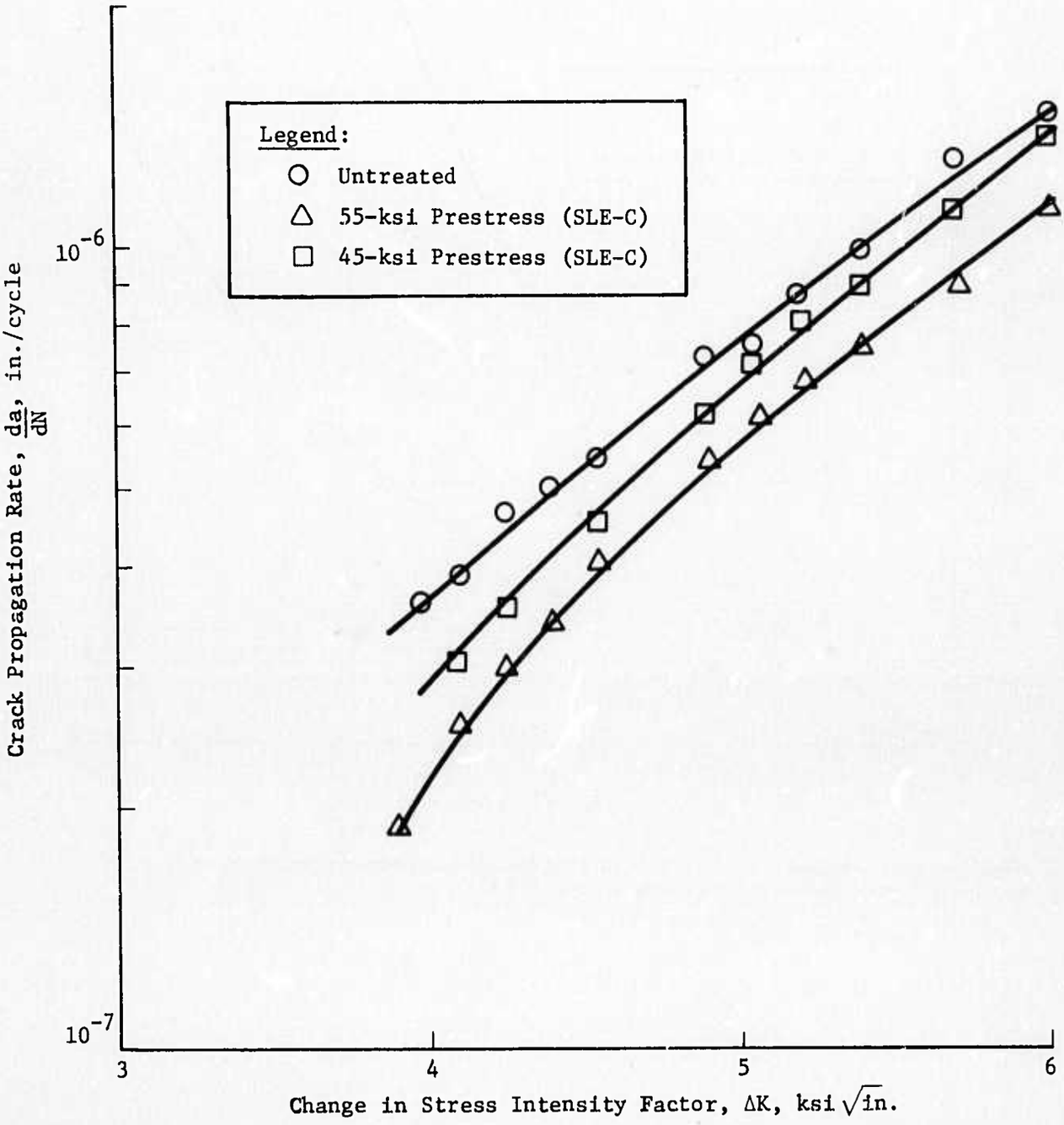

Fig. 11 Crack Propagation Rates of 2014-T6 Aluminum under Plane Stress Conditions, Center-Notched Specimens 0.125 in. Thick

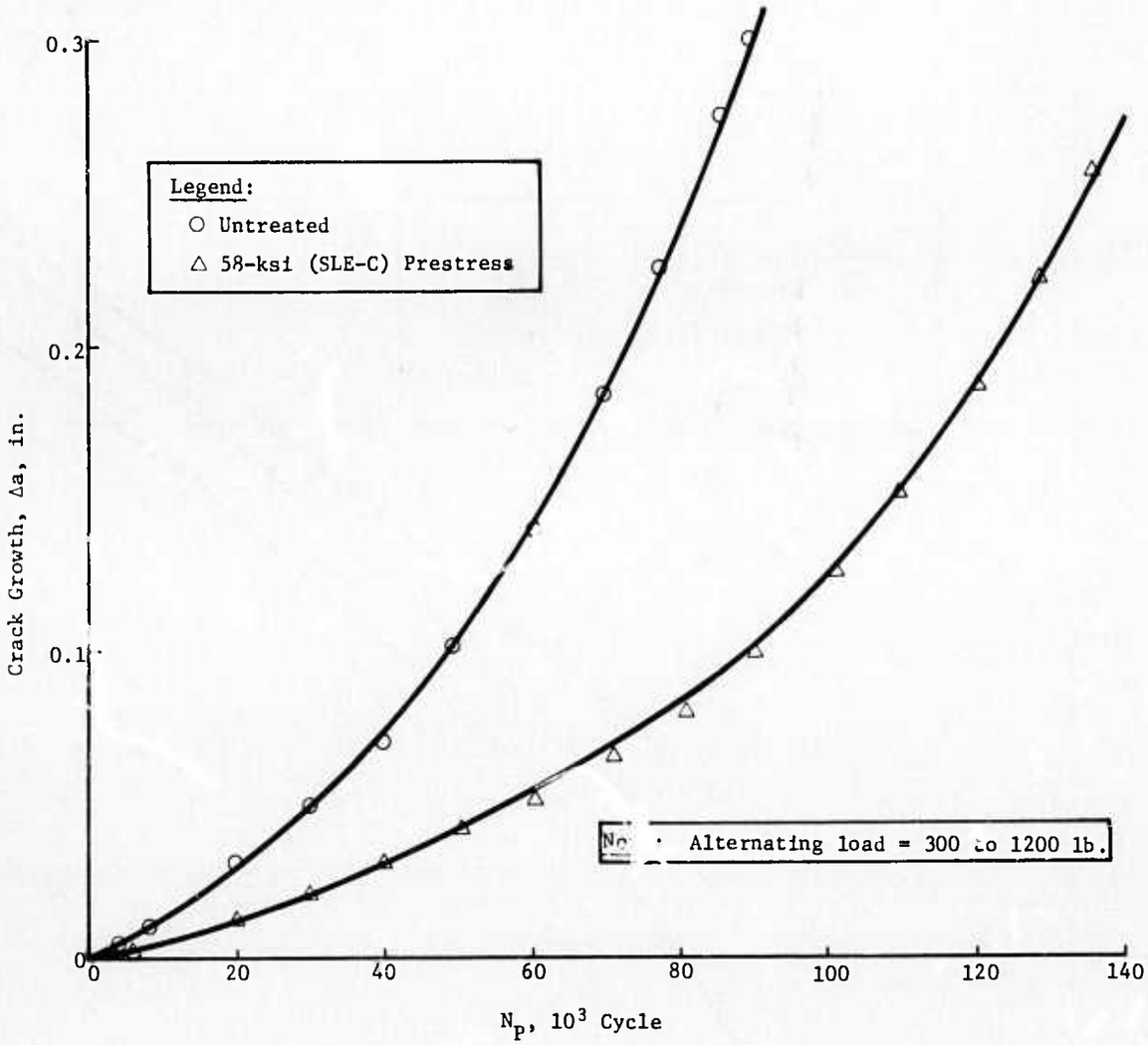

Fig. 12 Crack Growth of 2014-T6 Aluminum Compact-Tension Specimens under Plane Strain Conditions, Frequency = 1 Hz, R = 0.25

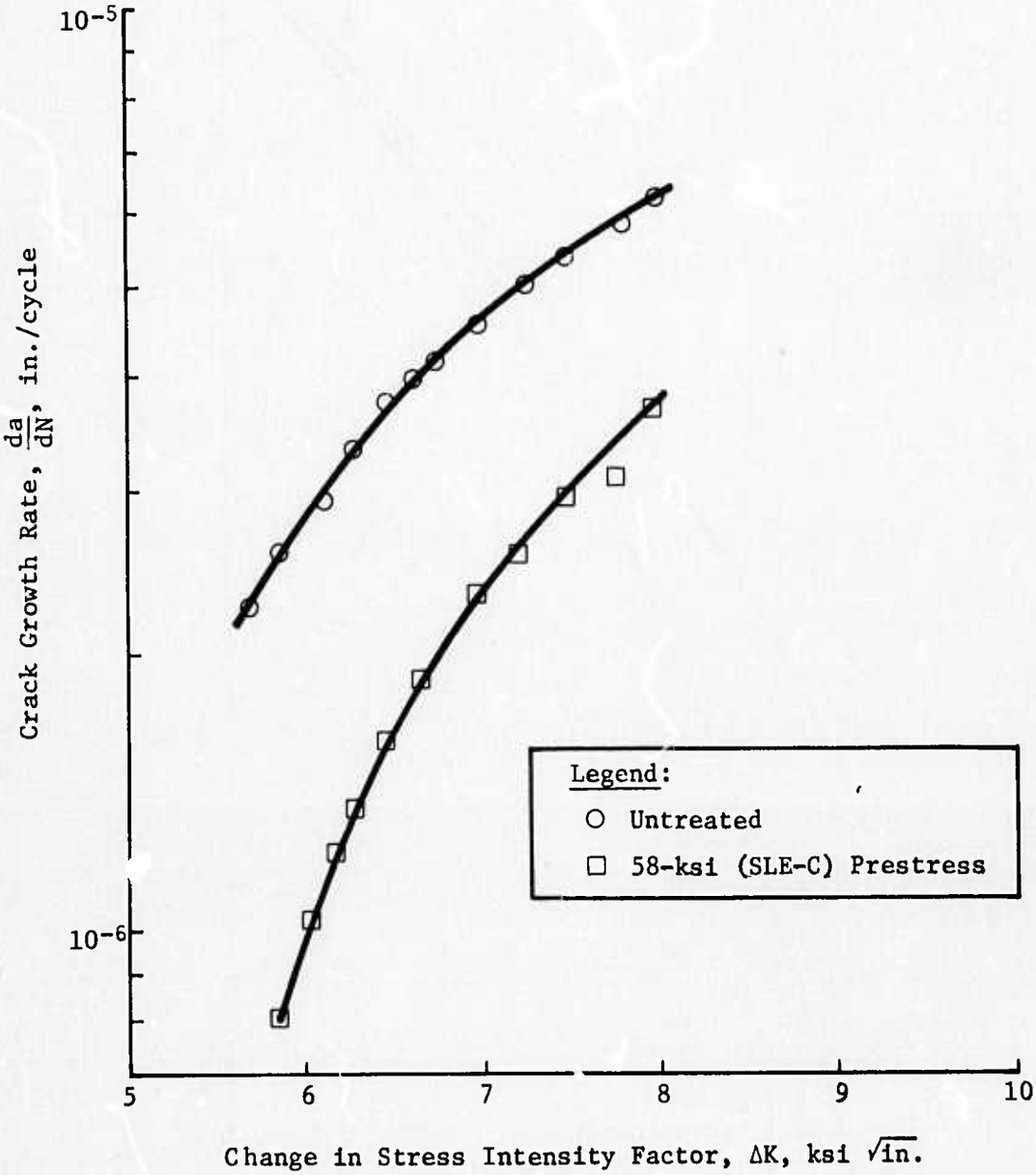

Fig. 13 Crack Propagation Rate of 2014-T6 Aluminum Compact-Tension Specimens, Frequency = 1 Hz, R = 0.25

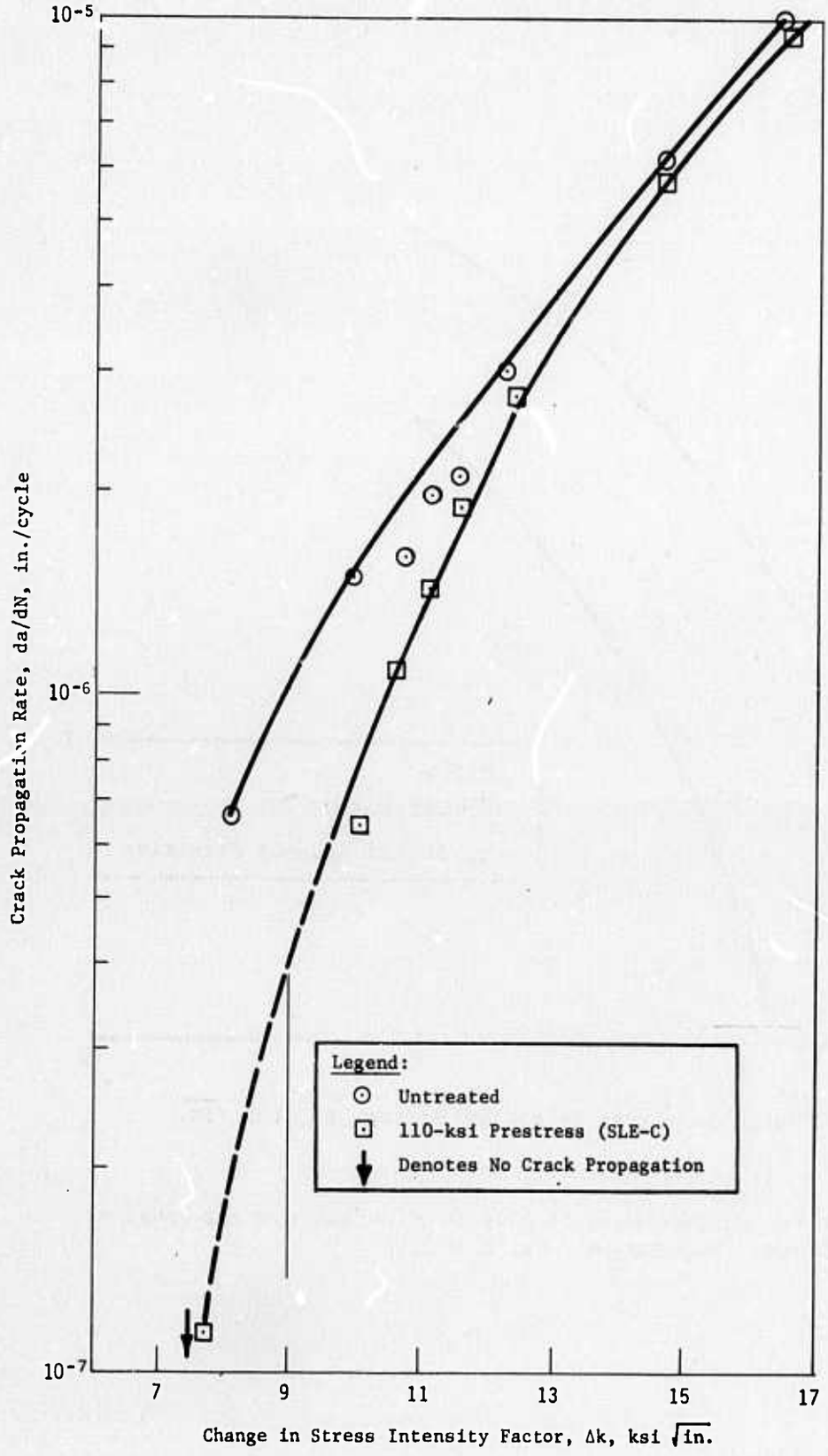

Fig. 14 Crack Propagation Behavior of Titanium 6Al-4V under Plane Stress Conditions, Center-Cracked Specimens 0.067 in. Thick.

D. WELDED 4130 STEEL

The effect of the SLE treatment on weldments of 4130 steel (YS = 100,000 psi) is shown in Fig. 15 thru 19. Figure 15 shows the increase in the crack resistance in the center of the weld for center-notched specimens (under plane stress) as a result of the SLE treatment at various prestress values. Like the specimens that were not welded, prestressing at a high value did not impart as much improvement in crack resistance as did prestressing at lower values.

As shown in Fig. 15, a large decrease in the crack growth was obtained when the prestress for the SLE treatment was 70,000 psi. Increasing this prestress to 80,000 psi greatly decreased the effectiveness of the SLE treatment.

Not shown in Fig. 15 is the crack growth behavior of specimens that were prestressed to 50,000 and 60,000 psi. For these specimens, practically no improvement was noted for the 50,000 psi prestress, and a slight improvement was found when the 60,000-psi prestress was used. The rates are shown in Fig. 16. The effect of prestressing to 150,000 psi in liquid nitrogen for the SLE treatment is also shown. Although an improvement was attained, it was less than that obtained by prestressing to 70,000 psi at room temperature.

The rates of crack growth in the center of the welds in 4130 steel as a function of ΔK are given in Fig. 16. Like the other data obtained for the 4130 steel, the SLE treatment decreased the crack propagation rate. For specimen prestressed to 70,000 psi before removing the surface layer, the crack velocity decreased by a factor of about 3 at a ΔK of about 9000 psi $\sqrt{\text{in.}}$ The curves tend to merge as ΔK increases, and at about 15,000 psi $\sqrt{\text{in.}}$ they coincide.

Figure 17 shows the effect of prestressing welded specimens of 4130 steel at liquid-nitrogen temperature in terms of the improvement in crack propagation resistance. For comparison, the crack velocity for the untreated and the 70,000-psi prestress, SLE-treated specimen is also shown. It is apparent that although prestressing at the temperature of liquid nitrogen did increase the crack propagation resistance, the process is not as effective or convenient to use as the 70,000-psi prestress combined with the SLE treatment.

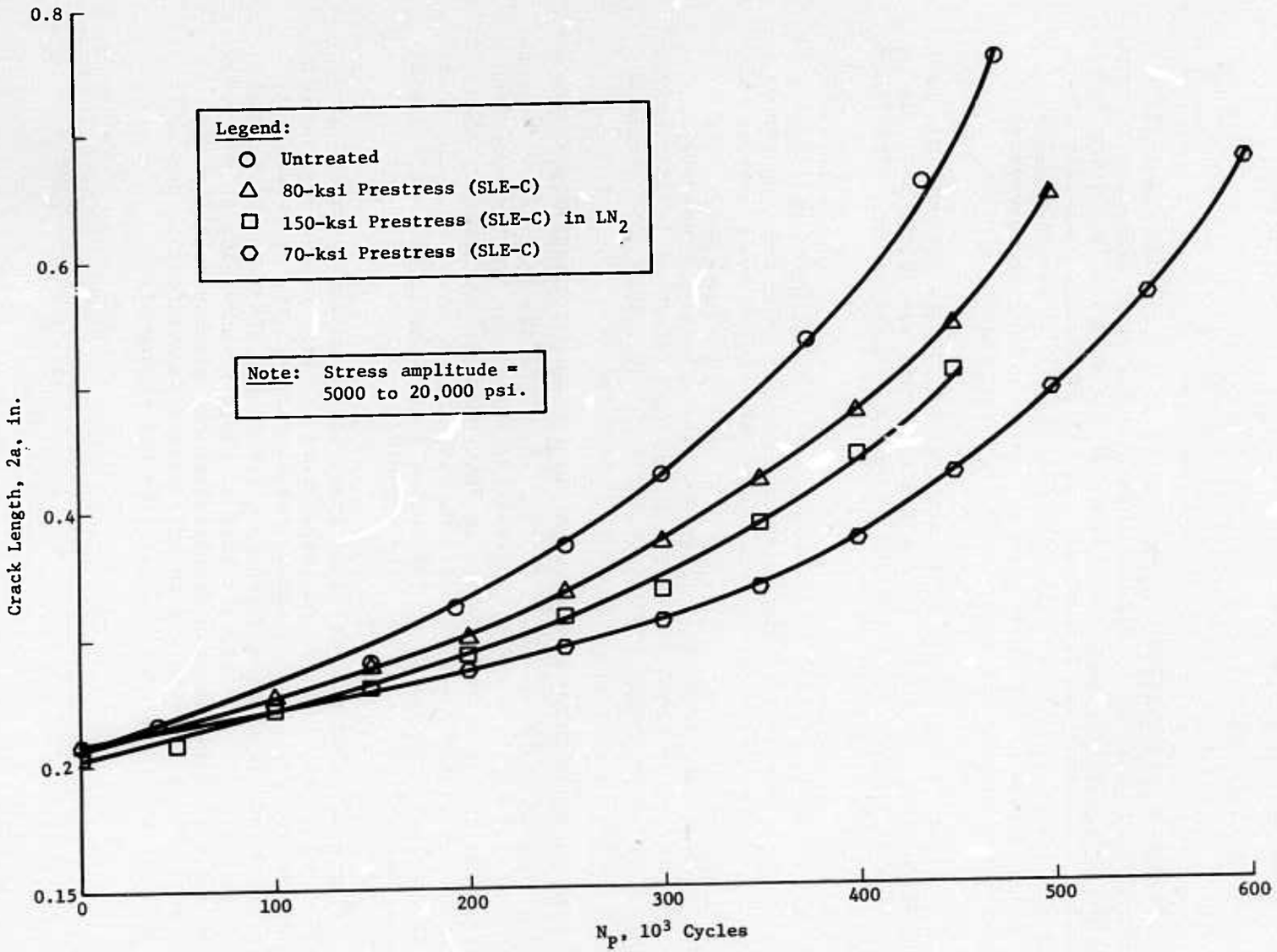

Fig. 15 Crack Growth in Center of Weld of 4130 Steel Center-Notched Specimens 0.06 in. Thick, YS = 100 ksi

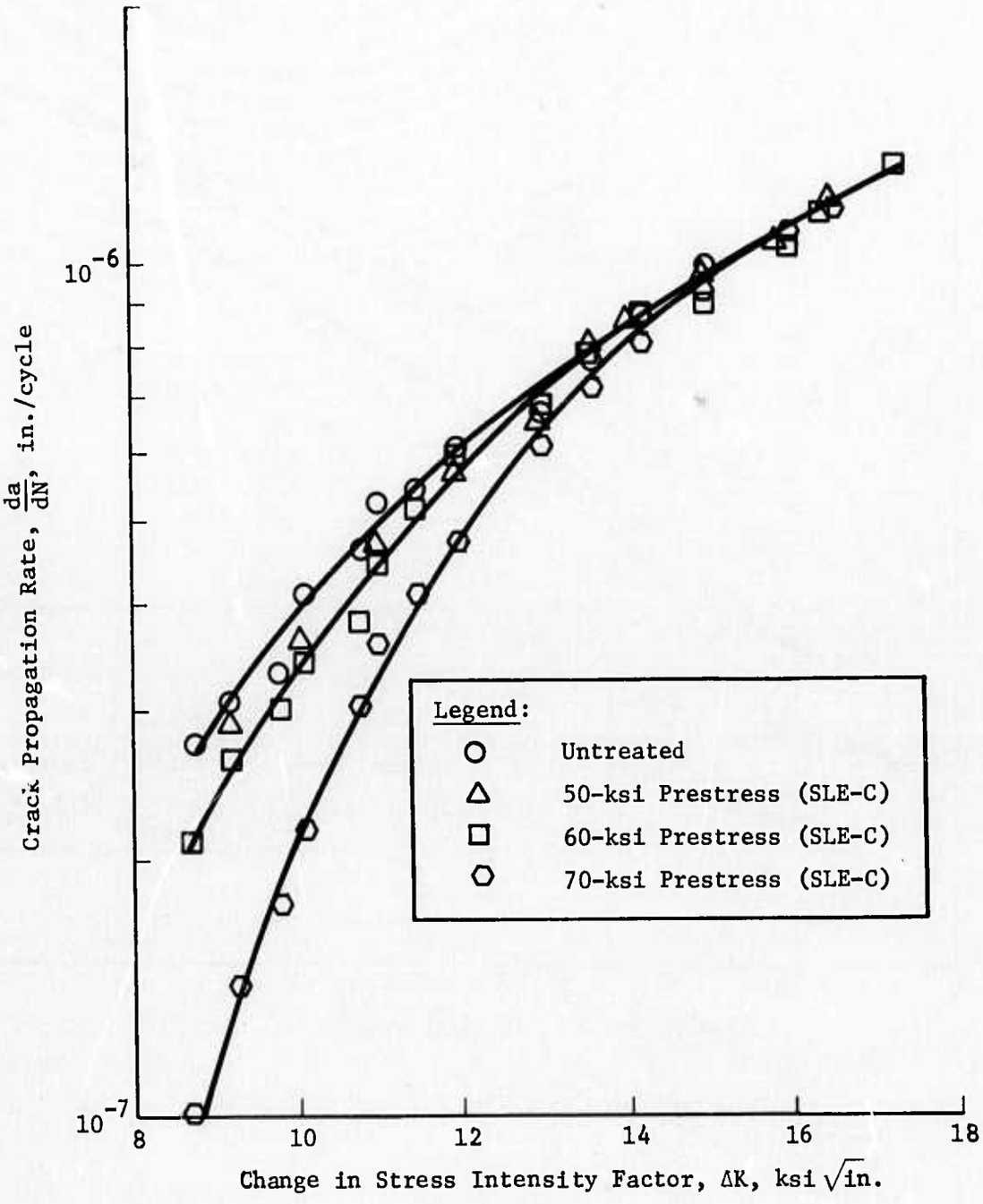

Fig. 16 Crack Propagation Rate in Center of Weld of 4130 Steel Center-Notched Specimens 0.06 in. Thick, YS = 100 ksi

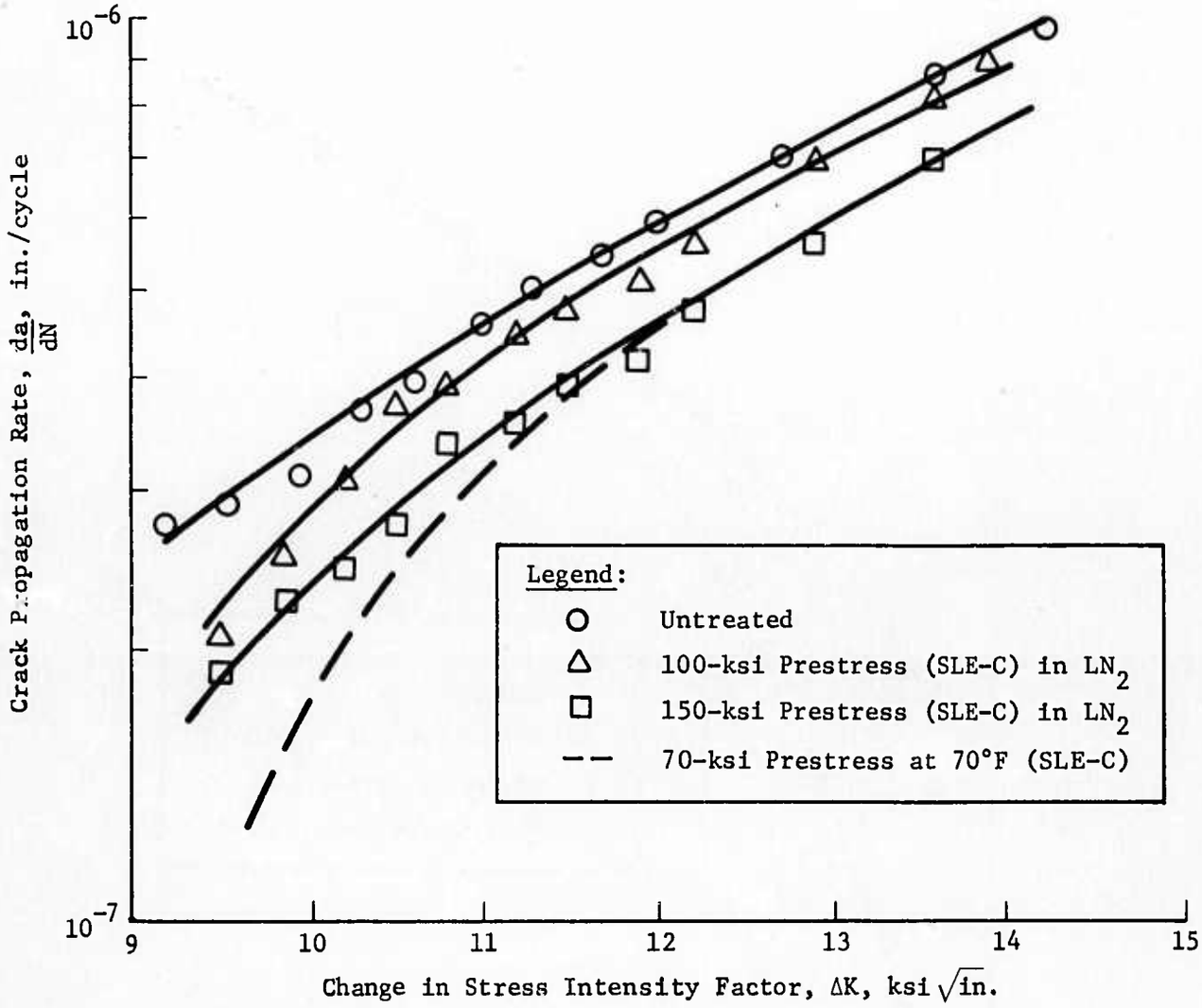

Fig. 17 Crack Propagation Rate in Center of Weld of 4130 Steel, SLE Treatment in LN_2, YS = 100 ksi

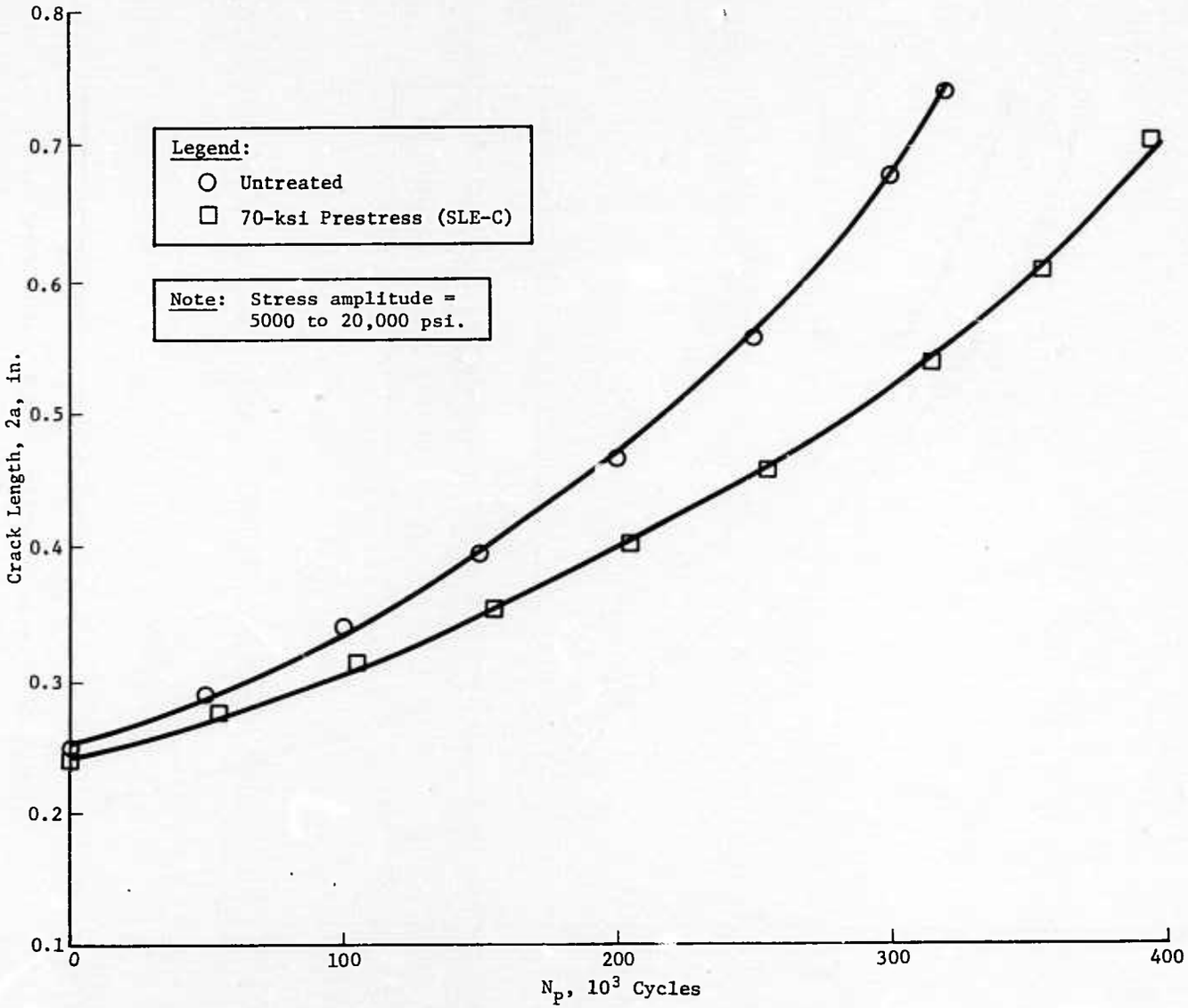

Fig. 18 Crack Growth in Heat-Affected Zone of 4130 Steel Center-Notched Specimens 0.06 in. Thick, YS = 100 ksi

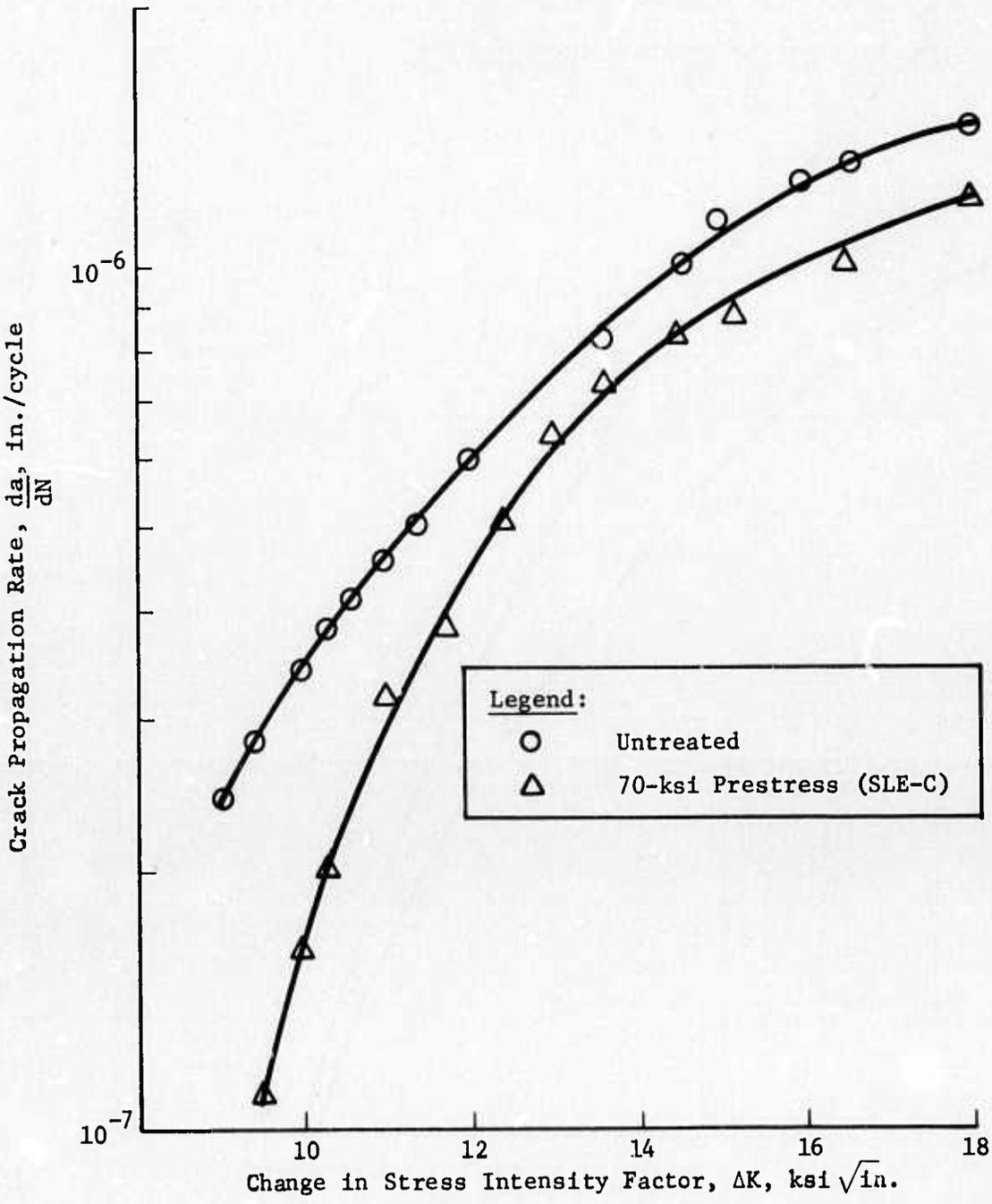

Fig. 19 Crack Propagation Rate in Heat-Affected Zone of 4130 Steel Center-Notched Specimens 0.06 in. Thick, YS = 100 ksi

Figures 15 and 16 show that prestressing the SLE-treated specimens to 50,000, 60,000 and 80,000 psi was not as effective in increasing the crack-propagation resistance as prestressing them to 70,000 psi. Therefore, the effectiveness of the SLE treatment on the crack propagation resistance in the heat-affected zone was determined at a prestress of 70,000 psi. For these measurements, the heat-affected zone was located by polishing the etching the weldment. The center-notched flaw was then placed in the midpoint of the heat-affected zone.

The crack growth in the heat-affected zone under a cyclic stress amplitude between 5000 and 20,000 psi is given in Fig. 18. The crack propagation rates are presented in Fig. 19 as a function of ΔK. These data show that, in addition to improving the crack propagation resistance within the weld, the resistance in the heat-affected zone was also increased. A comparison of the crack propagation rates in the heat-affected zone and in the weld at a ΔK value of 9,000 psi $\sqrt{\text{in.}}$, indicates the amount of improvement imparted by the SLE treatment was the same: the crack velocity was decreased by a factor of about 3.

E. WELDED TITANIUM (6Aℓ-4V)

The effect of the SLE treatment on weldment of the titanium (6Aℓ-4V) alloy is shown in Fig. 20 and 21. For this portion of the investigation, specimens were prestressed to 90,000, 105,000, and 115,000 psi for the SLE treatment. As seen in Fig. 20, prestressing to 105,000 and 115,000 psi had practically no effect on crack growth behavior. However, when the specimens were prestressed to 90,000 psi, the number of cycles required to initiate crack propagation increased from about 60,000 to 500,000 cycles, a factor of 8. The rate of crack propagation for the untreated and SLE-treated specimens was about the same (Fig. 21).

To determine the cause for the lack of improvement in the crack propagation rate, the weldments were examined metallurgically. As commonly found in titanium welds, it was noted that the grain size was very large. Figure 22, taken from the fractured faces of the specimen, shows that the crack followed an intercrystalline path. This behavior was found for both the untreated and SLE-treated specimens. We suspect that the large improvement in crack initiation imparted by the SLE treatment occurs because, initially, a transcrystalline crack starts in the large grain next to the flaw. However, shortly thereafter, the crack proceeds along the grain boundaries.

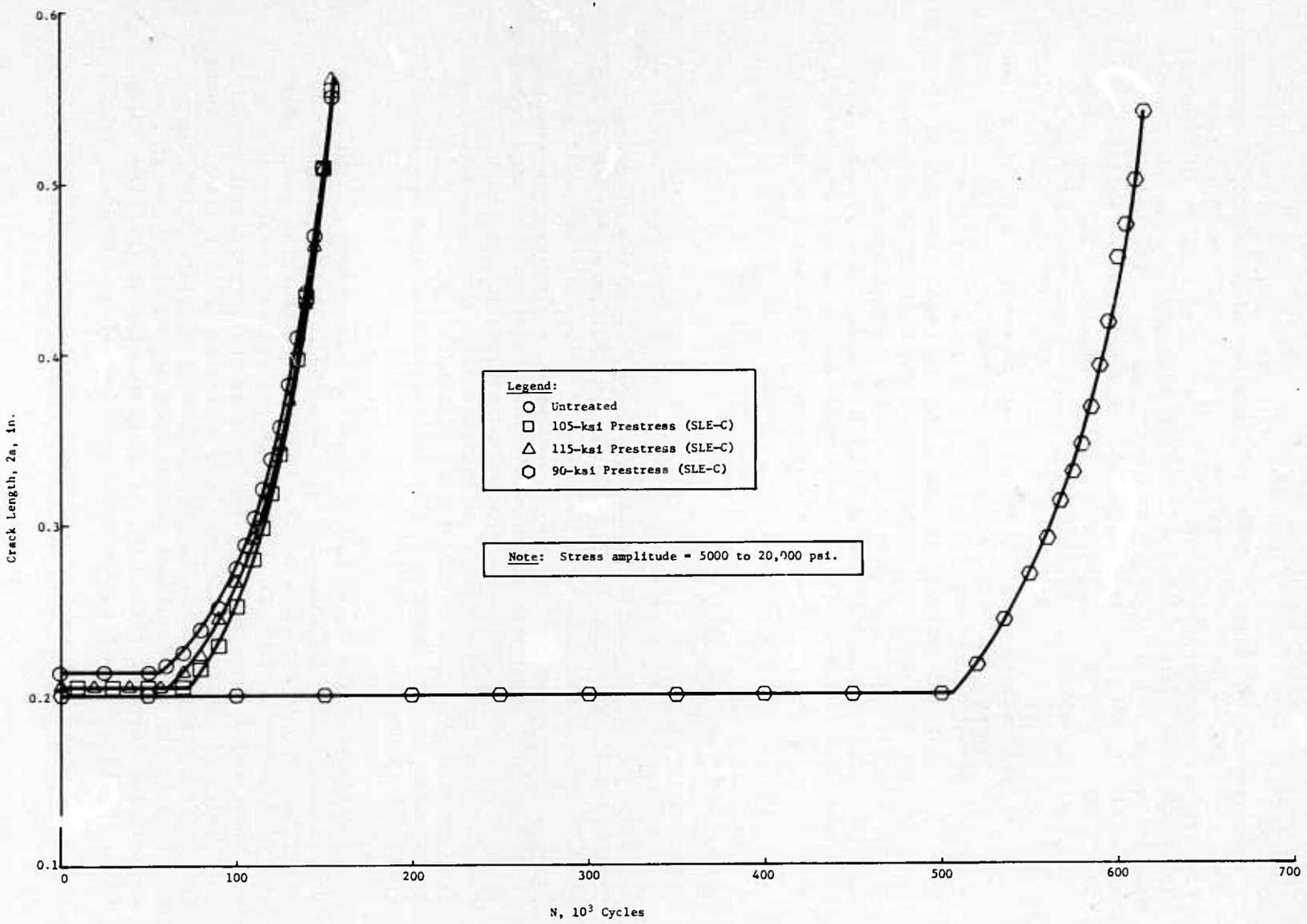

Fig. 20 Crack Growth in Center of Weld of Annealed Titanium 6Al-4V Center-Notched Specimen 0.125 in. Thick

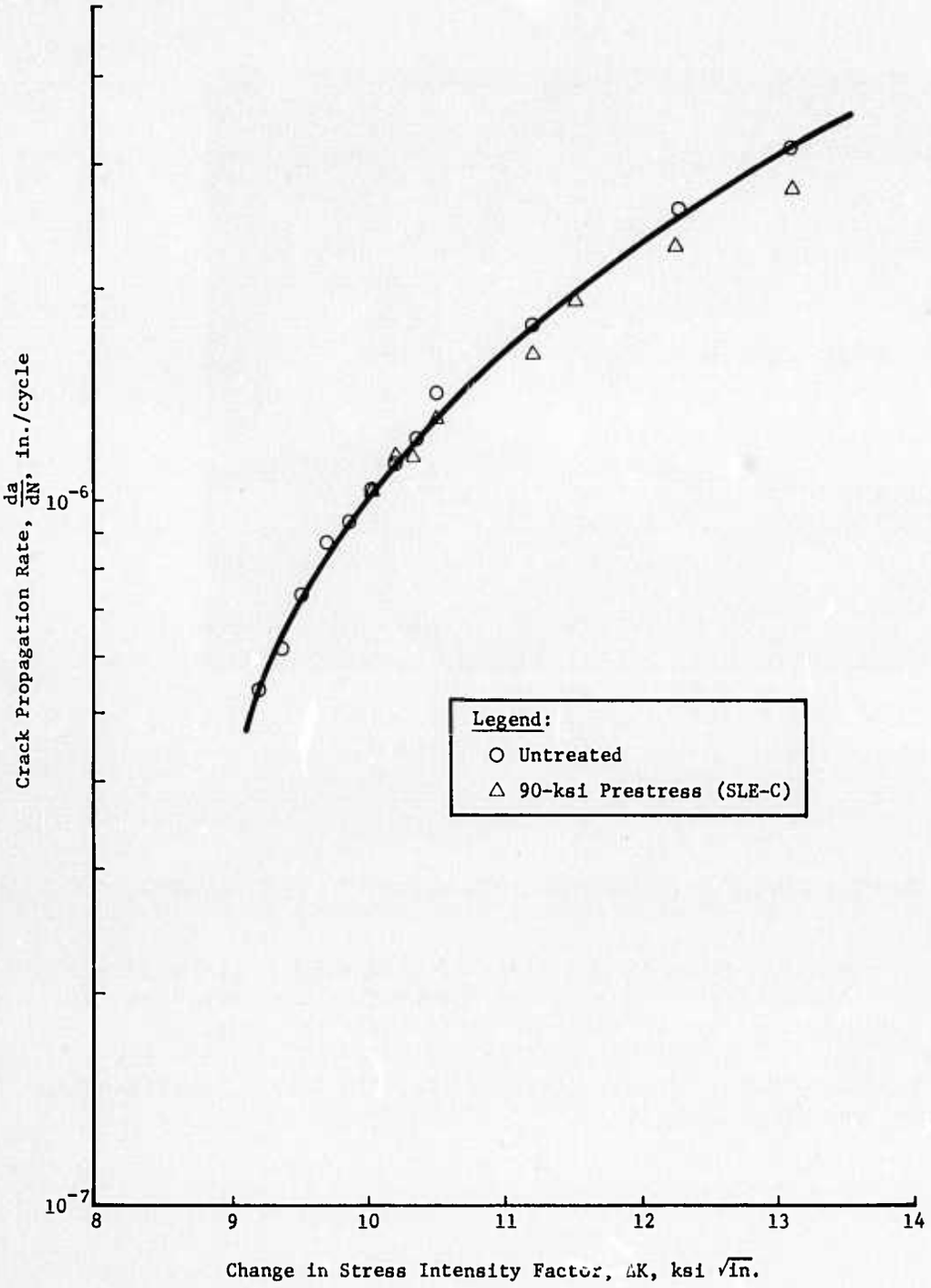

Fig. 21 Crack Propagation Rate in Center of Weld of Annealed Titanium 6Al-4V Center-Notched Specimens 0.06 in. Thick

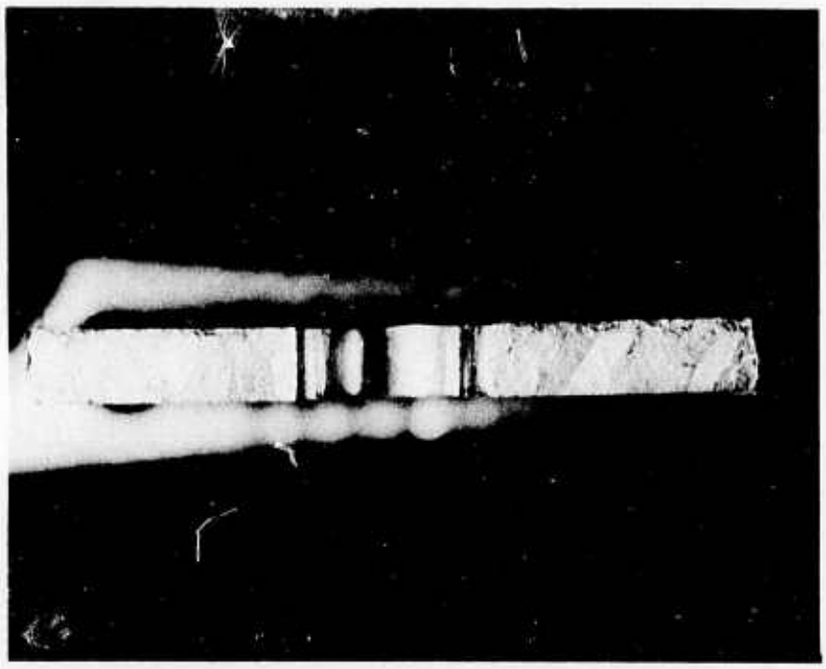

Fig. 22 Fractured Surface through Center of Weld of Titanium 6Al-4V Specimen (Magnified 3X)

A similar effect was found in the heat-affected zone of the welded titanium alloy. When the prestress in the SLE-treated specimens was 90,000 psi, the number of cycles required to initiate the crack increased from 50,000 to 175,000, a factor of 3.5 (Fig. 23). The crack propagation rates, however, for the untreated and SLE-treated specimens were about the same (Fig. 24).

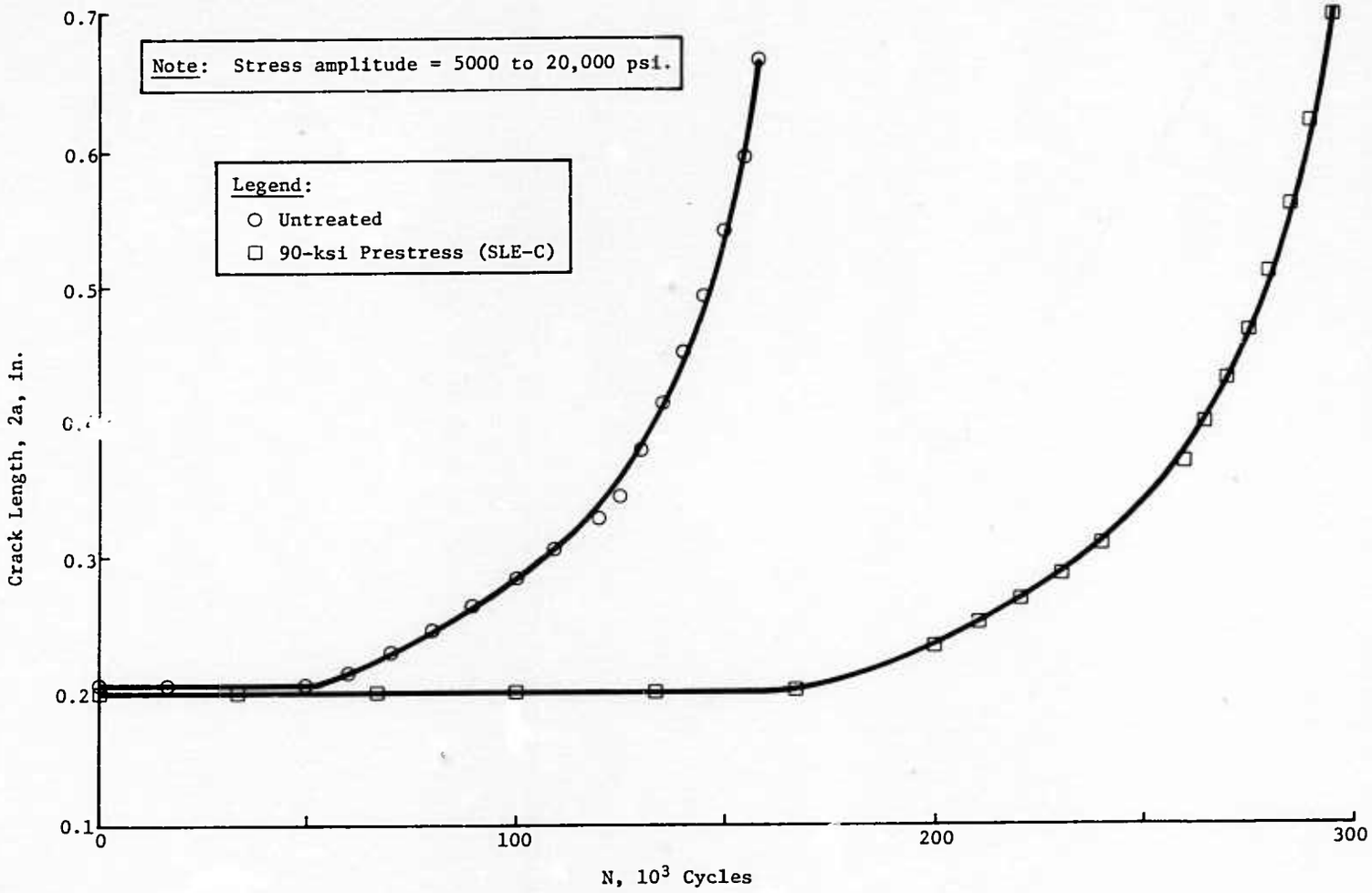

Fig. 23 Crack Growth in Heat-Affected Zone of Annealed Titanium 6Al-4V Center-Notched Specimens 0.06 in. Thick

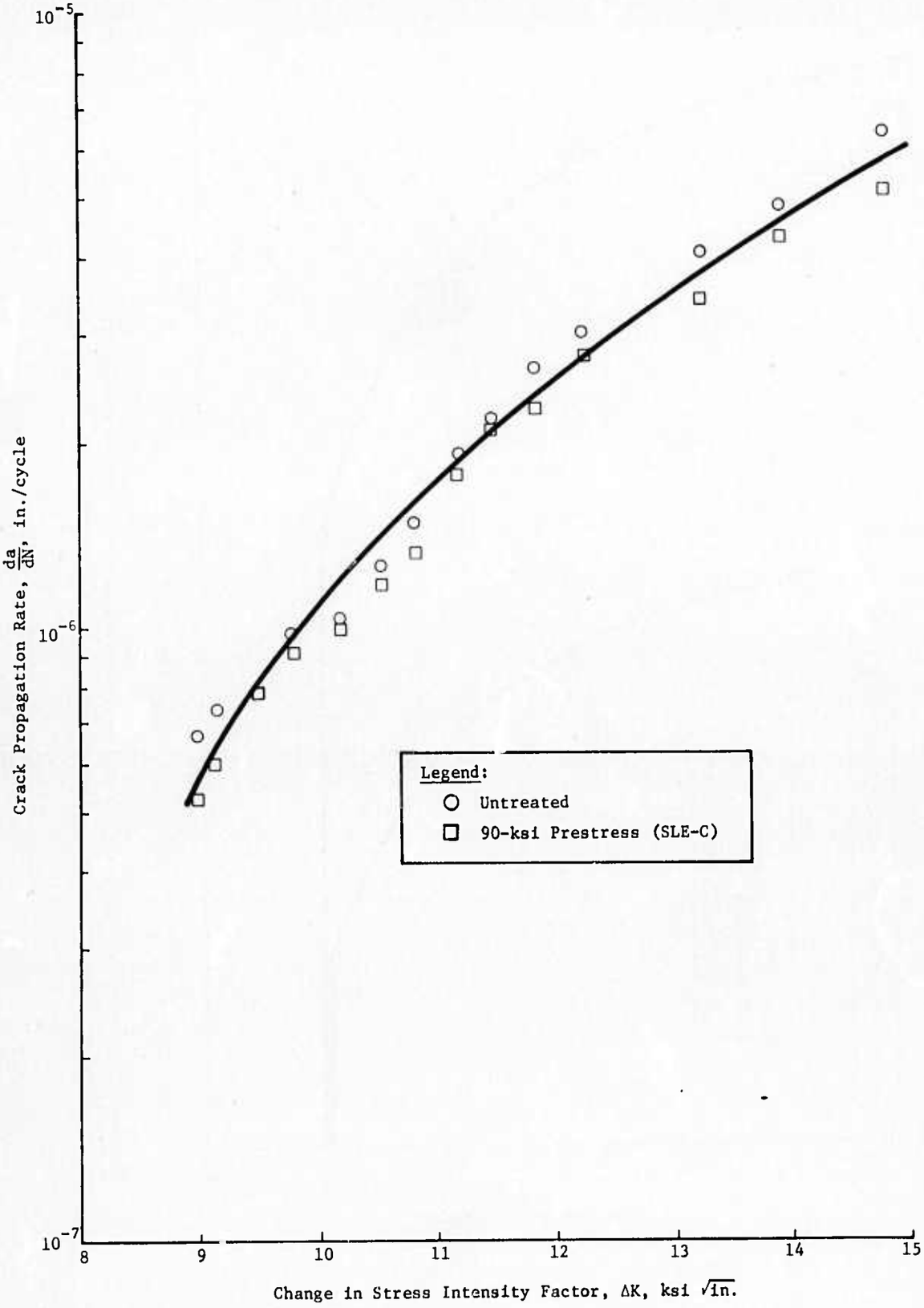

Fig. 24 Crack Propagation Rate in Heat-Affected Zone of Annealed Titanium 6Al-4V Center-Notched Specimens 0.06 in. Thick

F. FATIGUE OF TITANIUM TUBING

The effect of the SLE treatment on the fatigue properties of titanium tubing (6Aℓ-4V) in reverse, four-point bending is presented in Fig. 25. In these experiments considerable difficulty was experienced in obtaining fatigue fractures within the gage section. This was especially ture for SLE-treated specimens that were fatigued for long periods. To obtain the data shown in Fig. 25, over 50 tests were conducted. Nevertheless, the data are sufficient to show that the endurance limit was increased from 70,000 psi to 90,000 psi. In a previous investigation (Ref 14) on the fatigue behavior of titanium (6Aℓ-4V) rods tested in alternate tension-compression, the SLE treatment increased the endurance limit from 78,000 to 85,000 psi (Fig. 26).

The prestress used for the SLE treatment was 120,000 psi. This value was the average of the proportional limit of five specimens. It would, therefore, be expected that the finite fatigue life for the untreated and SLE-treated specimens be the same at that stress. Although the data are limited, it does a-pear that at lower stresses the fatigue life of the SLE-treated specimens is greater than that of the untreated specimens. For example, at a stress of ±100,000 psi, the fatigue life of the untreated specimens is 50,000 cycles, while that for the SLE-treated specimens is 100,000 cycles.

G. FATIGUE OF 4130 STEEL PRESSURE VESSEL

In order to select the proper stress amplitude to cause fatigue failures in a reasonable time, we made a preliminary investigation on surface-flawed specimens of 4130 steel heat-treated to the same yield strength as the tanks. For the SLE treatment, the specimens were prestressed to 60,000 psi and chem-milled before the EDM notch was put in. The specimen used is shown in Fig. 5.

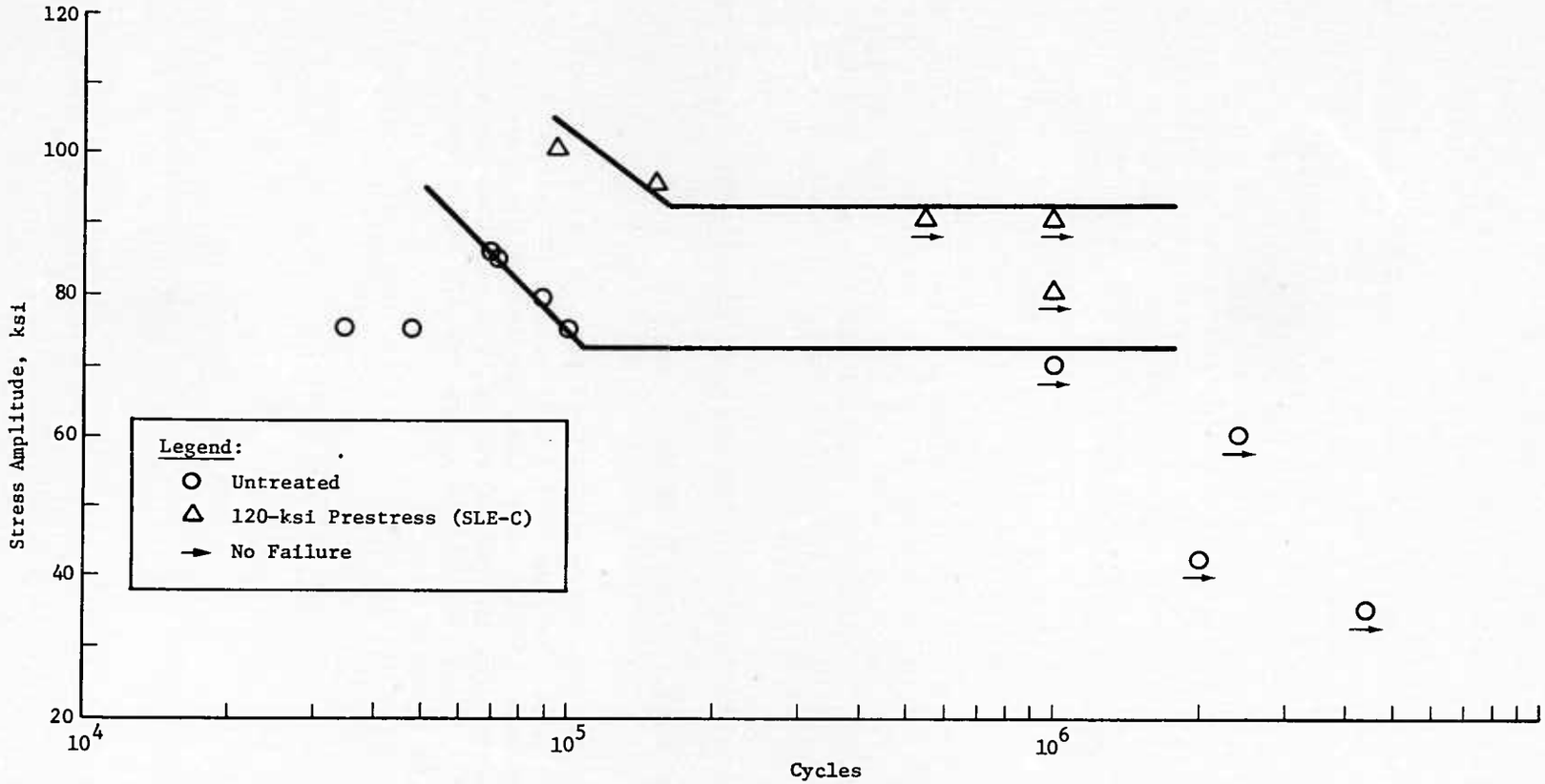

Fig. 25 Fatigue Life of Annealed Titanium 6Al-4V Tubing in Four-Point Reverse Bending, R = -1

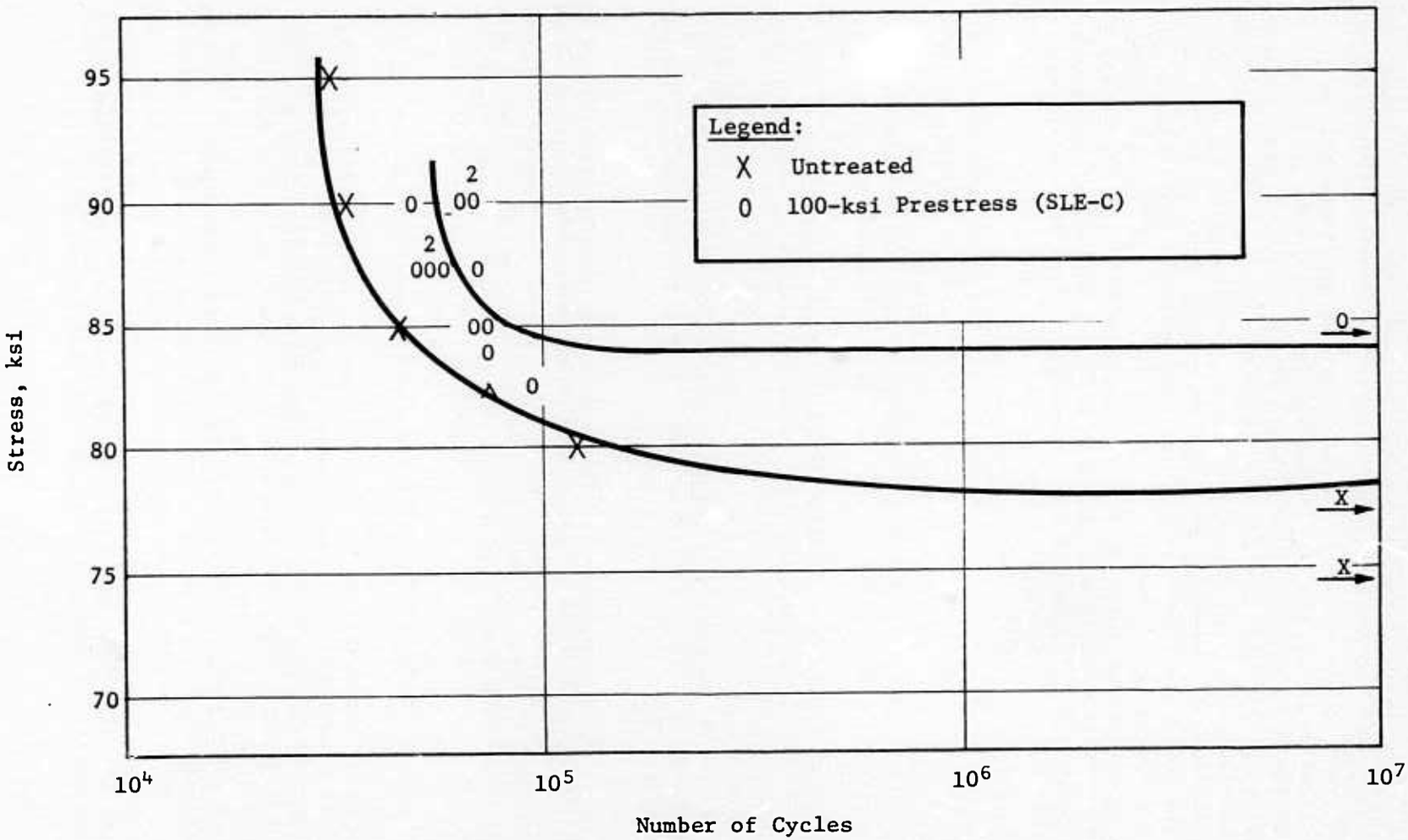

Fig. 26 Fatigue Life of Annealed Titanium 6Al-4V Rod in Tension/Compression, R = -1

The crack growth behavior of the untreated specimens tested at a stress amplitude of 6500 to 26,000 psi is shown in Fig. 27. As shown in the figure, crack growth began after 140,000 cycles and progressed rather rapidly, and at about 450,000 cycles the specimen was completely broken. With the above stress, the change in stress intensity factor, ΔK, covered the range from about 9000 to 14,000 psi $\sqrt{\text{in.}}$ (In comparison, for the SLE specimen tested at this stress amplitude, a propagating crack was not formed at 1.1×10^6 cycles.) The stress amplitude was then increased to between 6750 and 27,000 psi for 4.6×10^5 cycles, and then to between 7000 and 28,000 psi for an additional 2.7×10^5 cycles. Still, no propagating crack was formed. Since this latter load was at the limit of the capacity of the testing machine, the test was discontinued.

The fatigue life data for the 4130 steel pressure bottles tested at various values of ΔK is presented in Table 1 and in Fig. 28 thru 32. Bottles 1 to 5 were SLE-treated, bottles 8 to 11 were untreated, and bottle 6 was pressurized to 4800 psig, but allowed to relax.

The data in Fig. 28 show that there was a considerable variation in fatigue life: for example, at $\Delta K = 11{,}000$ psi $\sqrt{\text{in.}}$, the life of the SLE-treated vessels varied from about 1.5×10^5 to 3.8×10^5. In some cases, the SLE-treated tanks had a longer life than the untreated specimens; and in others, the opposite occurred. When the data were plotted in terms of K_{max} instead of ΔK, the scatter in results did not improve (Fig. 29).

In an attempt to clarify the situation, each of the five EDM notches was sectioned and the amount of crack growth was measured. In addition, the thickness of the tank at each notch was measured and the stress intensity factor at each location was calculated. These data revealed that there was a considerable range in crack growth within the same tank. For example, at $\Delta K = 9000$ psi $\sqrt{\text{in.}}$, the growth rate in tank 11 ranged from about 7×10^{-8} to 34×10^{-8} in./minute. Plotting the data in terms of K_{max} did not clarify the results.

From this investigation, it appears that the large scatter in the data relating to fatigue life and crack-propagation rates prohibits any conclusions to be drawn. The previous data obtained from the SLE treatment indicated that the degree of improvement was about 2 to 4; and the scatter in performance for the various tanks tested in these studies is about equal to or exceeds the expected improvement. However, the exact reasons for the large scatter are not known. We suspect that the failure to remove any of the decarburized layer may have contributed to the scatter. Furthermore, an inspection of the fractured faces also revealed that the metal was laminated in many regions; the lamination would, of course, decrease the crack propagation rate.

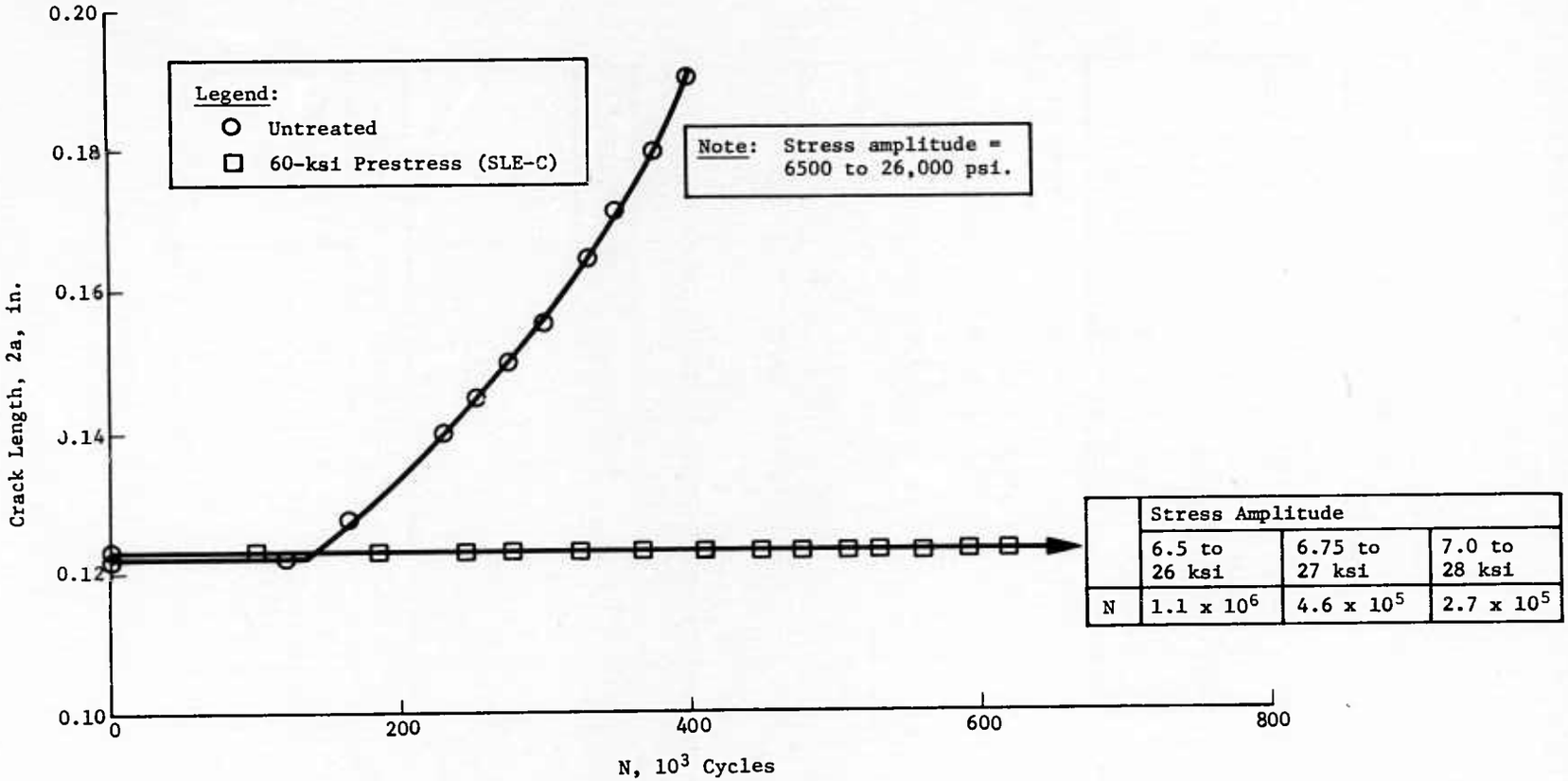

Fig. 27 Crack Growth of 4130 Steel Surface-Flawed Specimens, YS = 100 ksi

Table 1 Fatigue Test Data for 4130 Steel Bottles

Flaw	t, in	a, in.	a/2C	Δ a, in.	σ_{max}, ksi	Δ K, ksi $\sqrt{in.}$	K_{max}, ksi $\sqrt{in.}$
Bottle No. 1 (SLE-C; P_{max} = 2000 psig; P_{min} = 300 psig; N_F = 230,000)							
1	0.1870	0.0706	0.341	0.1360	36.4	12.1	14.2
2	0.1798	0.0689	0.340	0.0690	37.8	12.5	14.7
3	0.2048	0.0691	0.344	0.0900	33.3	11.1	13.0
4	0.1975	0.0709	0.352	0.0987	34.5	12.2	14.4
5	0.2067	0.0675	0.335	0.0806	33.0	11.0	12.9
Bottle No. 2 (SLE-C; P_{max} = 1600 psig; P_{min} = 100 psig; N_F = 156,800)							
1	0.1997	0.0678	0.34	0.0494	27.2	10.0	10.6
2	0.1824	0.0724	0.36	0.0972	29.7	10.9	11.6
3	0.1962	0.0683	0.35	0.0532	27.8	10.1	10.8
4	0.1865	0.0679	0.34	0.1043	29.2	10.7	11.4
5	0.1871	0.0680	0.34	0.1249	29.1	10.7	11.4
Bottle No. 3 (SLE-C; P_{max} = 1600 psig; P_{min} = 100 psig; N_F = 202,000)							
1	0.1953	0.0698	0.35	0.0481	28.0	10.2	10.9
2	0.1796	0.0691	0.33	0.1283	30.3	11.1	11.8
3	0.1900	0.0679	0.35	0.0596	28.6	10.5	11.2
4	0.1953	0.0690	0.35	0.0887	28.0	10.2	10.9
5	0.1953	0.0666	0.31	0.0537	28.0	10.2	10.9
Bottle No. 4 (SLE-C; P_{max} = 1500 psig; P_{min} = 100 psig; N_F = 367,200)							
1	0.1830	0.0698	0.33	0.1155	29.7	10.8	11.6
2	0.1988	0.0698	0.34	0.1114	27.4	10.0	10.7
3	0.1860	0.0687	0.33	0.0559	29.3	10.6	11.4
4	0.1933	0.0691	0.35	0.0532	28.2	10.3	11.0
5	0.2067	0.0702	0.35	0.0806	26.4	9.6	10.3
Bottle No. 5 (SLE-C; P_{max} = 1400 psig; P_{min} = 100 psig; N_F = 428,900)							
1	0.1810	0.0617	0.31	0.0677	26.3	9.5	10.3
2	0.1815	0.0622	0.32	0.1263	26.3	9.5	10.3
3	0.1881	0.0621	0.30	0.0565	25.3	9.1	9.8
4	0.1877	0.0628	0.31	0.0540	25.4	9.1	9.8
5	0.1832	0.0713	0.35	0.1218	26.0	9.4	10.1

Table 1 (concl)

Flaw	c, in.	a, in.	a/2c	Δ a, in.	σ_{max}, ksi	Δ K, ksi $\sqrt{in.}$	K_{max}, ksi $\sqrt{in.}$
Bottle No. 6 (SLE-R; P_{max} = 1500 psig; P_{min} = 100 psig; N_F = 344,300)							
1	0.1964	0.0712	0.32	0.1254	25.9	9.4	10.1
2	0.1994	0.0693	0.35	0.0564	25.5	9.2	9.9
3	0.1958	0.0692	0.35	0.0895	26.0	9.4	10.1
4	0.1862	0.0785	0.38	0.0601	27.4	9.6	10.3
5	0.1906	0.0709	0.34	0.1076	26.7	9.7	10.4
Bottle No. 8 (Untreated; P_{max} = 1600 psig; P_{min} = 100 psig; N_F = 460,000)							
1	0.1961	0.0664	0.33	0.1005	27.8	10.1	10.8
2	0.1938	0.0698	0.34	0.1402	28.0	10.2	10.9
3	0.2001	0.0718	0.34	0.0733	27.0	9.8	10.5
4	0.1900	0.0722	0.36	0.0765	28.6	10.5	11.2
5	0.1868	0.0712	0.36	0.1323	29.1	10.7	11.4
Bottle No. 9 (Untreated; P_{max} = 2000 psig; P_{min} = 300 psig; N_F = 164,000)							
1	0.1960	0.0709	0.33	0.0973	34.7	11.5	13.5
2	0.1858	0.0698	0.33	0.0906	36.6	12.1	14.3
3	0.1913	0.0711	0.34	0.0616	35.5	11.7	13.8
4	0.1874	0.0728	0.33	0.0684	36.3	12.0	14.1
5	0.1885	0.0706	0.34	0.1297	36.0	11.9	14.0
Bottle No. 10 (Untreated; P_{max} = 2000 psig; P_{min} = 300 psig; N_F = 157,600)							
1	0.2218	0.0679	0.33	0.0150	30.6	10.2	12.0
2	0.1690	0.0690	0.33	0.1126	40.3	13.3	15.7
3	0.1938	0.0706	0.34	0.0370	35.1	11.6	13.7
4	0.1871	0.0699	0.33	0.0562	36.4	12.1	14.2
5	0.2090	0.0700	0.33	0.0310	32.5	10.8	12.7
Bottle No. 11 (Untreated; P_{max} = 1600 psig; P_{min} = 100 psig; N_F = 405,300)							
1	0.2015	0.0737	0.37	0.1452	27.0	9.8	10.5
2	0.2166	0.0723	0.34	0.0346	25.2	9.2	9.8
3	0.2130	0.0706	0.35	0.0579	25.5	9.4	10.0
4	0.2043	0.0702	0.33	0.1497	26.7	9.7	10.4
5	0.2165	0.0710	0.36	0.1317	25.1	9.2	9.8

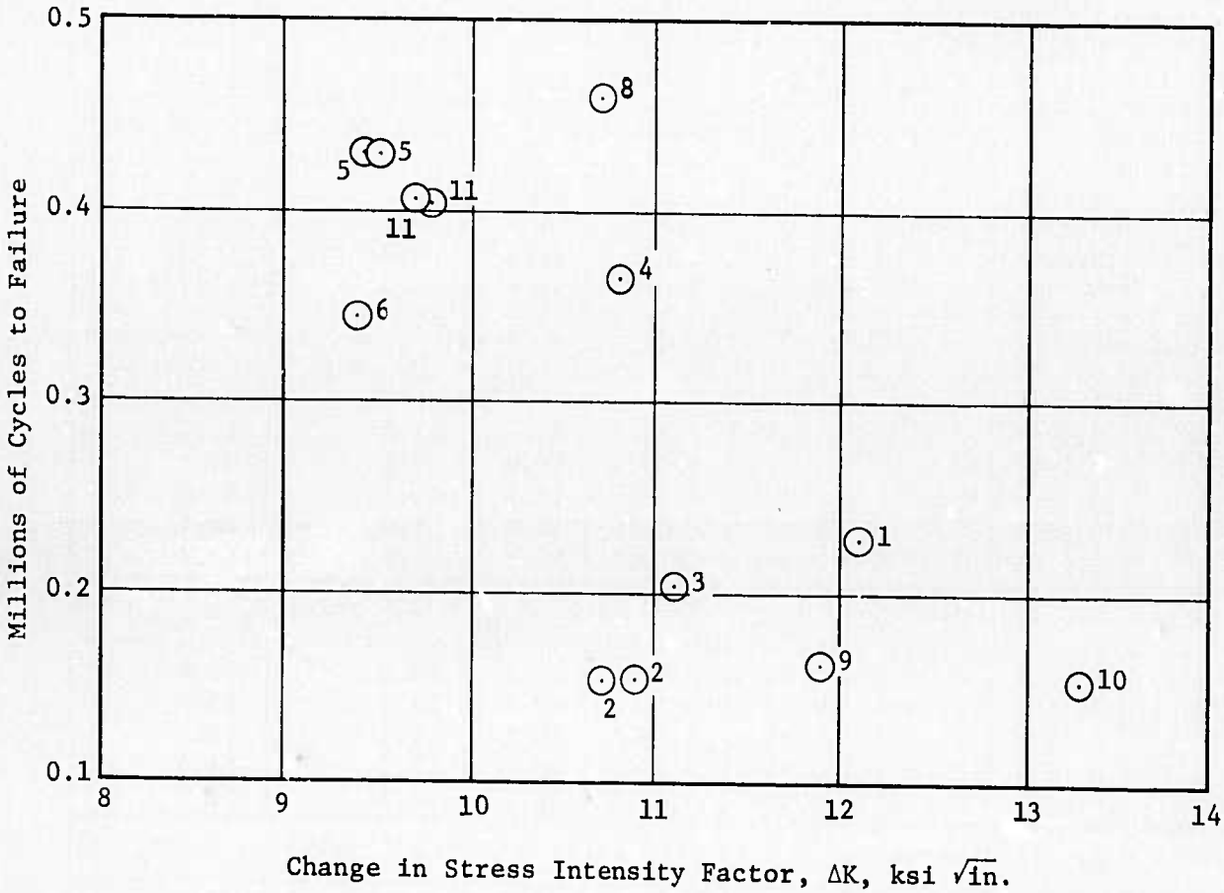

Fig. 28 Fatigue Life of 4130 Steel Pressure Bottles as a Function of ΔK

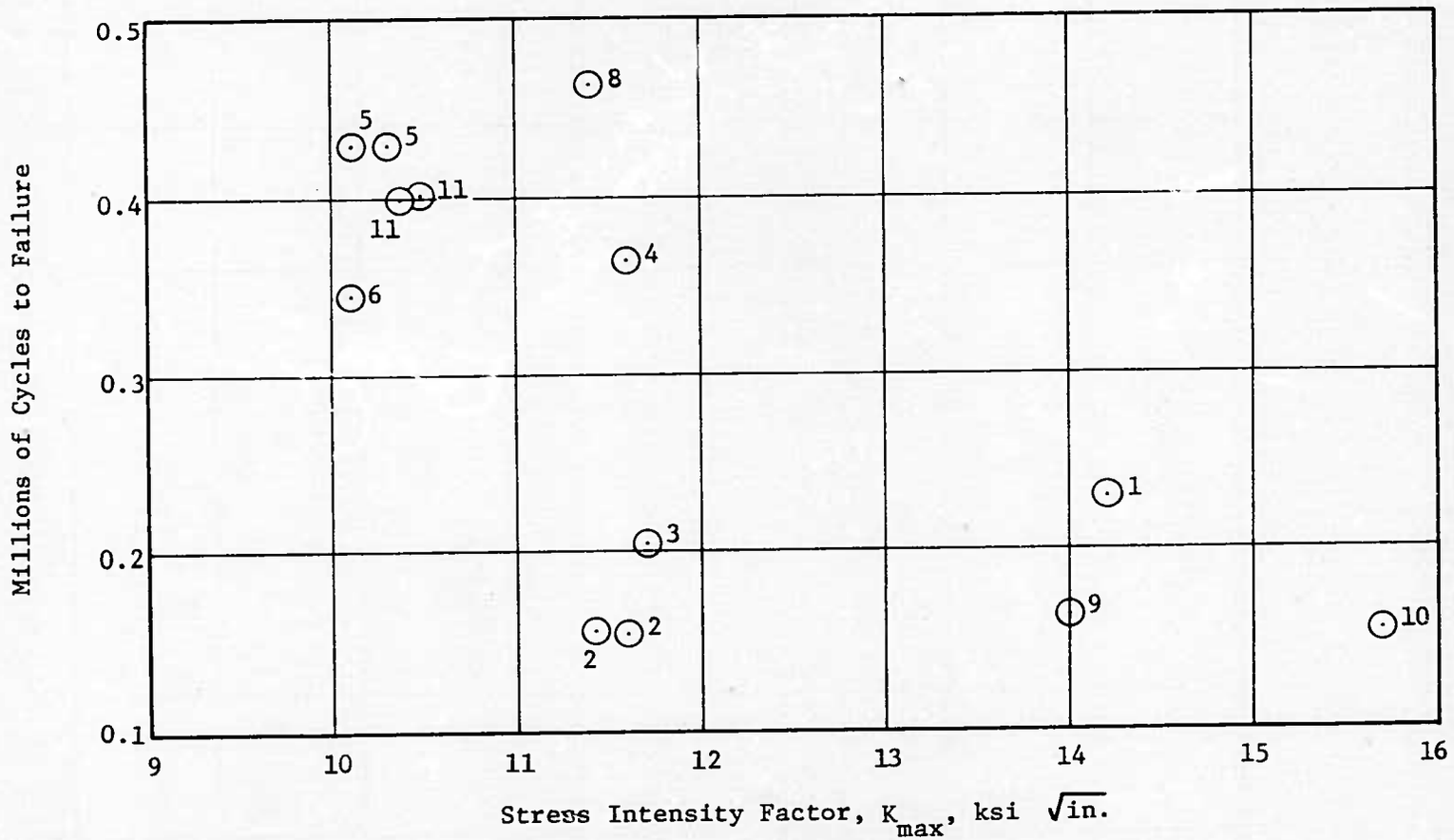

Fig. 29 Fatigue Life of 4130 Steel Pressure Bottles as a Function of Maximum Stress Intensity Factor

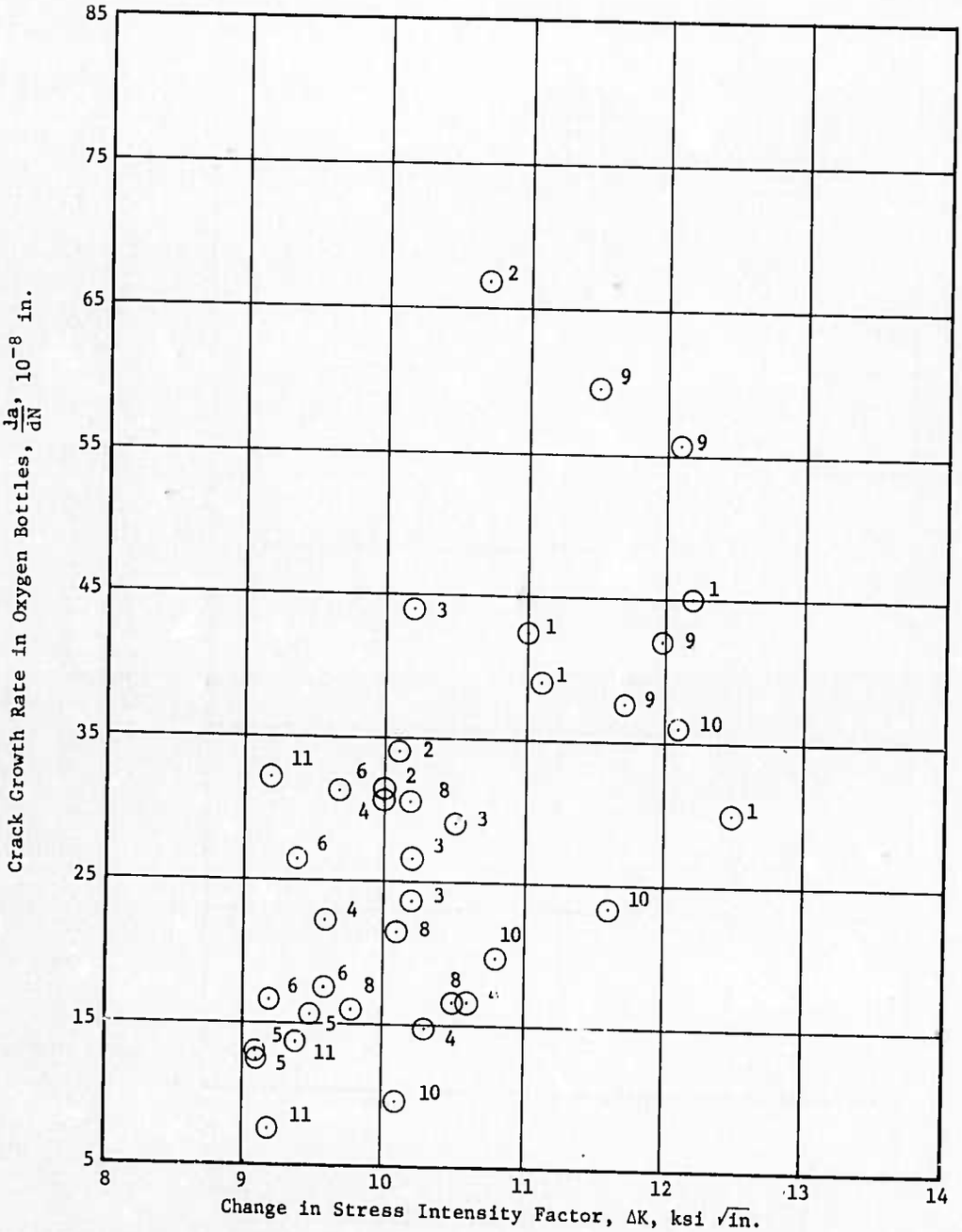

Fig. 30 Crack Growth Rate of Individual Flaws in 4130 Steel Pressure Bottles as a Function of ΔK

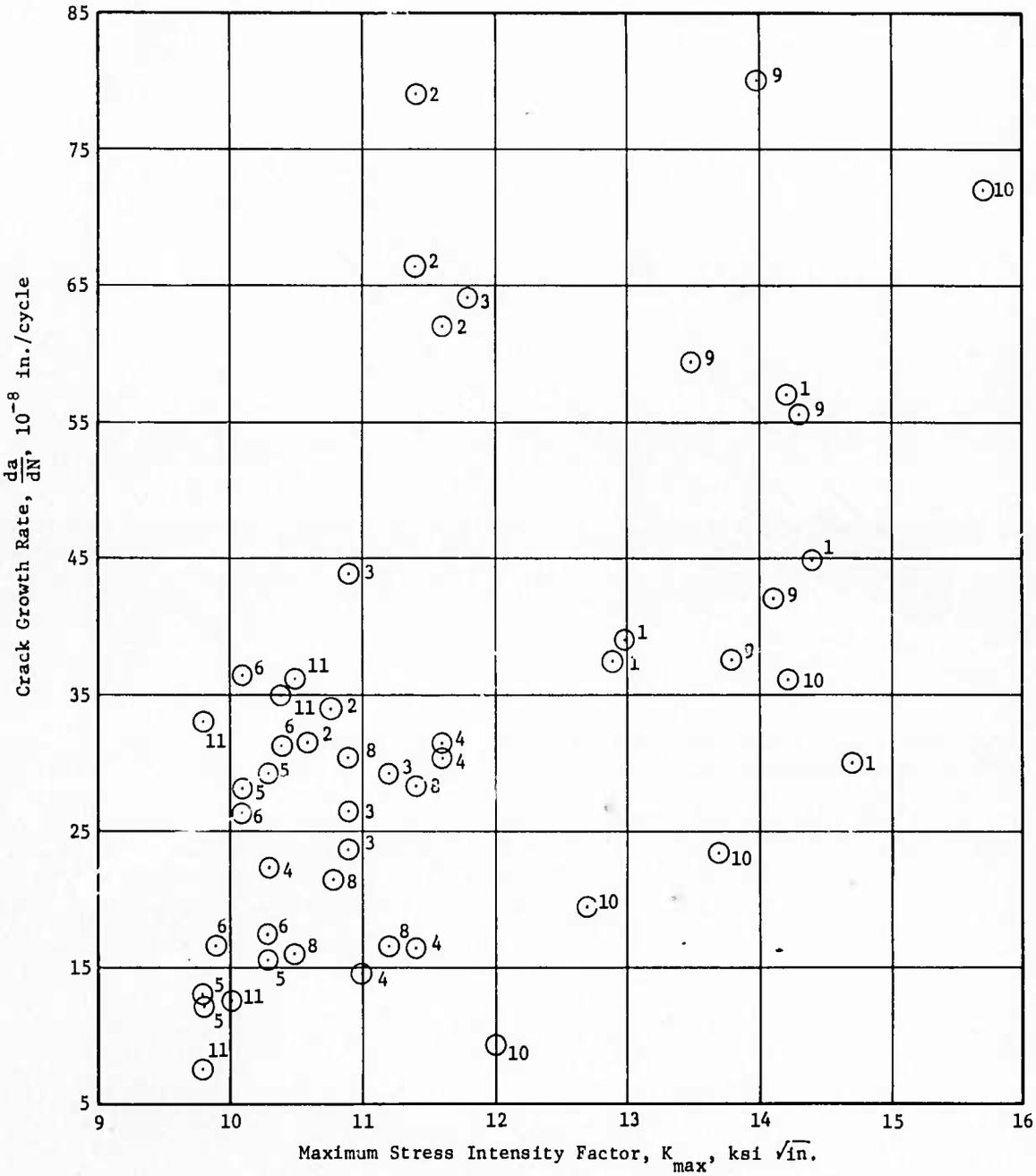

Fig. 31 Crack Growth Rate of Individual Flaws in 4130 Steel Pressure Bottles as a Function of Maximum Stress Intensity Factor

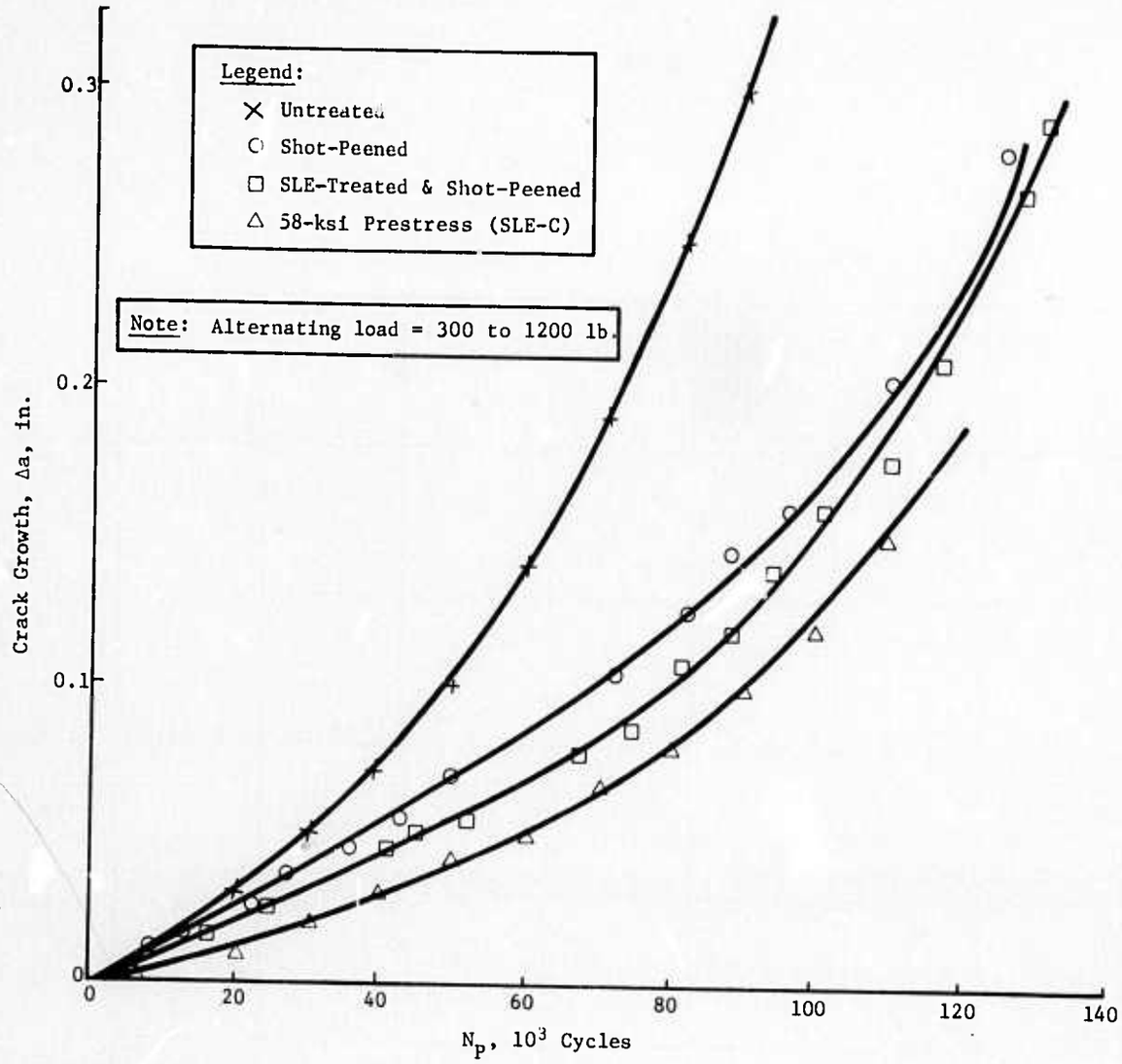

Fig. 32 Crack Growth Rate of Shot-Peened and SLE-Treated 2014-T6 Aluminum Compact Tension Specimens, Frequency = 1 Hz

H. SHOT PEENING

Since shot-peening is often used to enhance fatigue resistance, it became desirable to compare its effect with that of the SLE treatment. The curves in Fig. 32 show the crack-growth behavior after these treatments were given to compact tension specimens of 2014-T6 aluminum. The effect of shot-peening an SLE-treated specimen is also shown.

Figure 33 shows the crack propagation rates as a function of ΔK. Compared to the untreated specimens, the shot-peening treatment decreases the crack propagation rate. At a ΔK 5900 psi $\sqrt{in.}$, the rate decrease from 2.5×10^{-6} to 1.65×10^{-6} in./cycle, a factor of 1.5. In comparison, at the same ΔK value, the crack propagation rate in the SLE-treated specimen decreased by a factor of 3.2.

In general, Fig. 32 and 33 show that the SLE treatment is about twice as effective as the shot peening. They also show that shot peening after the SLE treatment reduces the crack propagation resistance imparted by the SLE treatment. The crack rates with the combined treatments are about the same as those for the shot-peened specimens.

In considering the effect of the shot-peening and the SLE treatment on the compact tension specimen, it should be noted that only the outside surfaces were treated; that is, the crack starts at the bottom of the untreated notch. Accordingly, this specimen does not afford a good measurement of the effect of these treatments on crack initiation. The tests do, however, show the very large influence of the surface layer on crack propagation. In the shot-peened specimens, the surface region is under a large residual compressive stress, but the dislocation density is high because of the large amount of cold work. In comparison, the residual compressive stress is not present in the SLE treated specimens, but the dislocation density is low. Apparently, the high dislocation density is more detrimental than the benefit imparted by the high residual compressive stress.

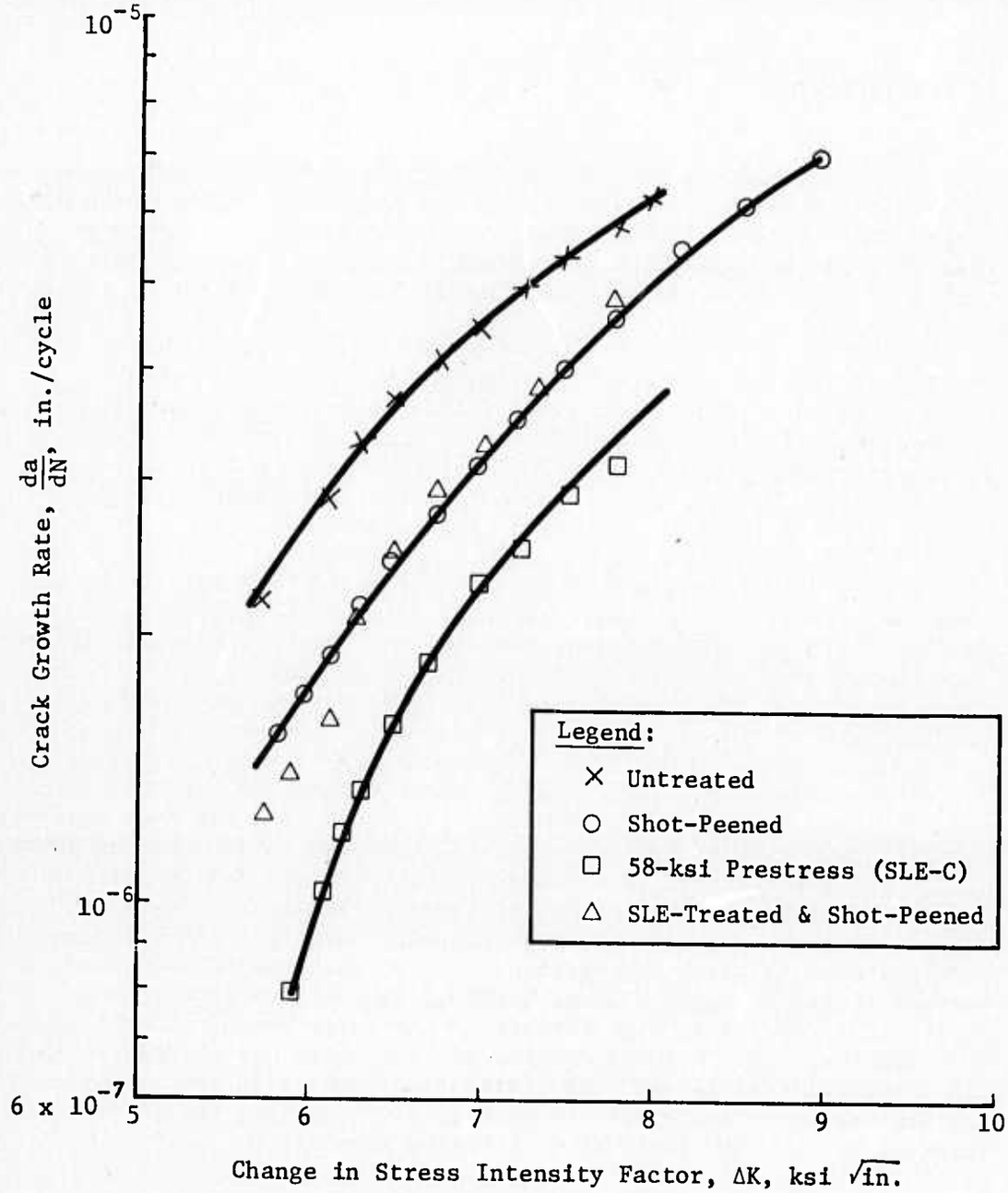

Fig. 33 Crack Growth Rates of Shot-Peened and SLE-Treated 2014-T6 Aluminum Compact-Tension Specimens, Frequency = 1 Hz

IV. REFERENCES

1. I. R. Kramer: *Trans. Am. Inst. Mining Engineers, 227*, 1003 (1963)
2. I. R. Kramer: *Trans. Am. Inst. Mining Engineers, 223*, 1462 (1956)
3. S. Kitajama, H. Tanaka, and H. Kaiede: *Journal I. M.*, 10 (1969)
4. G. Vellaikal and J. Washburn: *Journal of Applied Physics*, 40, 2280 (1969)
5. I. R. Kramer and N. Balasubramanian: *Acta. Met., 21*, 695 (1973)
6. C. Zener: *Fracturing of Metals*, ASM, 3 (1948)
7. A. N. Stroh: *Advances in Physics, 6*, 418 (1957)
8. A. H. Cottrell: *Trans. AIME, 212*, 192 (1958)
9. I. R. Kramer: AFML Report TR 68/65 (MCR-67-421), January 1968
10. I. R. Kramer: *Trans. Met. Soc., 239*, 520 (1967)
11. I. R. Kramer, A. Kumar, and N. Balasubramanian: Army Materials and Mechanics Research Center, Report AMMRC CR 71-2/4, July 1972, and CR 71-2/5, December 1972
12. O. H. Basquin: *Proc. ASTM, 10*, 625 (1910)
13. E. T. Wessel: *Eng. Fract. Mech. 1*, 77 (1968)
14. I. R. Kramer: *Proc. Air Force Conference on Fatigue and Fracture*, AFFDL-TR-70-144, editors H. A. Wood, R. M. Badger, W. J. Trapp, R. F. Hoener, and R. C. Donat, p 271

Enhancement of Crack Propagation Resistance by Elimination of the Surface Layer

I. INTRODUCTION

If our knowledge of fatigue failure processes was well understood, then (in addition to many others) we should be able to predict fatigue life under a variety of stress, temperature, and environmental conditions. Furthermore, we should expect to find methods of improving fatigue resistance. Unfortunately, our state of knowledge does not permit us to attain these goals at present, and in spite of the efforts expended during the past 20 years, our understanding of the mechanisms governing crack initiation and propagation has been relatively small. This latter is quite evident from the number of theories that have been proposed and the amount of disagreement among the investigators. It *is* generally agreed, however, that fatigue cracks usually originate in the surface region.

Thompson, *et al.* (Ref 1), showed that for high-purity metals, cracks formed within persistent slip bands. These slip bands form in soft metals in about the first 5% of the metal's fatigue life, and cracks are found somewhere around 10% of the fatigue life (Ref 2). In Ref 2, Grosskreutz also reported that, for structural-type alloys (2024-T3 aluminum and 4130 steel), the cracks formed between 60 and 70% of the fatigue life in unnotched specimens. In contrast, Kemsley (Ref 3) reported that persistent slip bands occurred when specimens were cycled at low stresses.

In addition to being related to these persistent slip bands, fatigue cracks were also reported to be associated with intrusions and extrusions (Ref 4 thru 7). Thus, we find fatigue cracks forming in high-purity metals in both intrusions and in persistent slip bands. These observations, together with the tapered section technique of Wood, *et al.* (Ref 7 and 8) for observing the cracks, show that the cracks do start in the region of the surface. However, because all these previous observations were conducted by optical microscopic techniques, the underlying mechanism leading to crack formation was uncovered.

The use of electromicroscopic techniques has also failed to provide the required information necessary to formulate a satisfactorily proven mechanism for fatigue crack initiation. This is, in part, due to the extreme difficulty in detecting an embryonic crack and the extremely small areas employed for the observations. It is also generally recognized that a rather large fraction of the dislocation is lost in preparing and observing the specimen. Nevertheless, a number of suggested mechanisms was advanced.

It has been proposed that cross slip, and therefore the stacking fault energy, strongly influence surface cracking in fatigue (Ref 9 and 10). These conclusions were based on observations of lithium fluoride, silver chloride, and sodium chloride, as well as copper and copper-zinc alloys. Later, Nine (Ref 11) concluded from studies of single crystals of copper fatigued in torsion that cross-slip was not basic to the formation of persistent slip bands, and therefore, to the formation of cracks. It has also been suggested (Ref 12) that cracking is associated with the geometry of slip band formation, and that a crack will form only on systems that produce a slip step. Investigators also proposed that cracks were mainly nucleated at grain boundaries since the extrusions were insufficient to cause cracks (Ref 3, and Ref 13 thru 16). These latter mechanisms are largely geometric in natures. From the above, it is apparent that there is no general agreement concerning the mechanism by which cracks are initiated.

In further attempts to obtain an understanding of fatigue failures, a large number of investigations (Ref 17 thru 26) were conducted on cyclic hardening and cyclic softening. When single-phase, well annealed fcc metals were cycled between fixed plastic strain limits, the materials hardened up to a given value; further cycling did not increase the hardening. Alden and Backoffen (Ref 27) reported that cracks nucleate when the hardening reaches this saturation phase. When these materials are cold-worked and then cycled, they soften.

A number of investigations involving the use of thin-film electron microscope techniques have also been used to determine the dislocation structure resulting from cyclic stressing. For low-stacking-fault-energy metals, a planar array of dislocations is usually reported (Ref 28); Grosskreutz, *et al.* (Ref 29), observed a well developed cell structure in polycrystalline Cu/30% Zn. In high-stacking-energy metals, the dislocations are arranged in long, interconnected bands. These bands are reported to contain a high density of dislocation dipoles, loops, and debris (Ref 30).

A question naturally arises as to whether the observations made with respect to cyclic hardening/softening and to the accompanying changes in dislocation configurations in the interior of the specimens are related to the fatigue cracks that form at the surface. It should be noted that the fatigue failures occur for specimens that work-harden, work-soften, and work-harden followed by work-softening. Therefore, it is difficult to consider a simple functional relationship between fatigue failures and cyclic hardening/softening unless one wishes to postulate a number of fatigue mechanisms. A relationship between cyclic

hardening/softening and fatigue life appears to be even less tenable in view of Grosskreutz (Ref 2). Grosskreutz reported "that two halves of a specimen failed in fatigue (and containing dislocation cell structures) can themselves be tested and exhibit fatigue lives comparable to the original specimen." He concluded that "damage" introduced into copper during fatigue hardening/softening is harmless and serves only to determine the flow stress.

There does appear to be a relationship between cyclic hardening/softening and surface effects. But when these cyclic experiments are conducted, no attempt is usually made to determine whether the hardening/softening is occurring in the interior, in the surface layer, or both; during cycling, the metal is treated as a "uniform" structure.

It has been reported (Ref 31 and 32) that, for high-purity polycrystalline aluminum and copper, the increase in hardening was due practically entirely to an increase in the hardening of the surface layer, and that the surface-layer stress reached a maximum at saturation. Measurements of the activation volume for deformation (Ref 33) also indicated that cyclic hardening was associated with the surface layer. These latter measurements showed that after cycling between fixed plastic strain limits, the activation volume decreased markedly (reflecting a large increase in dislocation density). When the surface layer was removed from cyclic-hardened specimens of copper by electromechanical means, the activation volume initially was the same as that of the uncycled specimen, but with continued unidirectional straining the activation volume values became the same as those of the cyclic work-hardened specimens (Ref 33). It was reported earlier (Ref 31) that with further deformation, either in tension or in compression, after the surface layer had been completely removed from cyclic-hardened specimens, the surface layer stress reformed during the next quarter cycle to a value equal to that before the layer was removed. In the above experiment, the hardening increased by a factor of about 3. It would not be unexpected that for single crystals, or under conditions wherein the cyclic hardening is very large, that both the interior and surface layer contribute to the hardening.

These data also indicate that when the cyclic hardening is primarily associated with the hardening of the surface layer, the microstructural changes that occur in the interior strongly influence the reformation of the surface layer.

A relationship between the surface layer stress, cyclic hardening, and fatigue may also be found when specimens are tested in various environments. For example, it is known that the fatigue life is

greatly increased when specimens are cycled at reduced pressures. When the tests were conducted in vacuum, the rate of cyclic hardening was less than that for specimens cycled at atmospheric pressure (Ref 34). The surface-layer stress was also found to be lower. Similarly, it was shown (Ref 33) that when titanium (6Aℓ/4V) specimens were tested in a CH_3OH-HCl solution, and copper in a $Cu(NO_3)_2$-NH_4OH solution, the surface-layer stress is increased markedly, the activation volume is decreased, and the fatigue life is correspondingly decreased.

The lack of agreement between electron transmission microscopy with observations based on dislocation etch pits, activation volume, and surface layer stress appears to be associated with relaxation of the dislocations in the surface region. It is important to note that in those experiments wherein thin foils were taken from the surface region, the results indicate that the surface layer is "soft" (Ref 35) and has a lower dislocation density than the bulk material (Ref 30 and 36). In contrast, when the surface layer of strained specimens is examined on the bulk of the specimen using the etch pit technique (Ref 37 thru 39), or by the formation of slip bands as a function of depth (Ref 39), the results indicate that the surface layer is "hard" and has a higher dislocation density than the bulk material. These latter observations are in accord with changes in the activation energy and activation volume, and the decrease in the unidirectional and cyclic work-hardening behavior of metals when the surface layer is removed (Ref 40 thru 42).

The existence of a surface layer was first shown in 1963 (Ref 41). Later (Ref 43) the surface-layer stress was measured by determining the difference in the initial flow stress of strained specimens with and without the surface layer. These measurements also indicated that the surface layer was hard.

During a study of the activation volume of polycrystalline aluminum (Ref 43), it was found that when a strained specimen was tested after an elapsed time, the activation volume increased, indicating a decrease in the dislocation density. Later, a systematic investigation of copper, aluminum, and titanium (Ref 44) showed that at room temperature the surface layer relaxed completely in about 50, 4, and 1 hr, respectively, at 20°C. In a separate study, the apparent activation energy for this relaxation in copper was found to be 3300 cal per mole (Ref 33); and from the change in strain during relaxation, it was apparent that the surface layer contained an excess number of dislocations of like sign (Ref 31). This low value of the apparent activation energy for relaxation of the surface layer was due to a stress, τ_s, acting on the dislocation; that is, the activation energy was decreased by $V^*\tau_s$, where V^* is the activation volume.

All the above observations show that there is a driving force associated with a dislocation gradient in the surface layer that tends to move the dislocations out of the surface region. In addition, the surface layer is under a residual compressive stress gradient. This compressive stress may be described in terms of the stress fields associated with the excess number of dislocations of like sign in the surface layer, and is eliminated when the surface layer is removed. When thin foils are cut from the surface layer, dislocations will glide out to reduce the energy gradient and the dislocation density will appear to be lower than that in the bulk. Electroplating techniques that attempt to prevent the egress of dislocations are not expected to function very satisfactorily when a dislocation gradient is present, for unless the electroplating system is operated in a completely irreversible manner, metal ions from the cathode will dissolve and dislocations will be lost. Barrett and others (Ref 40 and 41) have shown that a large number of dislocations are lost when the outer layers were removed from strained specimens. Furthermore, when a dislocation gradient is present, only a relatively short time is available to apply any method to prevent loss of dislocations. For example, for copper at 274°K, approximately 25% of the surface layer is lost within 10 minutes; and for high-purity polycrystalline aluminum, about 35% is lost in 1 minute. In addition, because of the compressive stress gradient in the surface layer, a bending moment is imparted to the foil when it is separated from the bulk material.

Fourie (Ref 35 and 45) reported that the residual compressive stress of his deformed copper crystals was 2 kg/mm^2. From simple beam theory, it may be shown that his foils (70 x 2 x 0.06 mm), after removal from the surface layer, will have a radius of curvature of 230 mm, and that plastic flow will start in the outer fiber at a stress 50% lower than that of a straight specimen. For his 0.6-mm specimens, a 25% error will be introduced.

In several previous publications the concept was advanced that the surface layer greatly influenced the fatigue life of metals (Ref 31, and Ref 47 thru 49). This concept was based on the observation that: (1) under both constant strain or constant stress cycling conditions, the surface layer stress increases; (2) that environments that decrease the fatigue life increase the surface layer stress; and (3) that when the surface layer stress was decreased or increased, the fatigue life was correspondingly increased or decreased (Ref 32, 34, and 50). We have also been able to show (Ref 50) that the surface layer stress at the root of a notch is much larger than that for unnotched specimens for the same strain. Thus, in a qualitative manner, we found that the

fatigue life decreases under conditions that cause the surface layer stress to increase and, importantly, vice versa.

In this investigation, measurements were made of the change in the surface layer stress with the number of fatigue cycles on three alloys [2014-T6 aluminum, titanium (6Aℓ/4V), and 4130 steel]. Previously (Ref 31 and 32), it was shown that when specimens of the aluminum alloy were fatigued, the proportional limit increased. However, if the surface layer was removed after fatiguing the specimens, then the proportional limit returned to its original value. As a result of these experiments, it was suggested that the surface layer, if sufficiently strong, could act as a barrier to the movement of mobile dislocations, and that cracking could occur in a manner similar to that suggested by Stroh (Ref 51) when the local stress associated with a pileup of dislocations exceeded the fracture stress. This implies that the surface layer stress must reach a critical value before fatigue cracks can form.

During this phase of the contract, it was also decided to reinvestigate the effect of the periodic removal of the surface layer on fatigue life. For the past 40 years or more, it has been common shop practice to machine shafts and take other steps to remove "cracks" and prolong fatigue life. Thompson, *et al.* (Ref 1), in a systematic investigation, showed that the periodic removal of 30 μ from the surfaces of copper specimens prolonged the fatigue life. This effect was attributed to the removal of persistent slip bands and cracks.

These types of experiments have also been conducted by many other investigators with similar results. Lissner and Moller (Ref 52), as well as Hempel (Ref 53), reported that the results of a rotating bend test showed that removing 0.1 mm from steel specimens after one-half of the fatigue life increased the remaining life of the material. Siebel and Stahli (Ref 54), by removing similar amounts at intervals corresponding to 40% of the fatigue life, found that the remaining life was also greatly extended. They terminated the tests after the life had been extended by a factor of 7.

In the research on copper, persistent slip bands were observed on specimens cycled below the fatigue limit. As pointed out by Kennedy (Ref 55), it might be expected that if the persistent slip bands are sources of fatigue cracks, these bands should not be developed at stresses below the fatigue limit. In consideration of the fact that a surface layer does exist in the fatigued materials, a question immediately arises as to whether the increase in life is due to the removal of the surface layer before a critical state is reached, or to the removal of cracks and slip bands.

In addition, data are reported on crack propagation rates from specimens with and without the surface layer initially. As described (Ref 32 and 34), this technique involves prestressing the specimen up to the proportional limit and then eliminating the surface layer. For brevity, the technique is referred to as the SLE (*S*urface *L*ayer *E*limination) treatment. In this procedure, when the metal is first stressed all grains with a "soft" orientation undergo plastic deformation and a surface layer is formed. The surface-layer stress is a function of strain (stress) (Ref 34, 43, and 44). After eliminating the surface layer by chem-milling or by relaxation and subsequently restressing the specimen, the surface layer reforms at a much higher stress than that required in the original specimens (Ref 39). For example, in the 2014-T6 aluminum alloy, by observing the appearance of slip lines it was found that plastic flow began in the surface grains at a stress of 5000 psi. After prestressing the material to the proportional limit (58,000 psi) and noting the formation of the slip lines after removing the surface layer, plastic flow and reformation of the surface layer began at 35,000 psi. At depths less than 0.002 in. plastic flow started at higher stresses. Similar data were also obtained on Fe/3% Si and single crystals of aluminum and copper (Ref 39).

II. EXPERIMENTAL APPROACH

The fatigue specimens used to measure the surface-layer stress and to determine the effects of removing the surface layer on fatigue life were machined from 5/8-in.-diameter rods of 2014-T6 aluminum, annealed titanium (6Al/4V), and 4130 steel. These specimens had a diameter of 0.16 in. and a gage length of 0.30 in. The specimens and alignment features used during the cycling were in accord with those recommended by Feltner (Ref 56).

After being machined, the aluminum alloy was stress-relieved at 250°F for 1 hr; the titanium was stress-relieved at 1300°F in vacuum. The 4130 steel specimens were austenitized at 1600°F, oil-quenched, and tempered at 800°F. This resulting product had a 0.2% yield strength of 180,000 psi. Before being tested, all specimens were electrochemically polished to remove about 0.004 in. to obtain the same surface finish.

The fatigue tests were conducted in an electrohydraulic machine (MTS) in tension-compression. The upper portion of the specimen was held in alignamatic grips, while the lower end was embedded in a fixture containing a low melting point alloy.

The crack propagation rates were measured under conditions of plane stress and plane strain. Compact tension specimens conforming to ASTM specifications were used for the latter. The plane strain specimens were 13 in. long and 2 in. wide, and had a through-the-thickness notch. For the SLE treatment, strips of the material about 15 in. long were first stressed to the proportional limit and then chem-milled to remove 0.005 in. from each side to eliminate the surface layer. The specimens, with the exception of the faces, were machined from this stock. All notches were put in after the final machining. The crack length measurements were made with the aid of a telecope and strobe light.

As reported previously, when the aluminum specimens were stress-cycled, the proportional limit increased; and when the surface layer was removed after cycling, the proportional limit returned to its original value. To reconfirm this observation, the same tests were conducted on the titanium and steel specimens. In all cases the behavior was the same, and it may be concluded that, for the stress amplitudes used, the "hardening" during cycling was confined to the

surface layer. Therefore, the increase in the surface-layer stress due to cycling was equal to the increase in the proportional limit.

The stress-strain measurements were made immediately after cycling to minimize surface-layer losses due to relaxation effects. An extensometer was attached to the specimen after the cycling sequence and measurements were begun in less than 1 minute. The sensitivity of the recording was as follows: 1 in. of chart was equal to an extension of 0.0005 in. and a load of 250 lb.

The curves shown in Fig. 1 give an example of the change in the load-deformation characteristics after the titanium specimens were cycled at a constant stress amplitude of ±80,000 psi. These curves are tracings from the recordings obtained from specimens that had the same cross-sectional areas. When the number of cycles was increased from 15,000 to 45,000, the proportional limit increased from 134,000 to 142,000 psi. In all cases the curves coincided at the higher strains. Typically, the stress-strain curves for the uncycled and cycled specimens were the same after a plastic strain of about 0.003. Note that in these tests the cycling stress was *always* below the proportional limit.

For that portion of the investigation devoted to the effects of surface removal on the fatigue life, both aluminum and titanium specimens were used. A series of preliminary investigations was first conducted to determine the appearance of the slip line in terms of the stress and number of cycles. The specimens were cycled and examined at a magnification of 1200 for evidence of persistent slip bands or cracks. In the cases chosen for further investigation, the slip bands were barely discernible and no evidence of cracks was found. Examination showed that removal of less than 0.001 in. from the radius was sufficient to remove all of the slip markings when examined at 1200 magnification.

In addition to the above, etch-pit and crack propagation rate studies were conducted on a Fe/3% Si alloy supplied by the U.S. Steel Company through the courtesy of Dr. W. C. Leslie. An investigation showed that the metallographic observations were best after this material was quenched from 1400°F and aged for 20 minutes at 300°F. The center-notched specimens, which were 2 in. wide and 0.60 in. thick, were used to measure the crack propagation rate after the above heat-treatment. The specimen blanks were cut in the rolling direction and then machined to remove any decarburized layers before being heat-treated. All specimens were then polished in a chromium trioxide-glacial acetic acid solution. The etchants and procedures were the same as those recommended by Hahn, *et al.* (Ref 57).

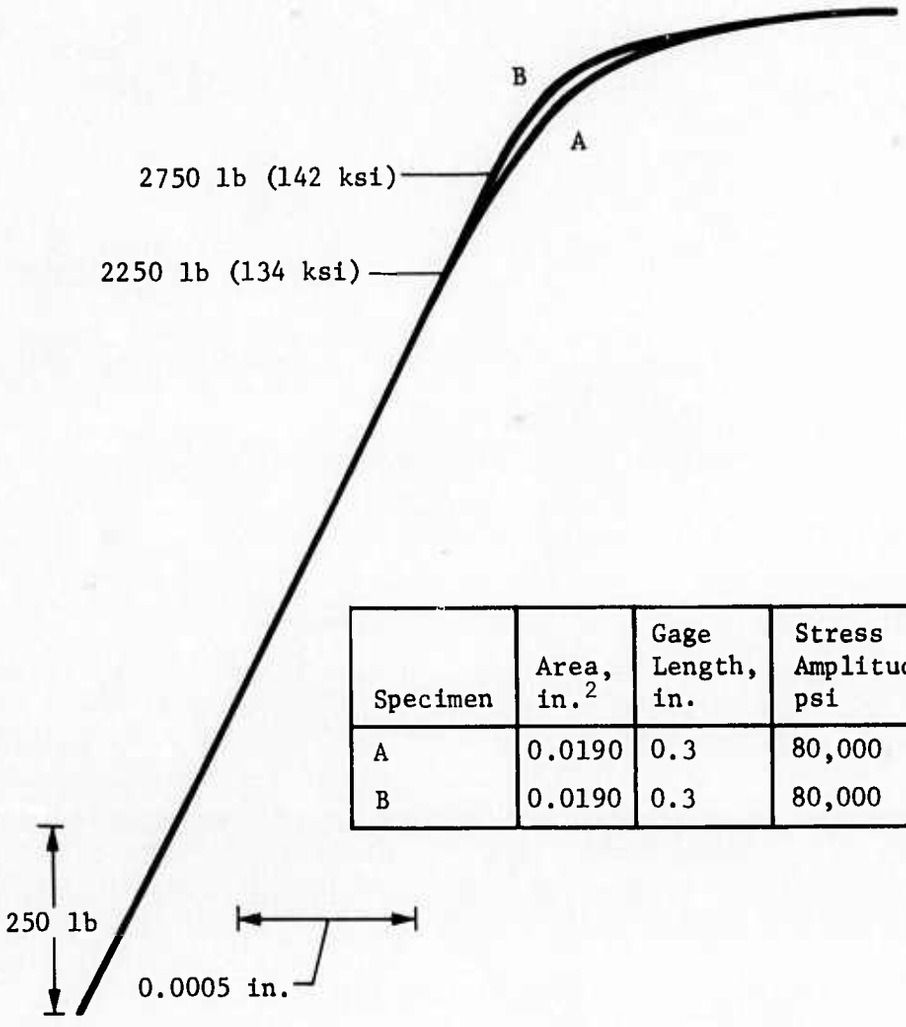

Specimen	Area, $in.^2$	Gage Length, in.	Stress Amplitude, psi	No. of Cycles
A	0.0190	0.3	80,000	15,000
B	0.0190	0.3	80,000	45,000

Fig. 1 Typical Load-Deformation Curves after Fatigue Cycling

III. RESULTS

The data presented in Fig. 2 thru 4 give the relationship between the increase in the surface layer stress, σ_s, and the number of cycles at various stress amplitude. The data may be represented by a linear curve. The asterisks designate the value of the surface layer stress at N_o, where N_o is the number of cycles required to initiate a propagating crack. Figure 5 shows N_F, the number of cycles to failure, as a function of the stress amplitude. As will be discussed later, these curves are linear when the data are plotted on a log-log basis.

The values of N_o were obtained by periodically examining the cycled specimens at 100X and 500X for the formation of propagating cracks. Depending on the particular metal and stress amplitude, the examination was made about every 2000 to 3000 cycles after some initial period. To ensure that the observations were made on propagating cracks, the crack lengths were measured as a function of the number of cycles with a graduated ocular lens. The extrapolation of the crack size data to zero length also aided in determining the value for N_o.

From the intersection of the σ_s curve at N_o, it is apparent that for all three materials propagating cracks are initiated when the surface-layer stress attains a critical value independent of the stress amplitude. These values are 11,000, 12,000, and 19,000 psi for the 4130 steel, 2014-T6 aluminum, and titanium (6Al-4V), respectively. These particular values of the surface-layer stress were obtained by dividing the increase in the load by the entire cross-sectional area.

The depth of the surface layer has been reported (Ref 39) to be about 0.002 in. for 2014-T6 aluminum strained unidirectionally. If this depth is used, then the barrier strength, σ_s', is approximately 40 times greater; i.e. $\sigma_s' \cong 40\ \sigma_s$.

The ratio of N_o / N_F was also measured to determine whether it varied with the stress amplitude. The materials used for these tests were the same, except for the 4130 steel, as those used in Fig. 2 and 3. A typical set of data relating the increase in crack length for the 4130 steel with the number of cycles at various stress amplitudes is shown in Fig. 6. The values of N_o / N_F as a function of stress amplitude for the three metals are given in Fig. 7. It is seen that, over

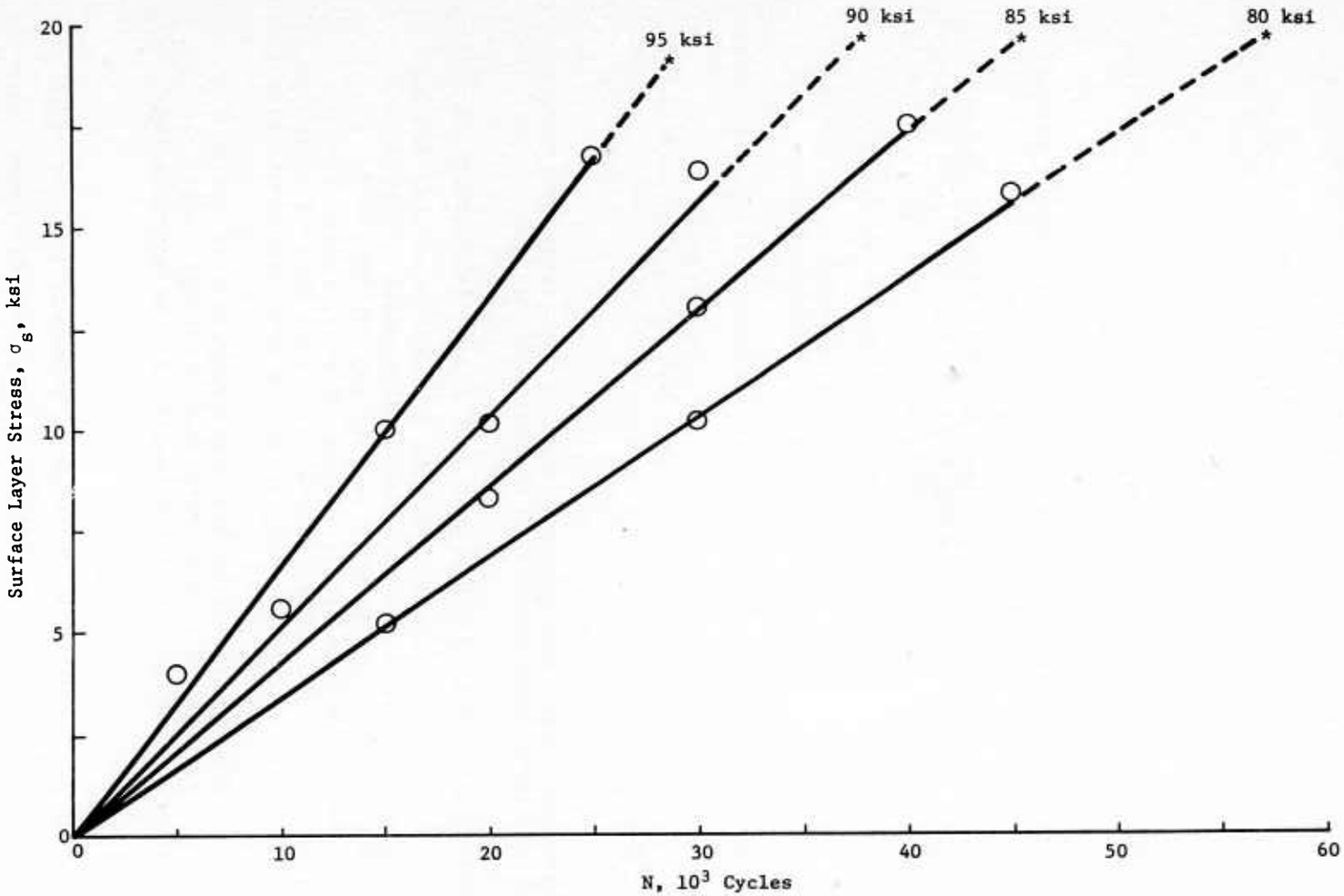

Fig. 2 Increase in Surface-Layer Stress in Titanium (6Al/4V) with Number of Fatigue Cycles and Stress Amplitude, R = -1

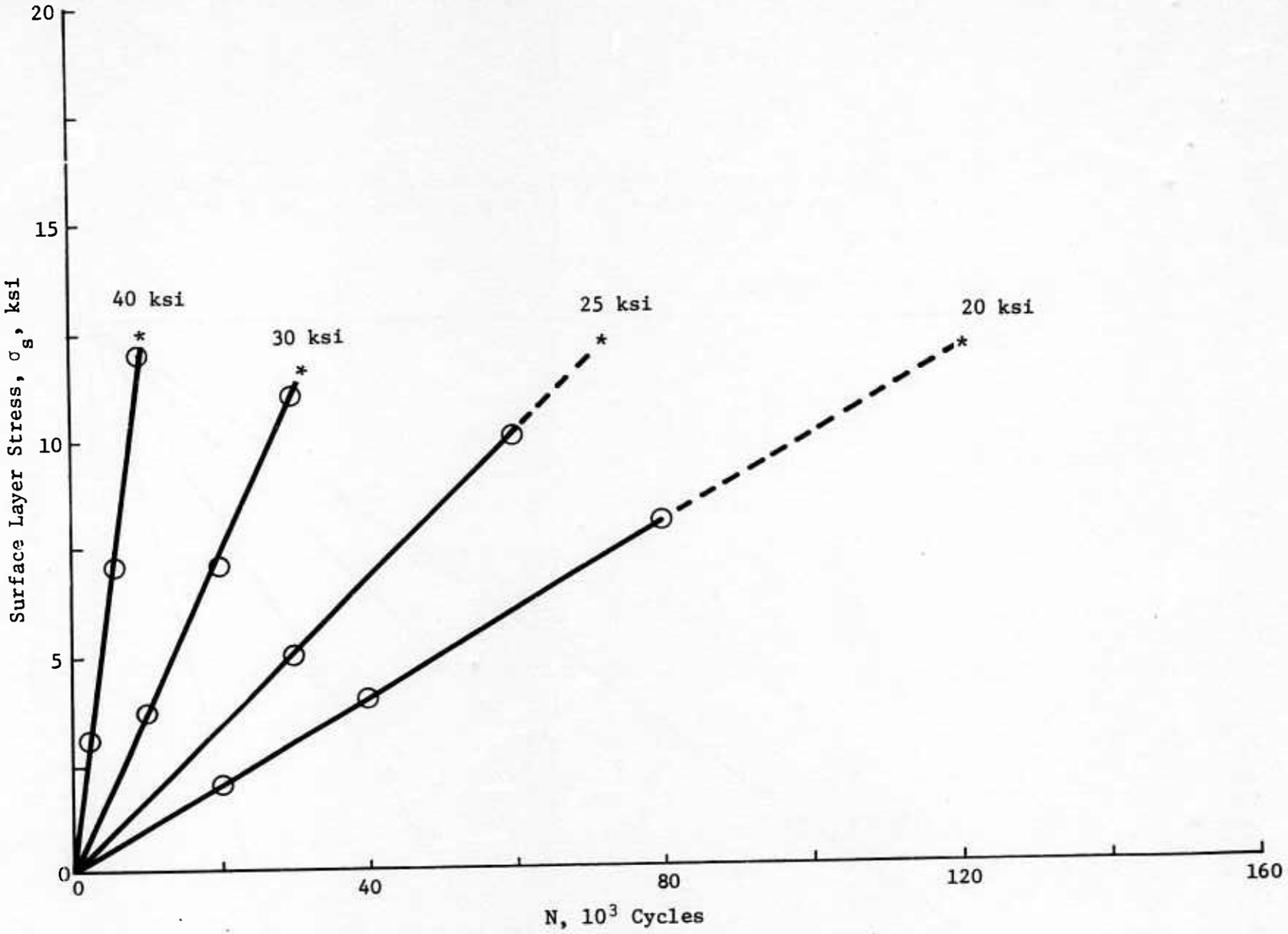

Fig. 3 Increase in Surface-Layer Stress in 2014-T6 Aluminum with Number of Fatigue Cycles and Stress Amplitude, R = -1

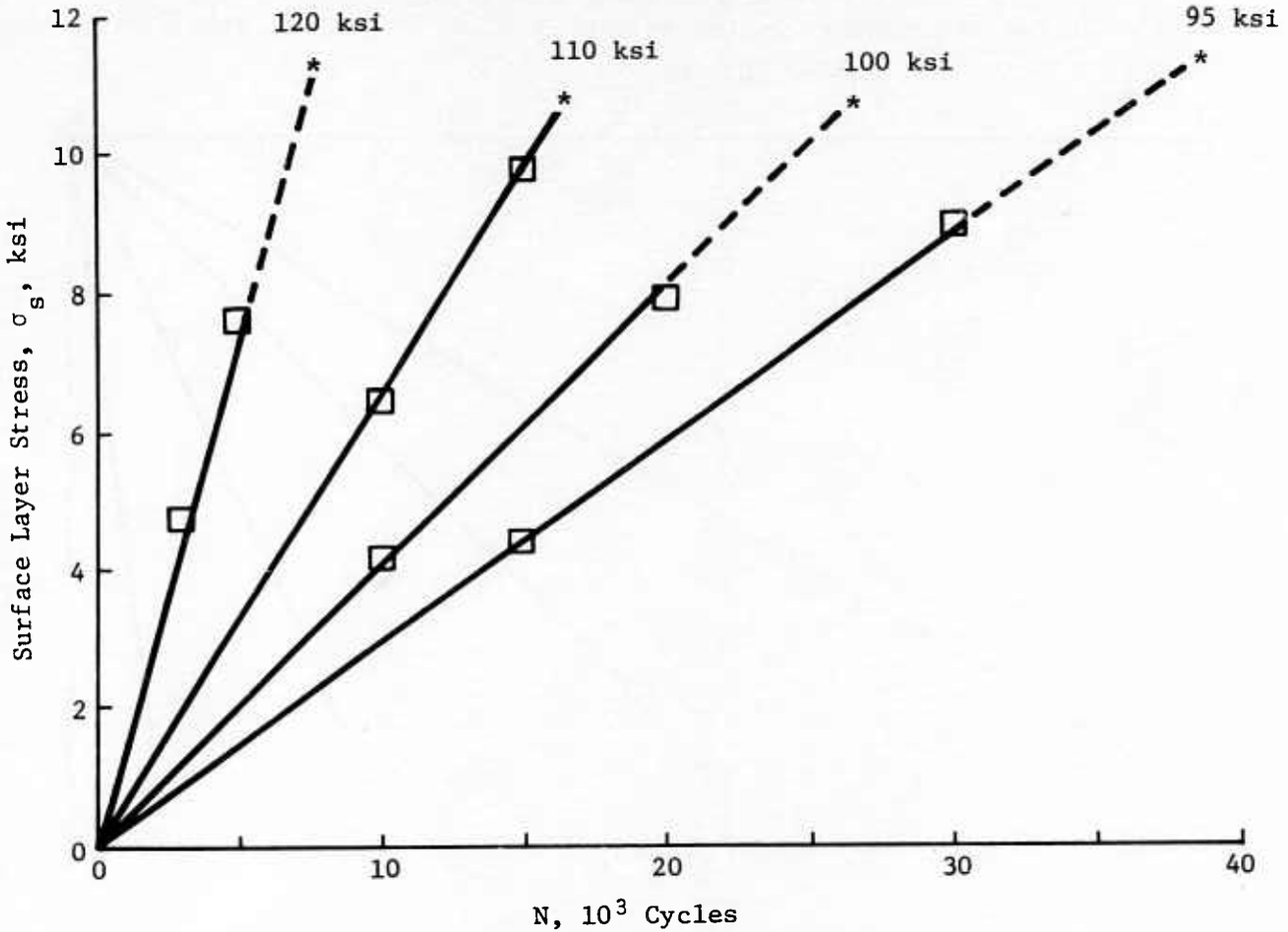

Fig. 4 Increase in Surface-Layer Stress in 4130 Steel with Number of Fatigue Cycles and Stress Amplitude, R = 1, σ_y = 180 ksi

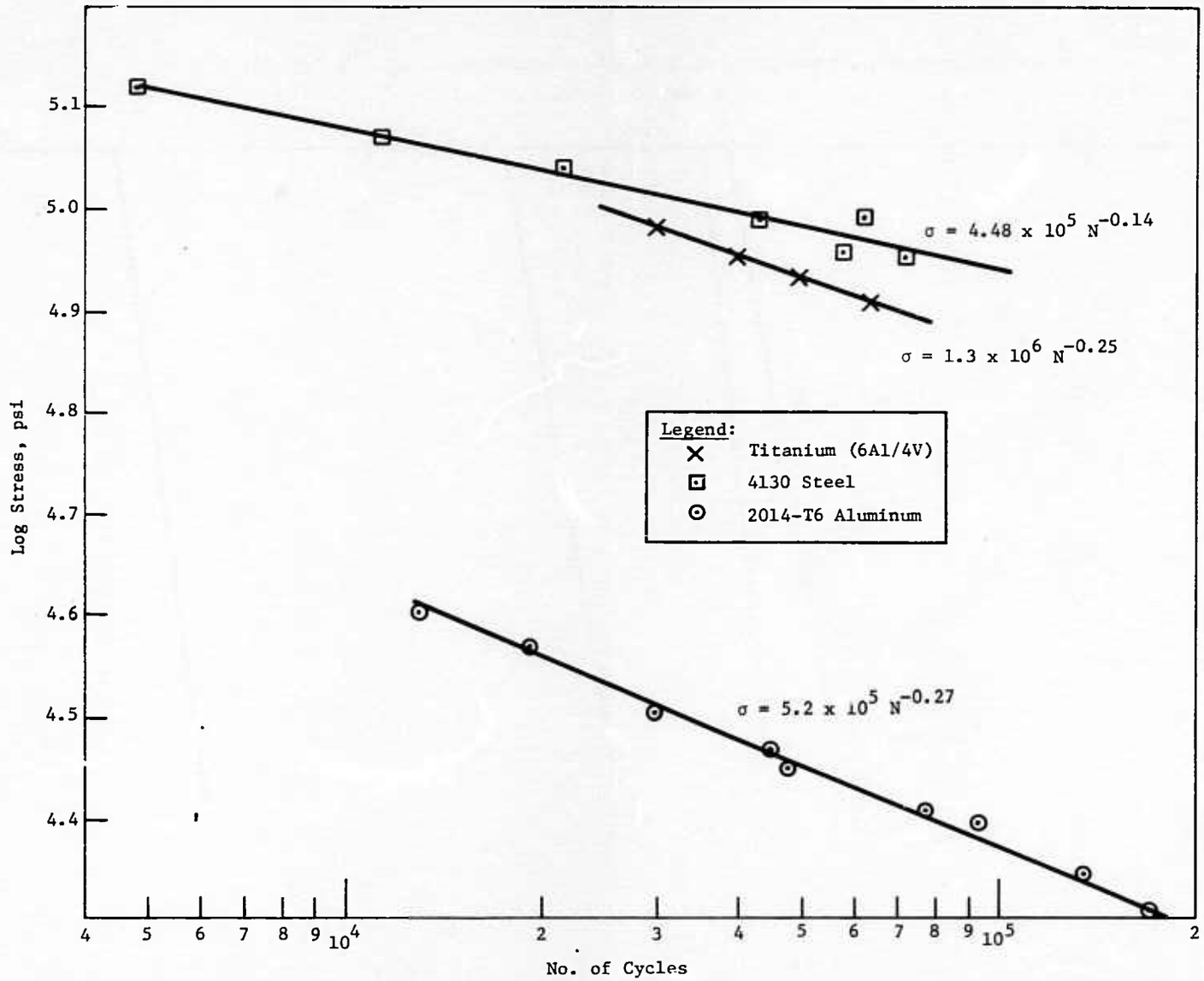

Fig. 5 Relationship between Fatigue Life and Stress Amplitude

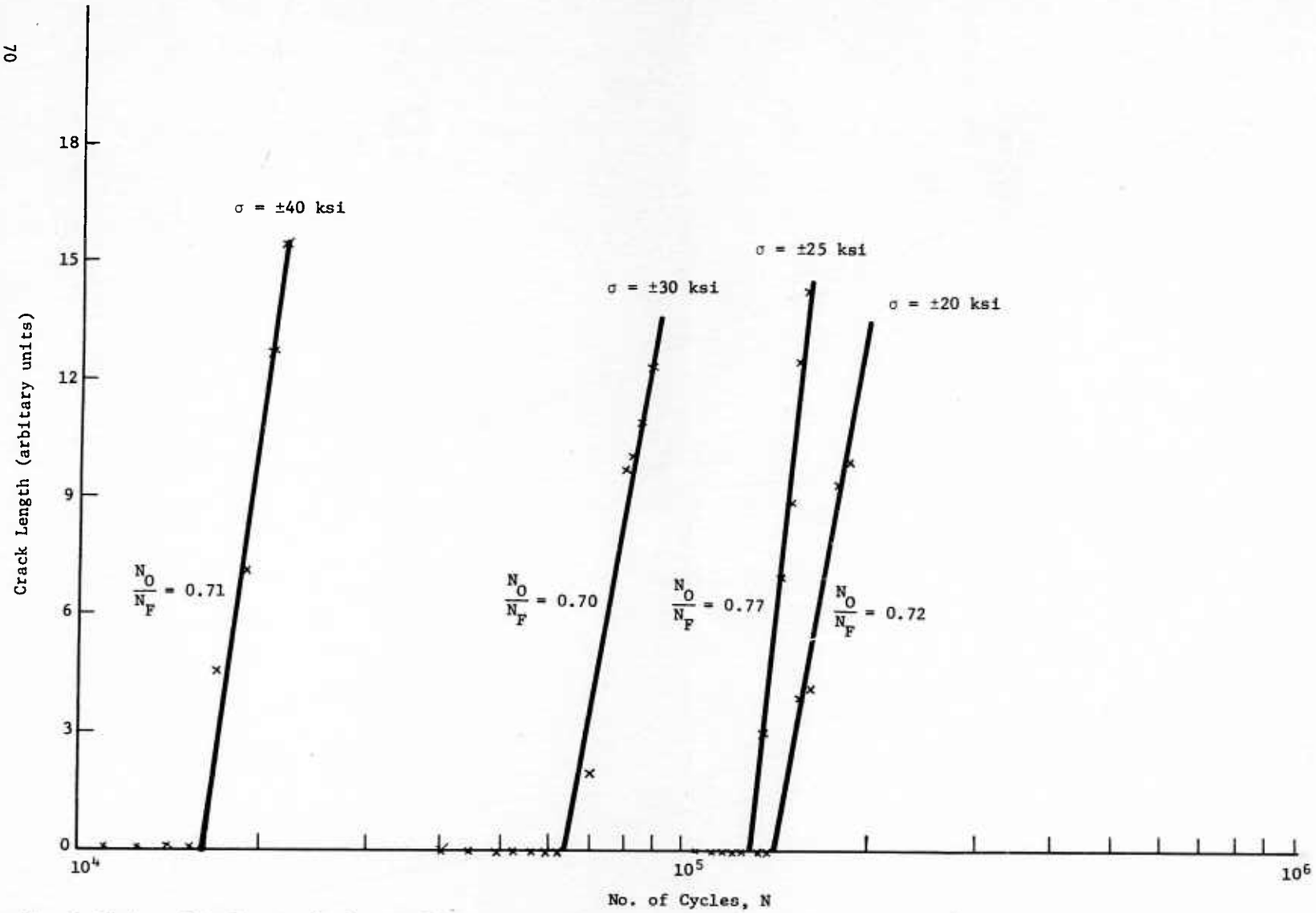

Fig. 6 Number of Cycles Required to Initiate a Propagating Crack in 2014-T6 Aluminum, Tension-Compression Cycling, R = -1

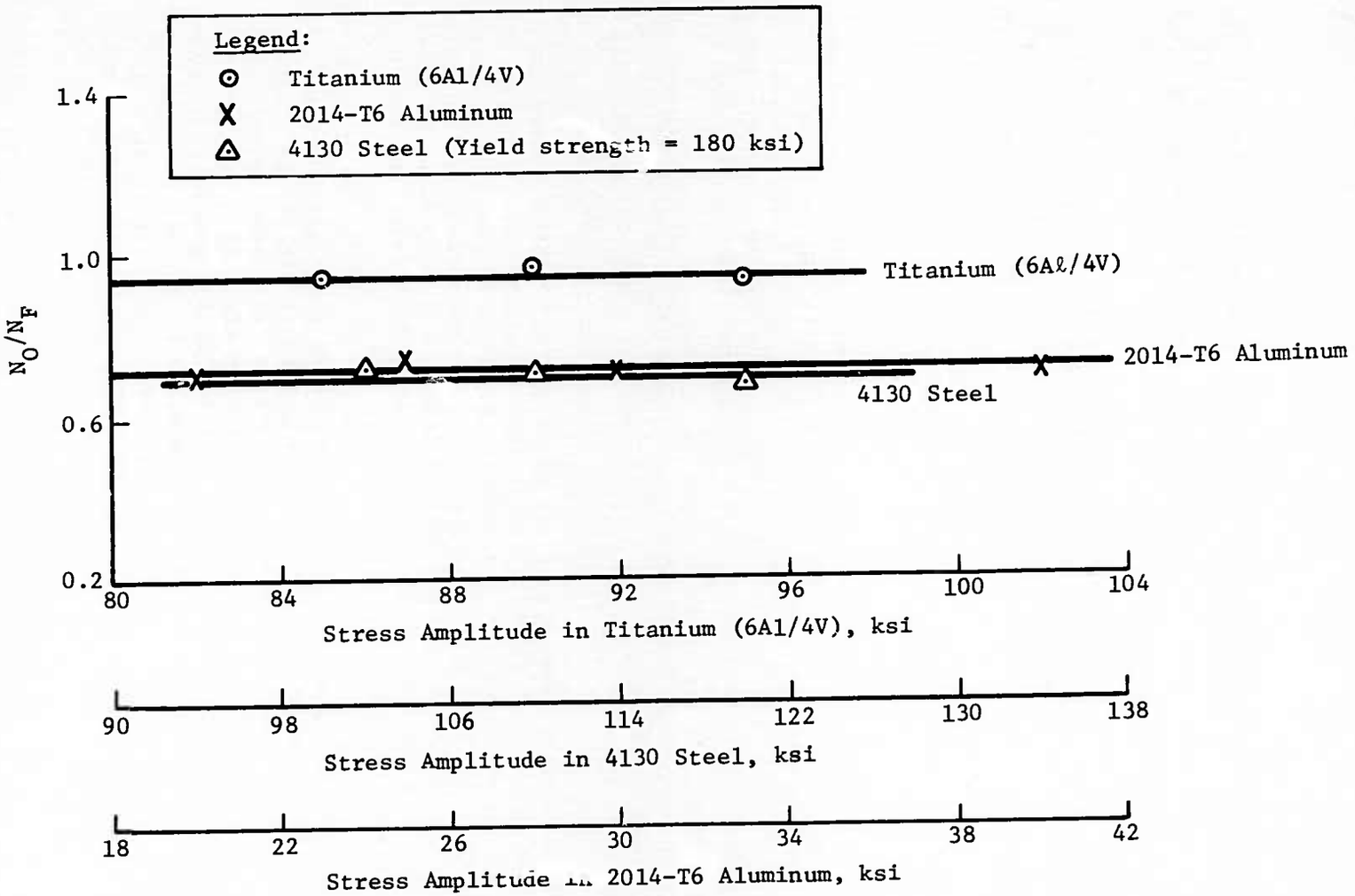

Fig. 7 N_O/N_F as a Function of Stress Amplitude

the stress amplitude employed, this ratio is independent of the stress amplitude. The average values are 0.7 for 2014-T6 aluminum and 4130 steel (YS = 180,000 psi), and 0.95 for the annealed titanium (6Aℓ-4V) alloy.

It was of interest to determine if the surface-layer stress was changed by cycling at stresses below the endurance limit. Accordingly, specimens of the aluminum were cycled 10^7 times at a stress amplitude of ±15,000 psi, and specimens of the titanium alloys were cycled up to 6×10^6 times at ±75,000 psi. No change in the surface-layer stress could be detected after these cycling periods. This indicates that below the endurance limit the surface layer does not increase (or at least increases very slowly) during stress cycling.

The effect of periodically removing the surface layer on fatigue life is presented in Fig. 8 and 9 and in Table 1. In these experiments the specimens were fatigued for various amounts, ΔN, and then the surface layer was removed by chem-milling 0.006 in. from the diameter. This process was repeated until the final diameter, D_f, was reached. Then, to determine whether the specimens suffered fatigue damage, they were cycled to failure after the final removal of the surface layer. The number of cycles required to fail the specimens is designated as N_p.

The detailed sequences used are given in Fig. 8 and 9, where the X represents the average number of cycles to failure for the uninterrupted tests, and 0 denotes the sequence employed in removing the surface layer. After each cycling period the entire surface of the specimen was carefully examined at 1200 magnification. No persistent slip bands or cracks were detected. The slip bands were faint and barely discernible at this magnification.

Figures 8 and 9, and Table 1 show that when the specimens were cycled less than about 50% of their normal life at the stress amplitudes that were employed, and when the surface layer was removed, fatigue failures did not occur. This behavior might have been expected in view of the work of others (Ref 1, 52, 53, and 54). However, in these experiments the conditions were selected so that persistent slip bands or cracks did not form. These new data, therefore, indicate that the persistent slip bands represent a *later stage of damage*.

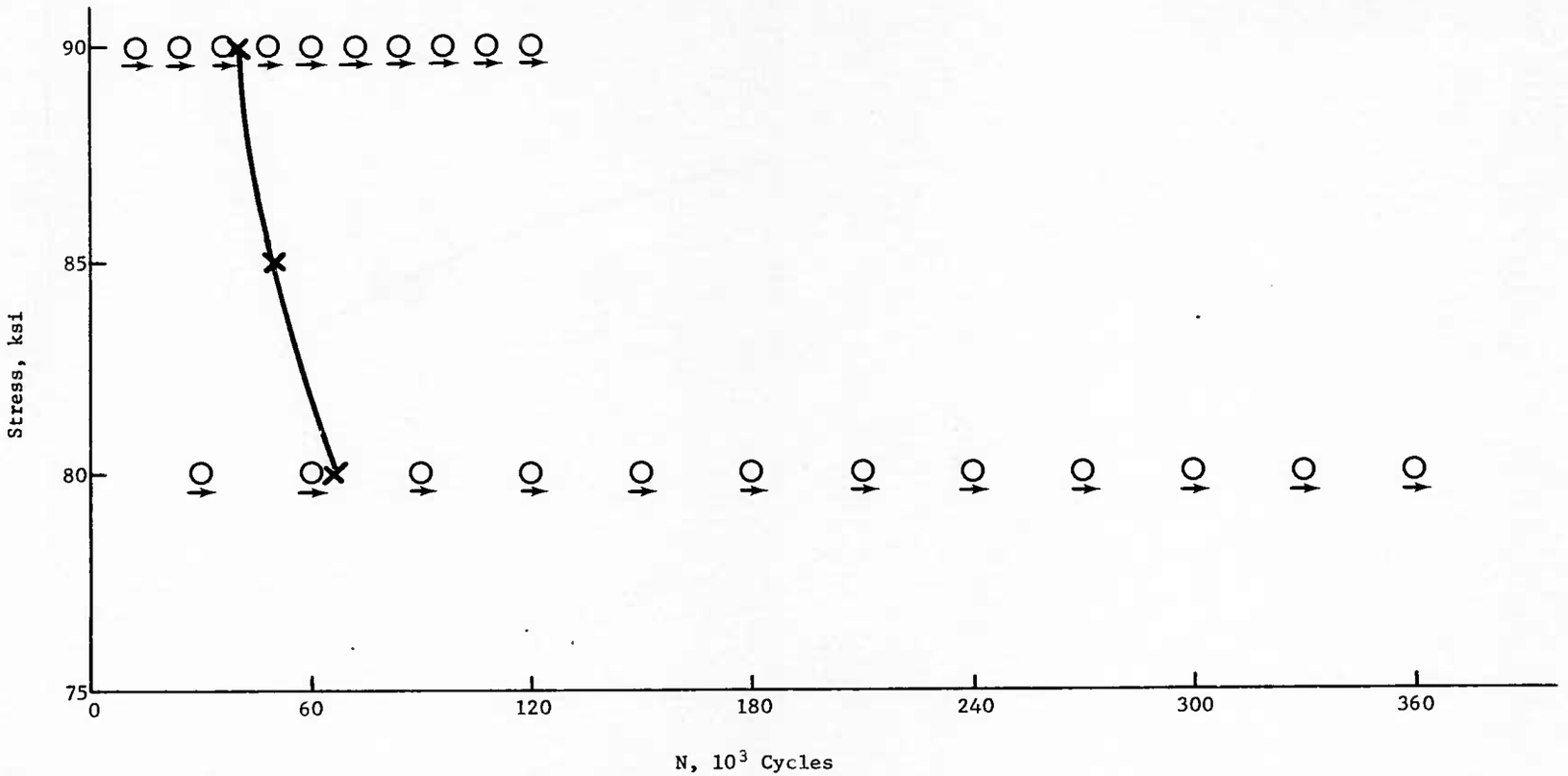

Fig. 8 Increase in Fatigue Life of Titanium (6Al/4V) by Removing Surface Layer, R = -1

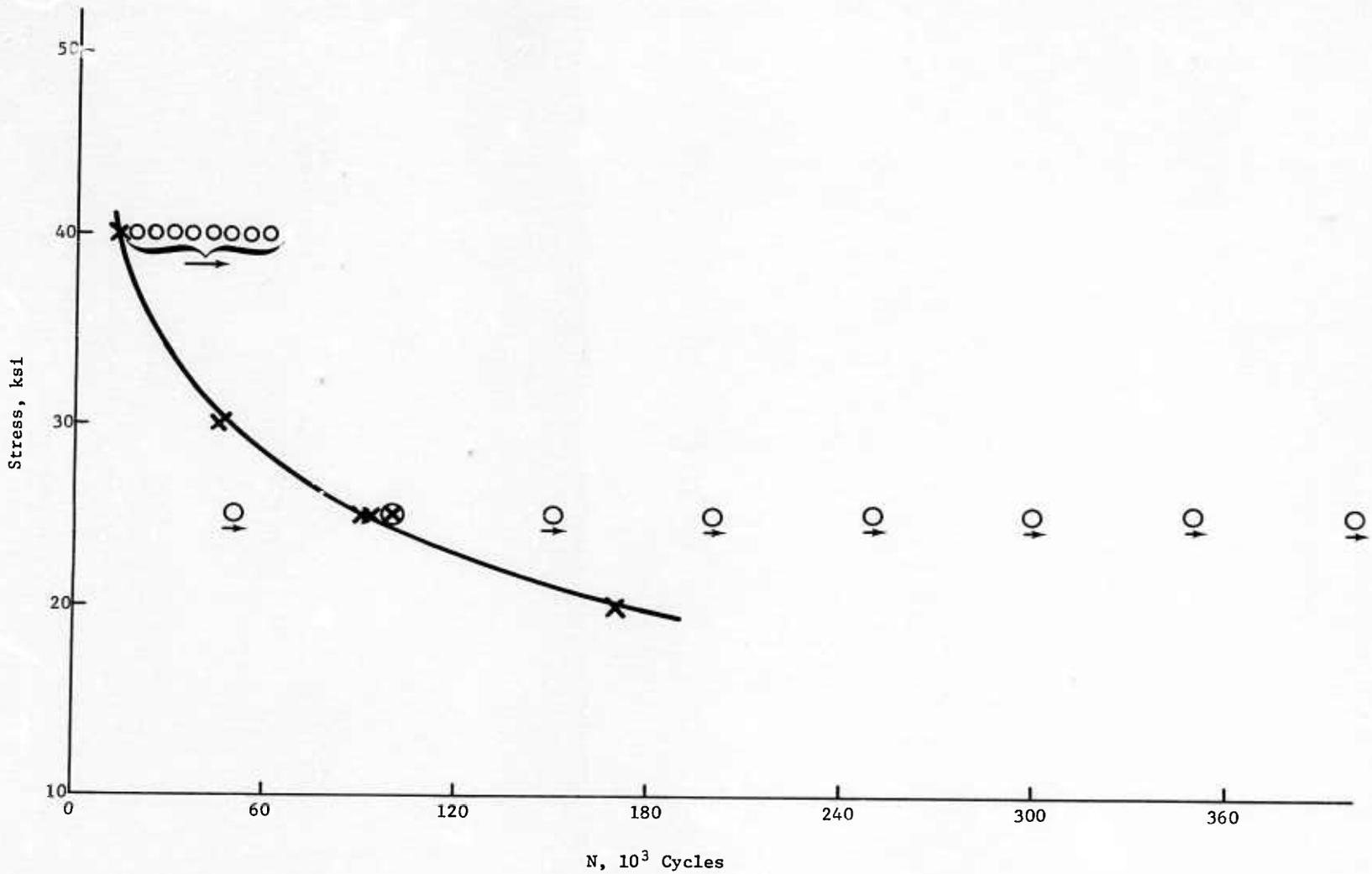

Fig. 9 Increase in Fatigue Life of 2014-T6 Aluminum by Removing Surface Layer, R = -1

Table 1 Extension of Fatigue Life by Removal of Surface Layer

Specimen Number	σ, ksi	N_F	ΔN	$\frac{N}{N_F}$	N_T	N_P	D_f, in.
Titanium (6Aℓ-4V)							
177	80	67,000	20,000	0.3	220,000	100,000	0.0523
178	80	67,000	30,000	0.45	360,000	180,000	0.0411
181	80	67,000	30,000	0.45	150,000	80,000	0.1375
179	90	40,000	12,000	0.30	132,000	63,000	0.0635
2014-T6 Aluminum							
38	25	95,000	50,000	0.53	500,000	150,000	0.598
41	40	12,000	6,000	0.5	60,000	56,000	0.489

To further investigate this hypothesis, a number of tests were conducted on the titanium and aluminum alloy specimens by fatiguing them for about 30% and 50% of their expected life, respectively, and removing only 0.001 in. from the radius between cyclic periods. This amount of removal was sufficient to remove slip band markings (at 1200X), but not the surface layer. In this case, only about a 30% increase in fatigue life was noted. It should also be stated that removing 0.010 in. from the diameter gave the same results as those obtained by removing only 0.006 in.

These results are in agreement with the conclusions reached by Grosskreutz (Ref 2) to the effect that cycling copper specimens did not produce damage in the unbroken portions. The data in Table 1 show that after the prolonged fatiguing and surface-layer-removal treatment, the residual fatigue resistance was unaffected. In fact, the number of cycles for failure, N_p, was always larger than that required to fail the specimens in the uninterrupted test. That is, $N_p > N_F$, even though the specimens were cycled 5 to 10 times their normal life.

The effect of the surface layer on crack propagation is shown in Fig. 10 thru 12; the data for 2014-T6 aluminum (Fig. 10) were obtained from compact tension specimens 1 in. thick. As previously described, some of the tests were run with specimen that had been prestressed to the proportional limit (58,000 psi) and for which the surface layer had not been removed, whereas for the SLE specimens, the surface layer was removed by chem-milling 0.005 in. from each face. It is quite apparent that the crack propagation rate of the prestressed specimen (which initially had a high surface-layer stress) is much higher than that of the untreated specimen. However, when the surface layer was removed, the crack propagation rate was much smaller than that of the untreated specimens. In addition, for the SLE-treated specimens, the numer of cycles required to initiate the crack increased from 100,000 to 250,000 cycles. Because there is a very small amount of plastic deformation imparted by prestressing to the proportional limit, a small compressive residual stress may be expected in those specimens that were not chem-milled after the prestressing treatment. This small compressive stress would not be expected to have any major effect. Moreover, the effect of the compressive stress--if any--would be to decrease the crack propagation rate, but the opposite effect was noted.

The effect of the surface layer on the crack propagation in titanium 6Aℓ-4V is shown in Fig. 11. For the SLE treatment the specimens were stressed to 110,000 psi, the proportional limit. To assess the effect of over-stressing, specimens were also stressed to 130,000 and 133,000 psi. A comparison between the crack propagation rates, da/dN, in terms of the change in the stress intensity, ΔK, for the untreated and the SLE-C treated specimens again shows that eliminating the surface layer decreased the crack propagation rate. At the higher ΔK values, the surface layer tends to reform and, as may be expected, the two curves, A and B, tend to coincide.

Comparing these two curves with two other curves (C and D) obtained from the overstressed specimens shows that large amounts of plastic strain have a very detrimental effect on crack propagation resistance, even when the surface layer is removed. We suspect that this decrease in the crack propagation rate may be associated with ruptures at inclusion-matrix interfaces that might produce local free surfaces and possibly unpin dislocations from precipitates.

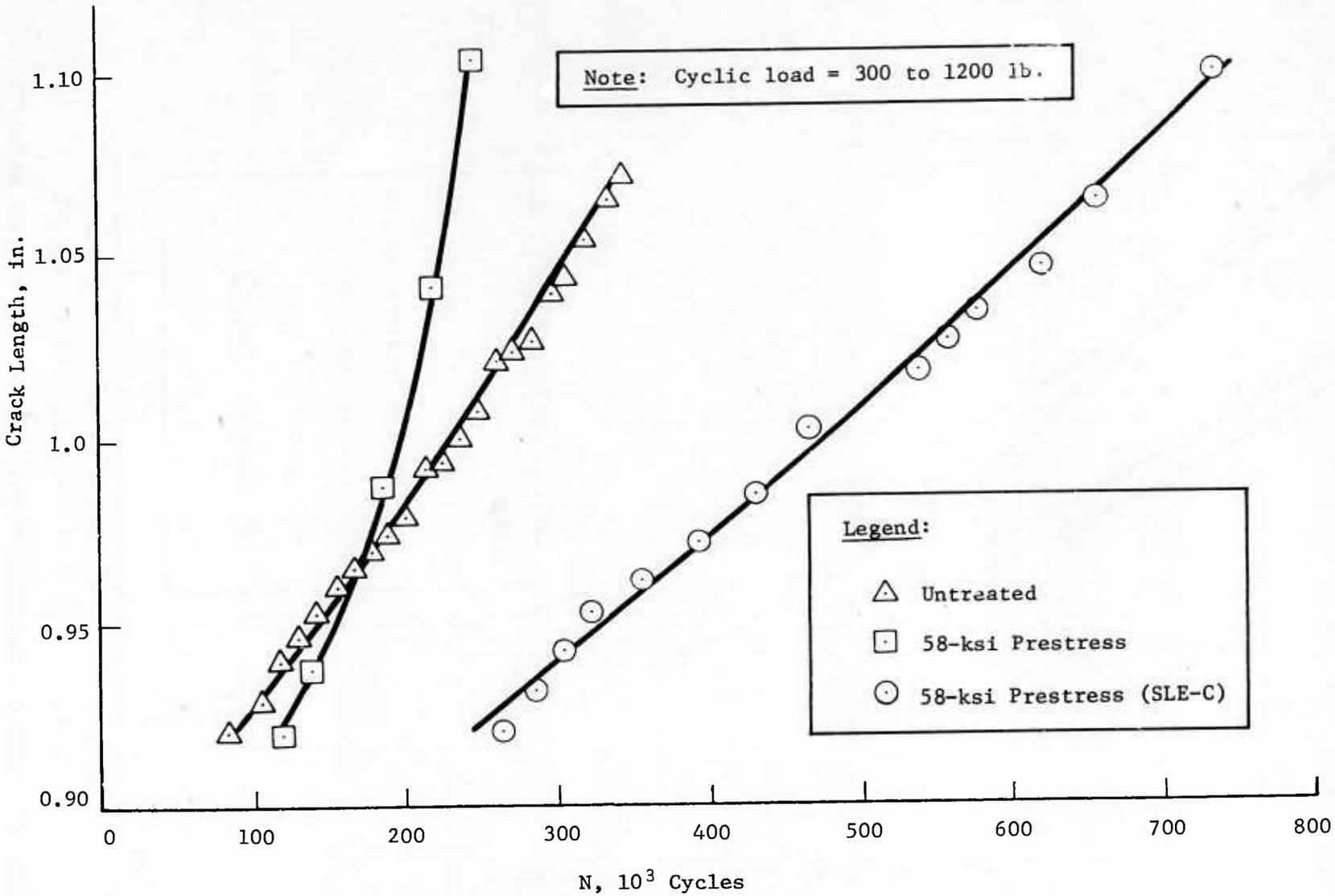

Fig. 10 Crack Propagation Behavior of 2014-T6 Aluminum under Plane Strain Conditions, Compact Tension Specimens 1-in. Thick

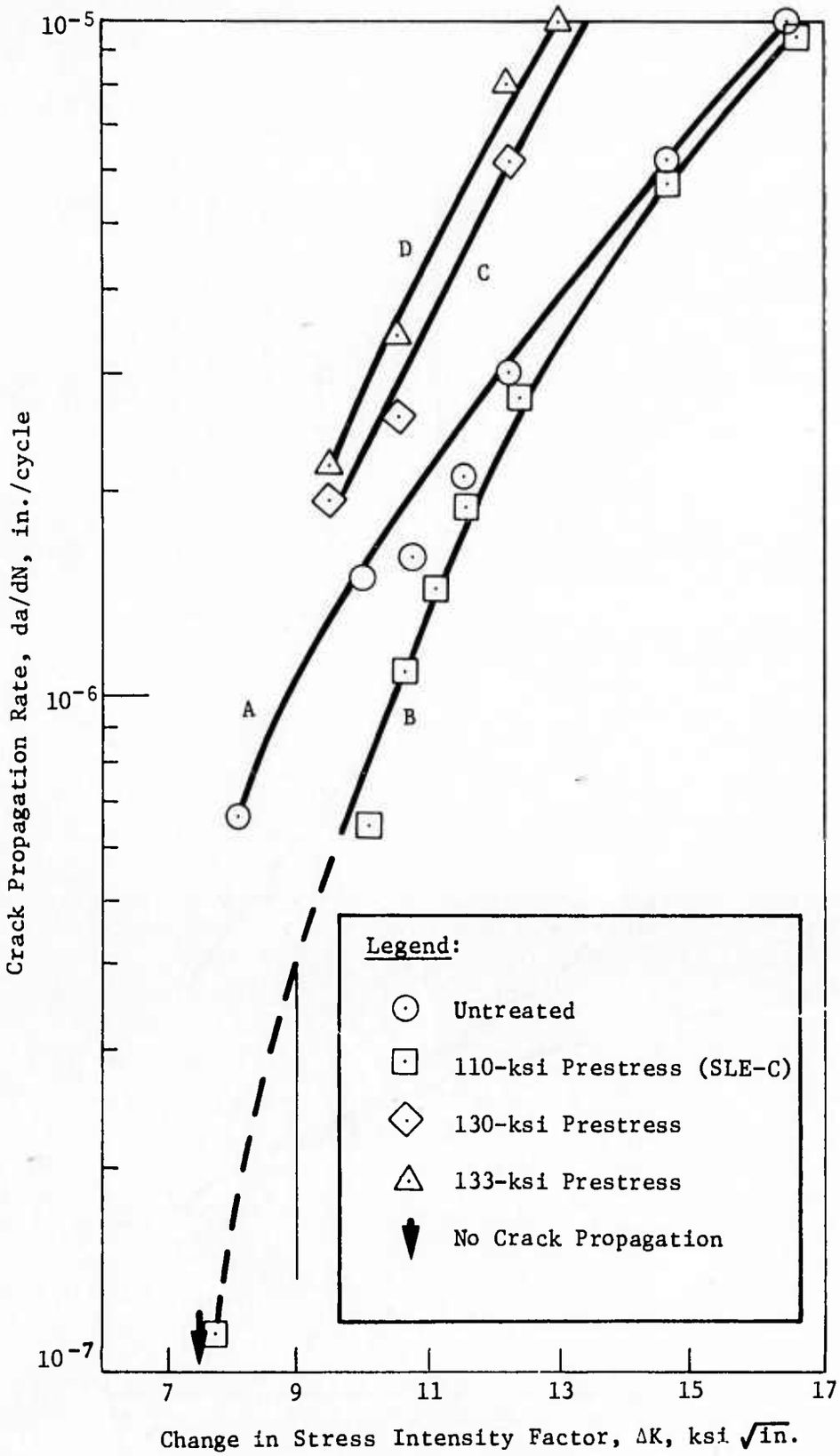

Fig. 11 Crack Propagation Behavior of Titanium (6Al-4V) under Plane Stress Conditions, Center-Cracked Specimens 0.067-in. Thick

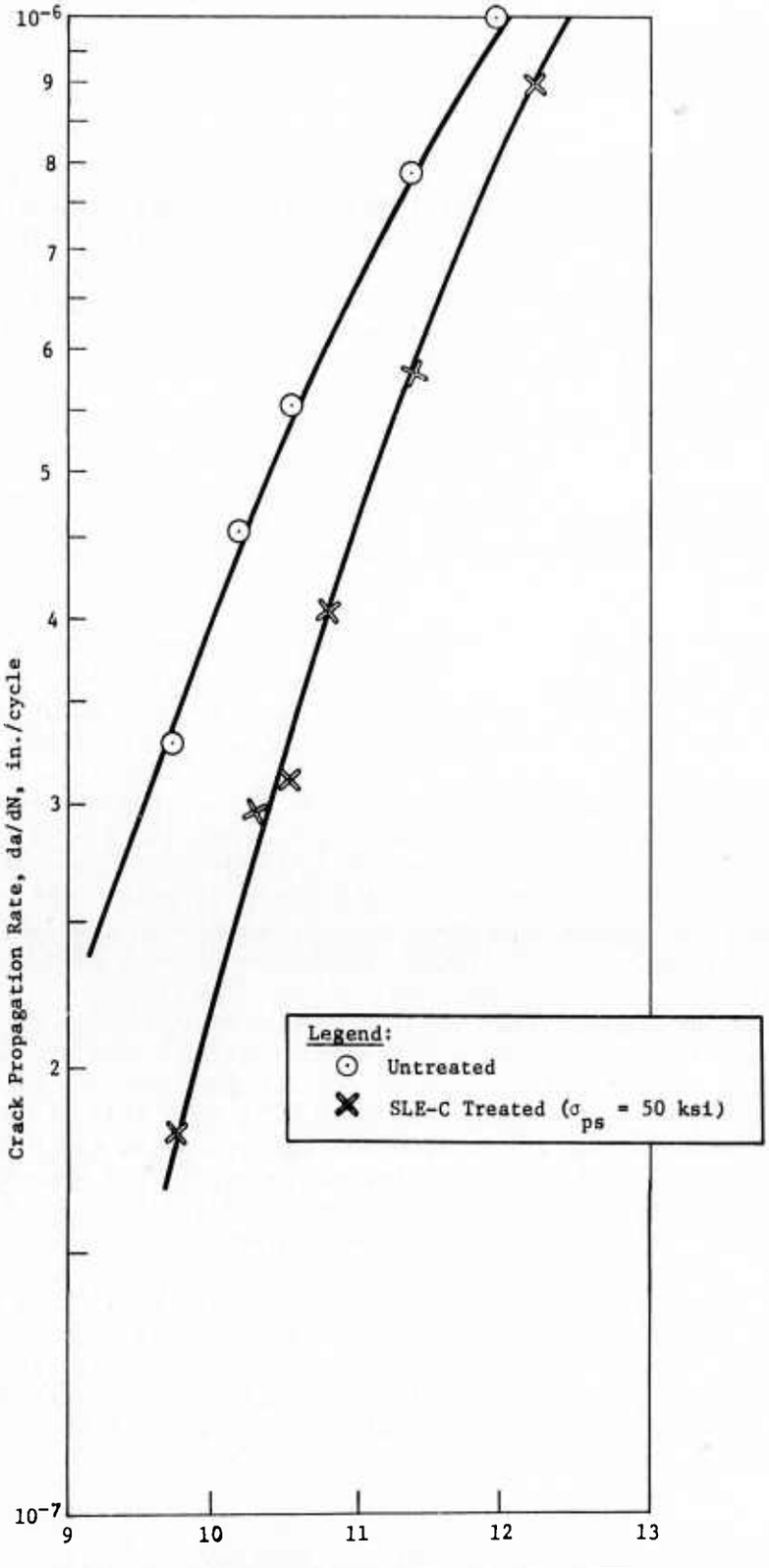

Fig. 12 Crack Propagation Rate of Fe/3% Si under Plane Stress Conditions

As previously discussed, the possibility that the large amount of plastic strain may precondition the rate of formation of the surface layer stress at the crack tip should not be discounted (Ref 31 and 32). Similar effects were found when 7075-T6 aluminum was overstressed small amounts. In this case, additional aging for 1 hr at 250°F after the prestress restored the fatigue resistance (Ref 32).

Additional evidence for the detrimental effect of the surface layer was found through an etch-pit and crack propagation investigation of Fe/3% Si alloy. The data presented in Fig. 12 compare the relationship between the crack propagation rate and the change in stress intensity factor, ΔK, for the SLE-treated and untreated specimens of this alloy.

The SLE-treated specimens were stressed to 50,000 psi (proportional limit) and the surface layer was removed by polishing 0.005 in. from each surface with the chromium trioxide-glacial acetic acid solution. Dislocation etch pits did not form during this polishing operation.

Figure 12 shows that the elimination of the surface layer initially increased the crack propagation resistance. At the low ΔK values, the improvement is about a factor of 2. (Similar to our other results, the two curves tend to meet at the high ΔK values.) The number of cycles required to initiate cracking increased from 290,000 to 400,000 for a stress amplitude of 6250 to 25,000 psi ($R = 0.25$).

The micrographs in Fig. 13 show the difference in the dislocation density in the vicinity of the crack. These micrographs were obtained as a function of depth from the surface of the fatigue specimen after the crack had propagated to a length, 2a, of 0.4783 in. This corresponds to about 490,000 and 700,000 cycles for the untreated and SLE-treated specimens, respectively. For these micrographs, the specimens, after cycling, were etched after removing 0.001, 0.003, and 0.006 in. from the surface through the use of 1 μ diamond paste.

It should be apparent that the dislocation etch pit density in the uncracked portion of the untreated specimen is greater than that for the SLE-treated specimens. Furthermore, for the untreated specimens the dislocation density *decreases* with the distance from the surface, while for the SLE-treated specimens, the dislocation density was essentially constant with depth.

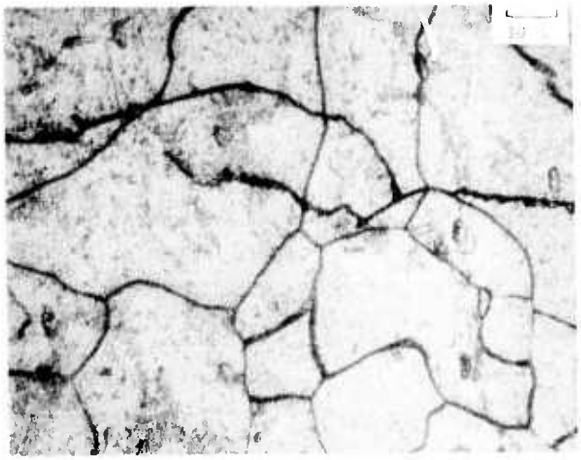

(a) Δx = 0.001 in.

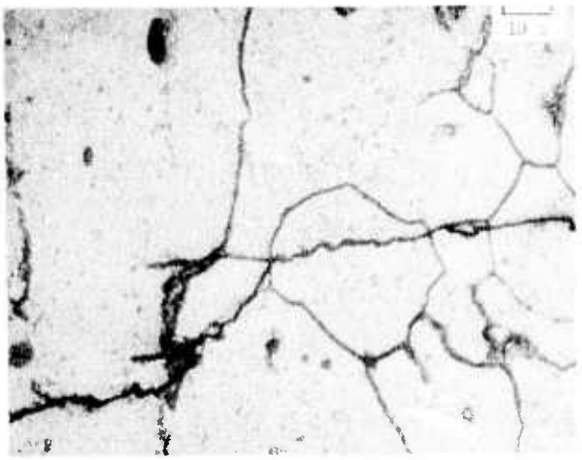

(d) Δx = 0.001 in.

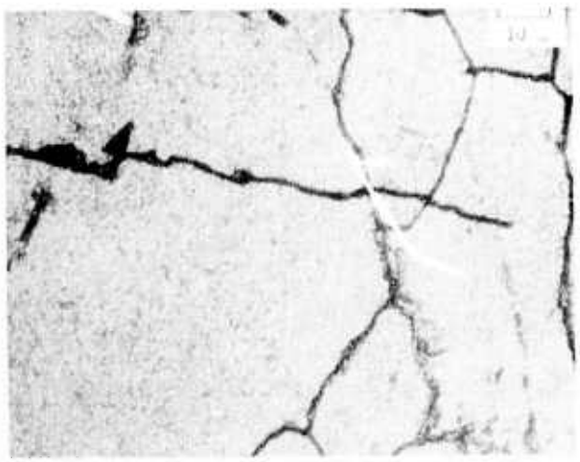

(b) Δx = 0.003 in.

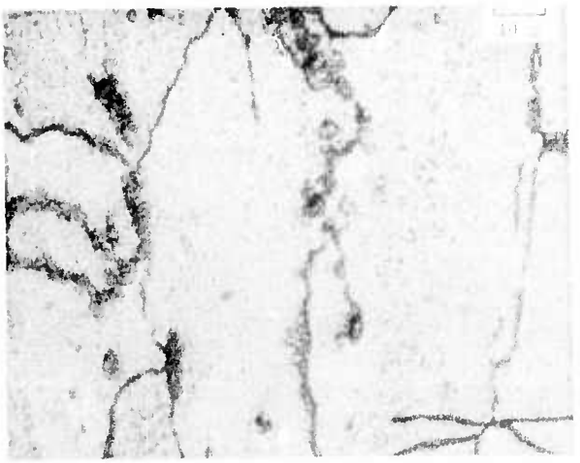

(e) Δx = 0.003 in.

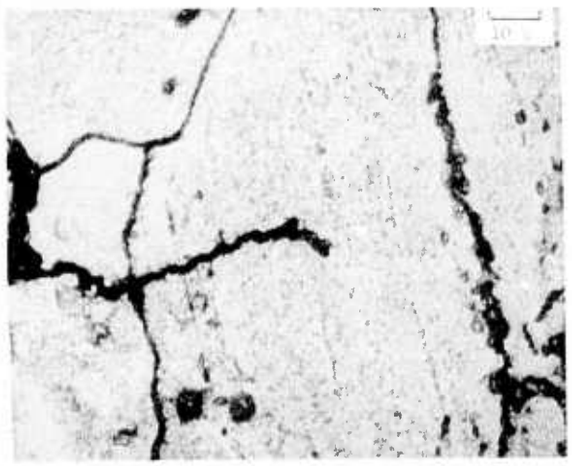

(c) Δx = 0.006 in.

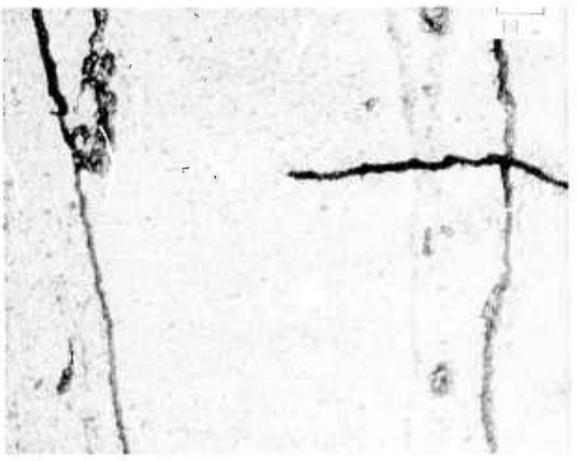

(f) Δx = 0.006 in.

Fig. 13 Dislocation Density as a Function of Depth, Δx, in Vicinity of Crack in Untreated (a, b, c) and SLE-Treated (d, e, f) Fe/3% Si

IV. DISCUSSION OF RESULTS

As seen from Fig. 2 thru 4, a linear relationship exists between the surface layer stress, σ_s, and the number of stress cycles. A cross plot of these data gives the slope as a function of the stress amplitude (Fig. 14). For the aluminum and titanium, as well as for the 4130 steel, a linear curve is obtained when the log of the slope is plotted against log σ, where σ is the stress amplitude. Accordingly,

$$S = k\,\sigma^{P} \qquad [1]$$

where $S = \frac{d\,\sigma_s}{dN}$;

and from Fig. 2 thru 4,

$$\sigma_s = SN, \qquad [2]$$

or

$$\sigma_s^{*} = S\,N_o, \qquad [2a]$$

where σ_s^{*} is the surface layer stress at N_o.

From Eq [1] and [2a]

$$o = \left(\frac{\sigma_s^{*}}{N_o k}\right)^{b}, \qquad [3]$$

where $b = \frac{1}{p}$.

Equation [3] implies a linear relationship between log σ and log N_o. The relationship for fatigue failure, N_F, and stress (Fig. 5) conform to this relationship and is in accord with Basquin (Ref 58). Using the data from Fig. 2, 3, 4, and 14, as well as Eq [3], it can be shown that N_o and N_p have the same stress dependence. In particular:

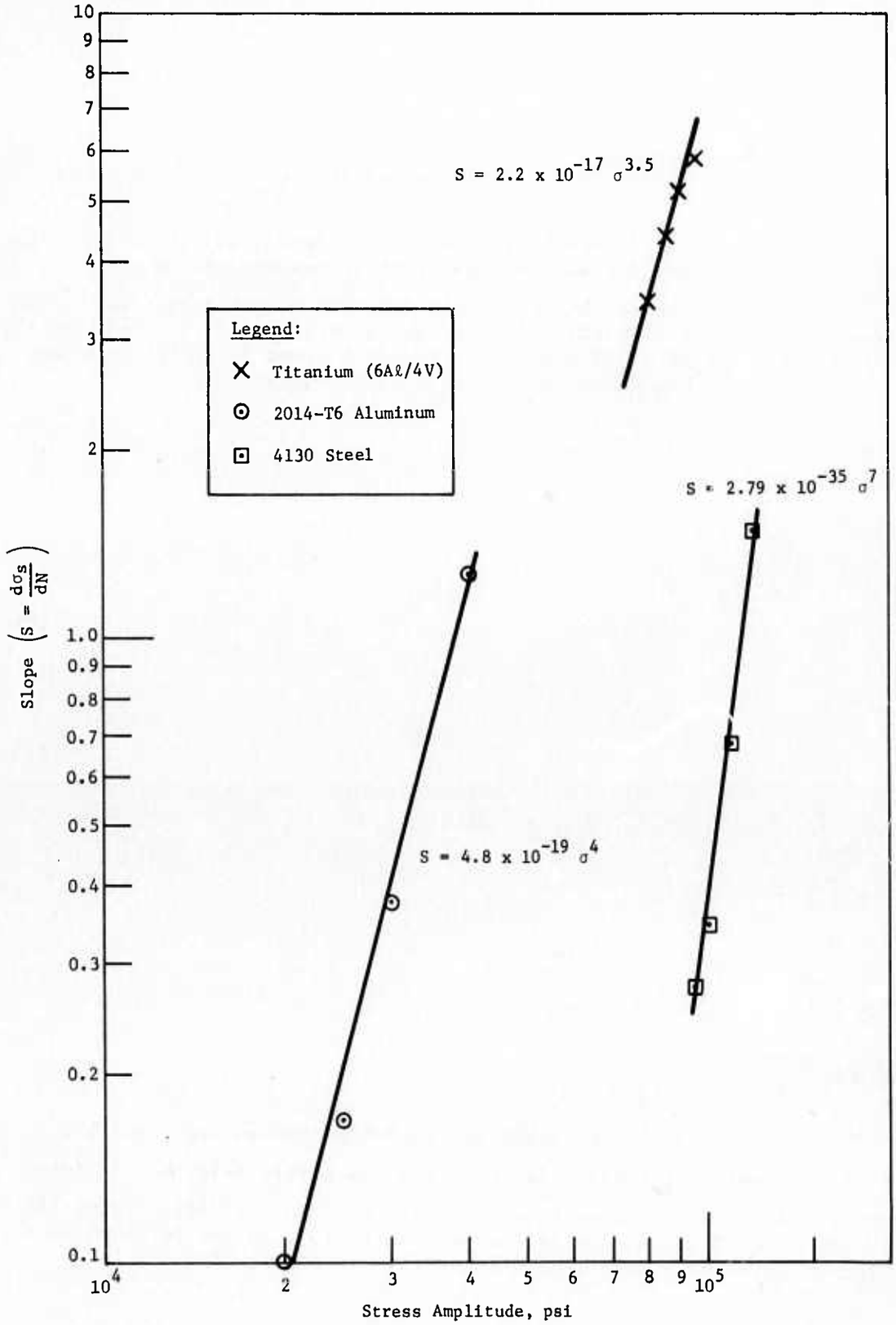

Fig. 14 Relationship between Slope and Stress Amplitude

1) For titanium (6Al-4V):

$$S = 2.2 \times 10^{-17} \sigma^{3.5} \quad [4]$$

$$\sigma = 4.2 \times 10^{5} N_o^{-0.3} \quad [4b]$$

$$\sigma = 10^{6} N_F^{-0.3} \quad [4c]$$

2) For 2014-T6 aluminum:

$$S = 4.8 \times 10^{-19} \sigma^{4} \quad [5]$$

$$\sigma = 4.0 \times 10^{5} N_o^{-0.25} \quad [5b]$$

$$\sigma = 4.3 \times 10^{5} N_F^{-0.25} \quad [5c]$$

3) For 4130 steel:

$$S = 2.79 \times 10^{-35} \sigma^{7} \quad [6]$$

$$\sigma = 3.26 \times 10^{5} N_o^{-0.14} \quad [6b]$$

$$\sigma = 4.48 \times 10^{5} N_F^{-0.14} \quad [6c]$$

It is also of interest to note that the linear addition of the curves in Fig. 2 thru 4 leads to a cumulative damage rule similar to that proposed by Miner (Ref 59). If the fatigue damage to initiate a propagating crack is represented by D, then

$$D = \frac{\sigma_s}{\sigma_s^*} , \quad [7]$$

and a crack will be initiated when

$$\sum \frac{\sigma_{si}}{\sigma_s^*} = 1, \quad [8]$$

or from Eq [2] and [2a] when

$$\sum \frac{N_i}{N_o} = 1. \qquad [9]$$

This suggests that deviations from the linear cumulative rule may be measured by the changes in the surface-layer stress as a function of prior cyclic history.

In considering fatigue process it is usually informative to consider both the initiation and propagation phases. In view of Fig. 5 and Eq [4] thru [6c], we may write

$$N_F = N_o + N_P = K_1 \sigma^{-\frac{1}{b}}, \qquad [10]$$

where N_P is the number of cycles required to propagate the crack to fail the specimen. Since N_o and N_P have the same stress dependence,

$$N_o = K_o \sigma^{-\frac{1}{b}}, \qquad [11]$$

$$N_P = K_P \sigma^{-\frac{1}{b}}, \qquad [12]$$

and

$$\frac{N_o}{N_F} = \frac{K_o}{K_P + K_o} = \text{constant}. \qquad [13]$$

Equation [13] is in agreement with the data presented in Fig. 7.

The experimental data in this investigation lend support to the concept that fatigue failures originate primarily in the surface layer. In particular, it was shown that propagating fatigue cracks form when the surface-layer stress attains a critical value. Support for the relationship between the surface layer and fatigue may be found in the series of experiments that showed the fatigue life is *not* extended when only slip bands are removed--the removal of the surface layer was also required. Additional support is provided by noting that decreasing the initial

value of the surface-layer stress decreased the crack propagation rate, and that, vice versa, the crack propagation rate increased under environmental conditions that increased the surface-layer stress.

The process may be described in terms of Fig 2 thru 4, where it was shown that the surface-layer stress increased with the number of cycles. In short, any procedure that removes or decreases the surface layer--either by physical, chemical, or thermal means--merely increases the number of cycles required for the surface layer to reach a critical value. The extension of fatigue life will depend on the amount of decrease in the surface-layer stress and the number of cycles before removal of the surface-layer stress. When cracks are present, it will be necessary to remove both the crack and the surface layer at the root of the crack.

The observed results suggest that the surface layer tends to act as a barrier to support an accumulation of dislocations that behaves similar to a "pileup" array. Fracture models in terms of linear arrays of dislocations, have been treated by Stroh (Ref 51), Zener (Ref 60), and Cottrell (Ref 61). The evidence that the surface layer can affect fracture behavior may also be found in an investigation concerned with the ductile-brittle transition temperature of molybdenum (Ref 62). In that investigation, the surface layer was continuously removed electrochemically at a rate of 6×10^{-4} in. per minute while the specimens were deformed. As shown in Fig. 15 (presented here for convenience), the ductile-brittle transition temperature was decreased 15°C by removing the surface layer. The temperature increase due to the electrochemical heating was only 0.5°C. In comparison, changing the strain rate by a factor of 100 decreased the transition temperature 25°C.

In those earlier studies, it was considered that the decrease in the ductile-brittle temperature may be explained in terms of the decrease in the barrier strength of the surface layer resulting from the electrochemical removal. Similarly, we propose that during fatigue cycling the barrier imposed by the surface layer increases in strength until, in the region of the slip bands near the surface (surface layer), the stress field from the accumulation of dislocations of like sign exceeds the fracture strength. At this point a crack will form. The crack will only propagate a small distance until it reaches a region where the stresses are less than the fracture strength. The distance traveled depend on the gradient of dislocations in the surface layer and the applied stress. During the next cycle(s) the crack propagates because the surface layer stress in the front of the crack increases very rapidly. Environmental effects may be explained simply in terms of their influence on the rate of formation of the surface-layer stress. That is, as explained earlier, conditions that decrease the surface-layer stress (such as vacuum)

increase the fatigue life, while conditions that increase the surface-layer stress decrease the fatigue life [e.g., CH_3OH-HCl for titanium, and $CuNO_3$ + NH_4OH for Cu (Ref 34)]. Any process that reduces the surface layer--such as annealing, chem-milling, etc--should extend the fatigue life.

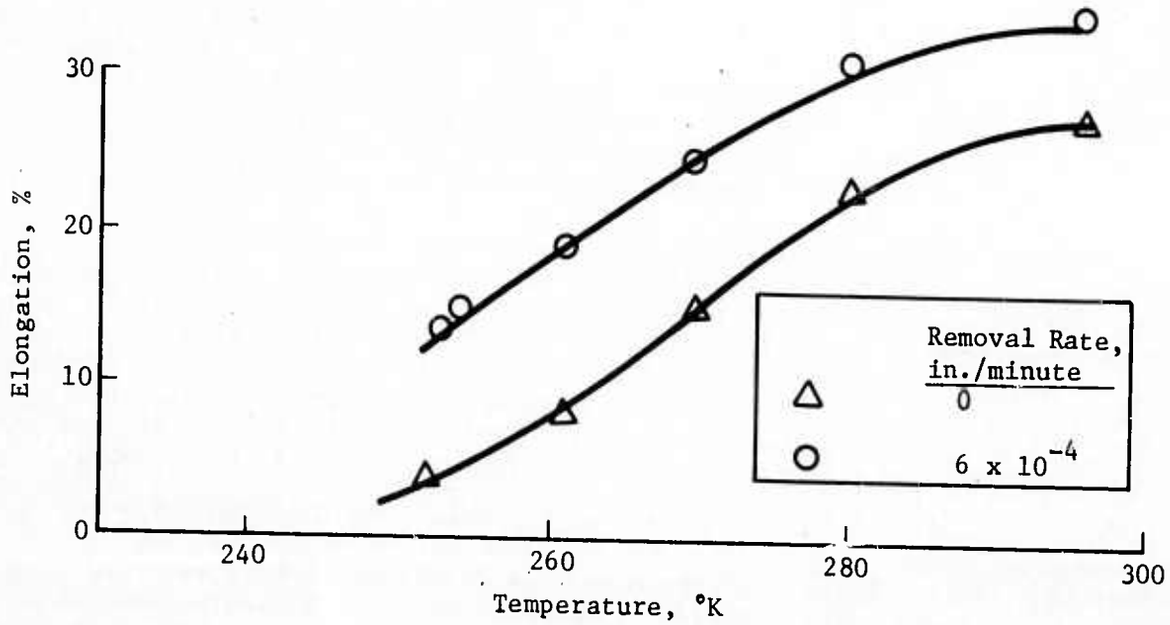

Fig. 15 Effect of Removing Surface Layer on the Ductile-Brittle Transition Temperature of Molybdenum (from Ref 9)

V. SUMMARY

1. The surface-layer stress was measured as a function of the number of stress cycles for 2014-T6 aluminum, annealed titanium (6Al-4V), and 4130 steel. The data show that a propagating fatigue crack forms when the surface-layer stress attains a critical value.

2. From the relationship of surface-layer stress, fatigue life, and stress amplitude, it was shown that

$$\sigma = \left(\frac{\sigma_s^*}{N_o^k} \right)^b$$

3. For the materials employed, it was shown that extending the fatigue life by surface removal techniques requires the elimination of the surface layer. Removing only slip bands is not sufficient.

4. Crack propagation resistance and fatigue life may be increased by decreasing or eliminating the initial surface-layer stress.

5. A model for fatigue failure is suggested. We propose that the surface layer acts as a barrier to cause an accumulation of dislocations. When the local stress associated with this accumulation exceeds the fracture strength, cracks are formed. In the propagation phase, the surface layer at the crack tip increases with cycling until the fracture strength is again exceeded. The depth of each cracking sequence will depend on the stress gradient in the surface layer. The effect of environment on fatigue may be explained in terms of its effect on the formation of the surface layer.

VI. REFERENCES

1. N. T. Thompson, N. J. Wadsworth and N. Louat: *Phil. Mag.*, 1965, Vol. 1, p 113

2. J. C. Grosskreutz: ASTM STP, 1971, Vol. 495, p 5

3. D. S. Kemsley: *Phil. Mag.*, 1957, Vol. 2, p 131

4. P. J. E. Forsyth: *Nature*, 1953, Vol. 171, p 172

5. P. J. E. Forsyth: *J. Inst. Met.*, 1955, Vol. 83, p 395

6. A. H. Cottrell and D. Hull: *Proc. Roy Soc.*, 1957, Vol. A242, p 211

7. W. A. Wood and R. L. Segall: *Bull. Inst. Metall.*, 1957, Vol. 3, p 160

8. W. A. Wood: ASTM Symposium on Basic Mechanisms in Fatigue, 1959, p 110

9. A. J. McEvily and E. S. Machlin: *Fracture*, p 450. John Wiley and Son, Inc., New York (1939)

10. J. T. McGrath and R. C. A. Thurston: *Trans. AIME*, 1963, Vol. 227, p 645

11. H. D. Nine: *J. Appl. Phys.*, 1967, Vol. 38, p 1678

12. M. L. Ebner and W. A. Backofen: *Trans. AIME*, 1959, Vol. 215, p 510

13. C. Laird and G. C. Smith: *Phil. Mag.*, 1963, Vol. 8, p 1945

14. D. S. Kemsley: *J. Inst. Met.*, 1956, Vol. 85, p 420

15. J. Porter and J. C. Levy: *J. Inst. Met.*, 1960, Vol. 89, p 86

16. R. C. Boettner, C. Laird and A. J. McEvily: *Trans. AIME*, 1965, Vol. 233, p 379

17. R. B. Davies: *Nature*, 1954, Vol. 174, p 980

18. P. P. Benham: *J. Inst. Met.*, 1961, Vol. 89, p 328

19. W. A. Wood and H. M. Bendler: *Trans. AIME*, 1962, Vol. 234, p 18

20. C. E. Feltner: *Acta Met.*, 1963, Vol. 11, p 817

21. M. H. Raymond and L. F. Coffin: *Acta Met.*, 1963, Vol. 11, p 801

22. D. S. Kemsley and M. S. Patterson: *Acta Met.*, 1960, Vol. 8, p 453

23. M. S. Patterson: *Acta Met.*, 1955, Vol. 3, p 491

24. R. N. Wilson and P. J. E. Forsyth: *J. Inst. Metals*, 1959, Vol. 87, p 336

25. J. C. Grosskreutz: *J. Appl. Phys.*, 1963, Vol. 34, p 372

26. R. K. Ham and T. Broom: *Proc. Roy. Soc. London*, 1959, Vol. A251, p 186

27. T. H. Alden and W. A. Backoffen: *Acta Met.*, 1961, Vol. 9, p 352

28. P. B. Hersch, P. Partridge, and R. L. Segall: *Phil. Mag.*, 1959, Vol. 4, p 721

29. J. C. Grosskreutz, W. H. Reimann and W. A. Wood: *Acta Met.*, 1966, Vol. 14, p 1549

30. P. Lukas and M. Klesnil: *Corrosion Fatigue*, NACE-2, 1971, p 118

31. I. R. Kramer: *Trans. ASM*, 1969, Vol. 62, p 521

32. I. R. Kramer: *Proc. Air Force Conference on Fatigue and Fracture*, AFFDL-TR-70-144, 1969.

33. I. R. Kramer and A. Kumar: *Met. Trans.*, 1972, Vol. 3, p 1223

34. I. R. Kramer and A. Kumar: *Corrosion Fatigue*, NACE-2, 1971, p 146

35. J. T. Fourie: *Can. J. Phy.*, 1967, Vol. 45, p 777

36. H. Mughrabi: *Phy. Stat. Solidi*, 1970, Vol. 29, p 317

37. S. Kitajama, H. Tanaka, and H. Kaeida: *Trans. J. I. M.*, 1969, Vol. 10, p 10

38. G. Vellaikal and J. Washburn: *J. Appl. Phys.*, 1969, Vol. 40, p 2280

39. I. R. Kramer and N. Balasubramanian: *Acta Met.*, 1973, Vol. 21, p 698

40. I. R. Kramer and L. J. Demer: *Progress in Material Science*, 1961, Vol. 9

41. C. S. Barett: *Acta Met.*, 1953, Vol. 1, p 2

42. I. R. Kramer: *Trans. Met. Soc.*, 1963, Vol. 227, p 1003

43. I. R. Kramer: *Trans. Met. Soc.*, 1964, Vol. 230, p 991

44. I. R. Kramer: *Trans. Met. Soc.*, 1965, Vol. 233, p 1462

45. I. R. Kramer and C. L. Haehner: *Acta Met.*, 1967, Vol. 15, p 199

46. J. T. Fourie: *Corrosion Fatigue*, NACE-2, 1971, p 164

47. I. R. Kramer: *Fundamental Phenomena in the Material Sciences* (Surface Phenomena), 1966, Vol. 3, p 171

48. H. Shen, S. Podlaseck, and I. R. Kramer: *Acta Met.*, 1966, Vol. 14, p 341

49. H. Shen and I. R. Kramer: *Trans. Inter. Vac. Met. Conference*, 1967, p 263

50. I. R. Kramer, A. Kumar and N. Balasubramanian: AMMRC Report CR 71-2/4, July, 1972

51. A. N. Stroh: *Advances in Physics*, 1957, Vol. 6, p 418

52. O. Lissner: Colloquium on Fatigue, Springer-Verlag, Berlin, 1955

53. H. Moller and M. Hempel: *Arch. Eisenhuttenw.*, 1954, Vol. 25, p 39

54. E. Siebel and G. Stahli: *Arch. Eisenhuttenw.*, 1942, Vol. 15, p 519

55. A. J. Kennedy: *Processes of Creep and Fatigue in Metals*, Oliver and Boyd, Edinburg and London, 1962

56. C. E. Feltner and M. R. Mitchell: *ASTM STP*, Vol. 465, p 27

57. G. Hahn, P. N. Mincer and A. R. Rosenfield: *Experimental Mechanics*, 1971, Vol. 11, p 1

58. O. H. Basquin: *Proc. ASTM*, 1910, Vol. 10, p 625

59. M. A. Miner: *J. Appl. Mech.*, September, 1945

60. C. Zener: *Fracturing of Metals*, ASM, 1948, p 3

61. A. H. Cottrell: *Trans. AIME*, 1958, Vol. 212, p 192

62. I. R. Kramer: AFML Report TR 68/65 (MCR-67-421), January, 1968

TECHNICAL REPORT DISTRIBUTION

No. of Copies	To
1	Office of the Director, Defense Research and Engineering, The Pentagon, Washington, D.C. 20301
12	Commander, Defense Documentation Center, Cameron Station, Building 5, 5010 Duke Street, Alexandria, Virginia 22314
1	Metals and Ceramics Information Center, Battelle Memorial Institute, Columbus, Ohio 43201
	Chief of Research and Development, Department of the Army, Washington, D.C. 20310
2	ATTN: Physical and Engineering Sciences Division
	Commanding Officer, Army Research Office (Durham), Box CM, Duke Station, Durham, North Carolina 27706
1	ATTN: Information Processing Office
	Commanding General, U.S. Army Materiel Command, Washington, D.C. 20315
1	ATTN: AMCRD-TC
1	AMCSA-S, Dr. C. M. Crenshaw, Chief Scientist
	Commanding General, Deseret Test Center, Fort Douglas, Utah 84113
1	ATTN: Technical Information Office
	Commanding General, U.S. Army Electronics Command, Fort Manmouth, New Jersey 07703
1	ATTN: AMSEL-GG-DM
	Commanding General, U.S. Army Missile Command, Redstone Arsenal, Alabama 35809
1	ATTN: Technical Library
1	AMSMI-RSM, Mr. E. J. Wheelahan
	Commanding General, U.S. Army Munitions Command, Dover, New Jersey 07801
1	ATTN: Technical Library
	Commanding General, U.S. Army Satellite Communications Agency, Fort Monmouth, New Jersey 07703
1	ATTN: Technical Document Center
	Commanding General, U.S. Army Tank-Automotive Command, Warren, Michigan 48090
2	ATTN: AMSTA-BSL, Research Library Branch
	Commanding General, U.S. Army Weapons Command, Research and Development Directorate, Rock Island, Illinois 61201
1	ATTN: AMSWE-RER-L, Technical Library

No. of Copies	To
1	Commanding General, White Sands Missile Range, New Mexico 88002 ATTN: STEWS-WS-VT
1	Command Offi-er, Aberdeen Proving Ground, Maryland 21005 ATTN: STEAP-TL, Bldg 305
1	Commanding Officer, Edgewood Arsenal, Maryland 21010 ATTN: Mr. F. E. Thompson, Dir. of Eng. & Ind. Serv., Chem-Mun Br
1	Commanding Officer, Frankford Arsenal, Philadelphia, Pennsylvania 19137 ATTN: Library, H1300, Bl. 51-2
1	Commanding Officer, Picatinny Arsenal, Dover, New Jersey 07801 ATTN: SMUPA-RT-S
4	Commanding Officer, Redstone Scientific Information Center, U.S. Army Missile Command, Redstone Arsenal, Alabama 35809 ATTN: AMSMI-RBLD, Document Section
1	Commanding Officer, Watervliet Arsenal, Watervliet, New York 12189 ATTN: SWEWV-RDT, Technical Information Services Office
1	Director, Eustis Directorate, U.S. Army Air Mobility Research & Development Laboratory, Fort Eustis, Virginia 23604 ATTN: Mr. J. Robinson, SAVDL-EU-SS
1	Librarian, U.S. Army Aviation School Library, Fort Rucker, Alabama 36360 ATTN: Building 5907
2	Command Officer, USACDC Ordnance Agency, Aberdeen Proving Ground, Maryland 21005 ATTN: Library, Building 305
1	Naval Research Laboratory, Washington, D.C. 20390 ATTN: Dr. J. M. Krafft, Code 6305
1	Commander, U.S. Army Foreign Science & Technology Center, 220 7th Street, N.W., Charlottesvilles, Virginia 22901 ATTN: AMXST-SDS
1	Chief of Naval Research, Arlington, Virginia 22217 ATTN: Code 471
2 1 1	Air Force Materials Laboratory, Wright-Patterson Air Force Base, Ohio 45433 ATTN: AFML (LAE), E. Morrissey AFML (LC) AFML (LMD), D. M. Forney

No. of Copies	To
	National Aeronautics and Space Administration, Washington, D.C. 20546
1	ATTN: Mr. B. G. Achhammer
1	Mr. G. C. Deutsch - Code RR-1
	National Aeronatucis and Space Administration, Marshall Space Flight Center, Huntsville, Alabama 35812
1	ATTN: R-P&VE-M, R. J. Schwinghamer
1	S&E-ME-MM, Mr. W. A. Wilson, Building 4720
1	Ship Research Committee, Maritime Transportation Res. Board, National Research Council, 2101 Constitution Ave., N. W., Washington, D.C. 20418
	Panametrics, 221 Crescent Street, Waltham, Massachusetts 02154
1	ATTN: Mr. K. A. Fowler
	Wyman-Gordon Company, Worcester, Massachusetts 01601
1	ATTN: Technical Library
	Lockheed-Georgia Company, Marietta, Georgia 30060
1	ATTN: Advanced Composites Information Center, Dept. 72-14 - Zone 402
	Director, Army Materials and Mechanics Research Center, Watertown, Massachusetts 02172
2	ATTN: AMXMR-PL
1	AMXMR-PR
1	AMXMR-AP
1	AMXMR-CT
2	AMXMR-EM, Dr. E. B. Kula
1	AMXMR- HW
	Director Advanced Research Projects Agency 1400 Wilson Blvd. Arlington, Va. 22209
3	ATTN: Program Management
	Department of the Navy Naval Air Systems Command P.O. Box 2128 Henderson, Nevada 89015 ATTN: Mr. H. W. Rosenberg Supervisor of Metallurgical Division (For related Contracts N 00019-70-C-0023
1	and NN00019-70-C-0143)

No. of Copies	To
	Department of Navy Naval Air Systems Command ATTN: Mr. J. E. Ehrhardt PCO Mr. Goodwin AIR-52031A/154 Washington, D. C. 20360 (For related contracts N00019-70-C-0023
1	and N00019-71-C-0143)
	Air Force Office of Scientific Research ATTN: Mr. Marvin L. Roberts, PCO (PND) 1400 Wilson Blvd. Arlington, Virginia 22209
1	(for use of contract F44620-69-C-0065)
	TRW Equipment TRW Inc. 23555 Euclid Avenue Cleveland, Ohio 44117
1	ATTN: Elizabeth Barrett, T/M 3417
	Lockheed Missiles and Space Company P. O. Box 504 Sunnyvale, California 94088 ATTN: Dr. M. I. Jacobson
1	Orgn. 47-01, Bldg. 150
	Metcut Research Associates Inc. 3980 Rosslyn Drive Cincinnati, Ohio 45209
1	ATTN: Mr. W. P. Koster